

**PETROLOGY AND GEOCHEMISTRY OF THE ULTRAMAFIC ROCKS
FROM PARTS OF THE MANIPUR OPHIOLITE
BELT WITH REFERENCE TO CHROMITE
MINERALISATION**

THESIS SUBMITTED TO NAGALAND UNIVERSITY IN PARTIAL
FULFILMENT FOR THE AWARD OF THE DEGREE OF

DOCTOR OF PHILOSOPHY IN GEOLOGY

By

LEIMAPOKPAM ROMENDRO SINGH

Ph.D. Registration No. 751/2017

Dated 14/9/2015



**DEPARTMENT OF GEOLOGY
NAGALAND UNIVERSITY
KOHIMA CAMPUS, MERIEMA**

AUGUST, 2021



Department of Geology
Nagaland University
Kohima Campus
Meriema, 797004

Certificate

This is to certify that the thesis entitled "*Petrology and Geochemistry of the Ultramafic Rocks from Parts of the Manipur Ophiolite Belt with Reference to Chromite Mineralisation*" is the outcome of the original and bonafide research work undertaken by **Shri Leimapokpam Romendro Singh** (Nagaland University Ph. D. Registration No. 751/2017, dated 14/9/2015) under my guidance and supervision. That the thesis, as a part or as a whole, hasn't been submitted to any other University or Institution for the award of any degree or diploma.

(Dr. Chabungbam Mangi Khuman)
Assistant Professor.
Department of Geology
Nagaland University
Kohima-797004

Kohima,
Dated 18th Aug. 2021

DECLARATION

I, **Shri Leimapokpam Romendro Singh**, do hereby declare that the subject matter of this thesis is the record of work done by me, that the content of this thesis did not form basis for the award of any previous degree to me or the best of my knowledge to anybody else, and that this thesis has not been submitted by me for any research degree to any other university or institute.

This thesis is being submitted to the Nagaland University for the award of Doctor of Philosophy degree in Geology.

Candidate

L. Romendro Singh

(L. Romendro Singh)

Ph.D. Regd. No. 751/2017

Coran

Supervisor

Dept. of Geology

18/08/2021

Head

Dept. of Geology

Head

**Department of Geology
Nagaland University, Kohima**

Chang

ACKNOWLEDGEMENT

At the very outset, I would like to express my profound gratitude to my supervisor Dr. Ch. Mangi Khuman, Department of Geology, Nagaland University, Kohima Campus Meriema, for his dedicated, innovative and proficient guidance extended to me throughout my research work. Without his continuous encouragement and benevolent guidance and father like advice, completion of such a thesis with a horizon of new concepts could have not been possible.

I also would like to place my sincere acknowledgements to Prof. B.V. Rao, Prof. S.K. Singh and Prof. G.T. Thong, the present and former Heads of the Department of Geology, Nagaland University, Kohima Campus (during my research tenure) for rendering their constant support, cooperation, encouragement and suggestions in carrying out the doctoral research.

I am grateful to Prof. N.V. Chalapati Rao and Dr. Dinesh Pandit of the Centre of Advanced Study, Department of Geology, Banaras Hindu University, Varanasi for their kind co-operation in carrying out the EPMA Analysis of my samples. I also would like to extend my sincere thanks Dr. R.K. Bikramaditya, Assistant Professor, Department of Geology, Banaras Hindu University for his hospitality, co-operation and support during my visit in his department in connection with EPMA analysis.

I express my heartfelt thanks to Dr. Krishnakanta Singh, Scientist E, Wadia Institute of Himalayan Geology (WIHG), Dehradun for helping me to bring out the XRD and ICP (MS) analyses at his esteemed institution.

I, also convey my sincere and deep sense of gratitude to Prof. R.A.S. Kushwaha, the then HOD and Dr. Maibam Bidyananda, Associate Professor, Department of Earth Sciences, Manipur University for providing me the facilities available in their respective laboratories in connection with capturing of many of the photomicrographs. I also express heartfelt thanks to Mr. Bapin Toijam, a vibrant research scholar of the Department of Earth Sciences, Manipur University for his co-operation and valuable help in handling the microscope at the time of capturing the photomicrographs.

My sincere thanks also go to Dr. Radhapyarai Devi, Guest Faculty, Department of Earth Sciences, Manipur University for her support and help in making slides and carrying out XRD analysis at the USIC facility of Gauhati University, Guwahati during her research tenure there.

I also gratefully acknowledge Dr. Th. Ranjit Singh, Associate Professor, Department of Geology, D.M. College of Science, Imphal for his moral support and encouragement by providing some important books and journals related to my research work.

I also express my heartfelt thanks to the Government of Manipur, especially the Department of Higher Education, Government of Manipur. My sincere and heartfelt gratitude also goes to Ms. O. Chaoba Devi, Principal, Thoubal College, Thoubal for rendering me necessary support and encouragement during the course of my research, and also for making me availed the opportunity of getting the benefits of study leave for the research work.

My thanks also go to all the teaching and non-teaching staff and fellow researchers of the Department of Geology, Nagaland University, Kohima Campus Meriema, for their fruitful help and for rendering thought provoking discussion and valuable suggestion at different stages of the progress of the research work.

I will not be satisfied if I don't express my benevolent thanks to Smt. Chabungbam Ongbi Nirmala Devi, wife of my supervisor, Dr. Ch Mangi Khuman, for her support and encouragement, and warm and homely treatment during my long stay at their quarter throughout my research work.

My acknowledgement may remain uncompleted if I don't express my sincere thanks to my half soul, Smt. Leimapokpam Ongbi Amita Devi, for her constant mental and moral support, and for running the family at par in my absence and also for meeting all the social obligations during my research work.

Last, but not the least I thank to the Almighty God for keeping me and my family in good health all throughout the research work.

L. Romendro Singh
(L. Romendro Singh)

Contents

	Page
Acknowledgement	i
List of Tables	ii
List of Figures	iii
Chapter 1: Introduction	1-36
1.1 General Idea about the Research Work	1
1.2 Ophiolite: Development and Evolution of Concept	5
1.3 Ophiolite: Global Distribution	12
1.4 Ophiolites around the Indian Plate	14
1.5 Manipur Ophiolite	19
1.6 Chromite and Its Occurrence in Ophiolites	22
1.7 General Account of Manipur	23
1.7.1 Relief and Topography	27
1.7.2 Drainage	31
1.7.3 Climate	33
1.8 Objectives of the Present Work	35
1.9 Methodology	35
1.9.1 Field Studies	36
1.9.2 Laboratory Studies	36
Chapter 2: Geological and Tectonic Setting	37-62
2.1 General geological setting	37
2.2 General tectonic setting	47
2.3. Ophiolite Melange Zone of Manipur	50
2.3.1 The Ophiolite Suite	50
2.3.2 The Oceanic Pelagic Sediments	56
2.3.3 The Exotics Rocks/ Bodies	59

Chapter 3: Ultramafic Rocks	63-101
3.1 Petrography and Mineralogy	64
3.1.1 Modal Analysis	70
3.2 Mineral Chemistry	74
3.2.1 Olivine	74
3.2.2 Orthopyroxene	78
3.2.3 Clinopyroxene	81
3.2.4 Spinel	84
3.3 Bulk Rock Geochemistry	90
3.3.1 Geochemistry of Major and Minor Element Oxides	92
3.3.2 Trace and Rare Earth Elements Geochemistry	95
Chapter 4: Serpentinisation	102-116
4.1 Petrography and Mineralogy	104
4.2 Mineral and Bulk Rock Geochemistry	111
Chapter 5: Chromite and Chromite Mineralisation.	117-137
5.1 Petrography and Mineralogy	119
5.2 Mineral Chemistry	124
Chapter 6: Discussion and Conclusion	138-151
6.1 Discussion	139
6.1.1 Geological and Tectonic Setting (Field Setting)	139
6.1.2 Ultramafic Rocks	142
6.1.3 Serpentinisation	145
6.1.4 Chromite and Chromite Mineralisation	147
6.2 Conclusion	150
Bibliography	152-164
Annexure I:	List of Conferences and Seminars attended.
Annexure II:	List of Papers Published.

List of Tables

1. **Table 1.2.1:** Correlation of ophiolite stratigraphy with oceanic lithosphere.
2. **Table 2.1.1:** Generalized stratigraphic succession of Manipur.
3. **Table 2.2.1:** Plate motion at various points in and around Manipur.
4. **Table 3.1.1.1:** Modal proportions of ultramafic rocks from Manipur Ophiolite Belt
5. **Table 3.1.1.2:** Recalculated modal proportions of Olivine, Orthopyroxene and Clinopyroxene.
6. **Table 3.2.1.1:** Olivine composition of representative ultramafic rock (Sample F3-2) from MOB in percent (EPMA data).
7. **Table 3.2.1.2:** Recalculation of Olivine Analysis (EPMA) data.
8. **Table 3.2.2.1:** Orthopyroxene composition of ultramafic rocks from Manipur ophiolite Belt in percent (EPMA data).
9. **Table 3.2.2.2:** Recalculation of Orthopyroxene Analysis (EPMA) data.
10. **Table 3.2.3.1:** Clinopyroxene composition of ultramafic rocks from Manipur ophiolite Belt in percent (EPMA data).
11. **Table 3.2.3.2:** Recalculation of Clinopyroxene Analysis (EPMA) data.
12. **Table 3.2.4.1A:** Composition of one type of spinel from host Ultramafic rocks (Sample F3-3B) from Manipur Ophiolite Belt in percent (EPMA data).
13. **Table 3.2.4.1B:** Composition of one type of spinel from host Ultramafic rocks (Sample F1M1) of Manipur Ophiolite Belt in percent (EPMA data).
14. **Table 3.2.4.1C:** Composition of one type of spinel from host Ultramafic rocks (Sample F1-S2B) from Manipur Ophiolite Belt in percent (EPMA data).
15. **Table 3.2.4.2A:** Recalculation of Spinel Analysis.
16. **Table 3.2.4.2B:** Recalculation of Spinel Analysis.
17. **Table 3.2.4.2C:** Recalculation of Spinel Analysis.

18. **Table 3.3.1:** Chemical analysis (XRF) data of ultramafic rocks from Manipur Ophiolite Belt (Major and Minor elements in wt %).
19. **Table 3.3.2.1:** Chemical analysis (XRF) data of Ultramafic rocks from Manipur Ophiolite Belt (Trace elements in ppm).
20. **Table 3.3.2.2A:** Data of selected REE in ppm (ICPMS) of Ultramafic from Manipur Ophiolite Belt.
21. **Table 3.3.2.2B:** Normalised (ICPMS) analysis data of selected REE in ppm of Ultramafic from Manipur Ophiolite Belt.
22. **Table 3.3.2.3:** Average amount of trace elements in ophiolitic metamorphic peridotite, ultramafic rocks and gabbros compared with that of Manipur ophiolite Ultramafic in ppm.
23. **Table 3.3.2.4:** Normalised values of amount of rare earth elements in ophiolitic metamorphic peridotite, mafic-cumulate, ultramafics and gabbros compared with that of Manipur Ophiolite Ultramafic in ppm.
24. **Table 4.2.1:** Serpentine Composition of ultramafic rocks from parts of MOB in percent.
25. **Table 4.2.2:** Recalculation of Serpentine Analysis.
26. **Table 4.2.3:** Recalculated values of XRF data of some Serpentinites from Manipur Ophiolite Belt.
27. **Table 4.2.4:** X- ray diffraction data of serpentinised Ultramafic rocks from MOB (Showing different types of serpentines).
28. **Table 5.2.1A:** Microprobe data of representative chromite sample (No. F₁-S₂A).
29. **Table 5.2.1B:** Recalculation of Chromite analysis (Sample No F₁-S₂A).
30. **Table 5.2.2 A:** Microprobe data of representative chromite sample (No. F₂-B₁).
31. **Table 5.2.2 B:** Recalculation of chromite analysis data (Sample No. F₂-B₁).
32. **Table 5.2.3 A:** Microprobe data of representative chromite sample (No. F₃-5A₁).

- 33. Table 5.2.3B:** Recalculation of chromite analysis data (Sample No. F₃-5A₁).
- 34. Table 5.2.4A:** Microprobe data of representative chromite sample (No. F₃-5A₂).
- 35. Table 5.2.4B:** Recalculation of chromite analysis data (Sample F₃ 5A₂, Phangrei).
- 36. Table 5.2.5:** Summary of microprobe data of four representative chromite samples from MOB.
- 37. Table 5.2.6:** Percentage Fe⁺³, Cr, Al in chromites of Manipur Ophiolite Belt.

List of Figures

1. **Fig. 1.1.1:** Layerings of the Earth.
2. **Fig. 1.1.2:** Diagrammatic representation of the concept of sea floor spreading.
3. **Fig. 1.2.1:** Lithology and thickness of a typical ophiolite sequence, based on Semail ophiolite in Oman.
4. **Fig. 1.3.1:** Global distribution of major Mesozoic and Cenozoic ophiolite belts.
5. **Fig. 1.4.1:** Regional tectonic setting of the Himalaya showing Tethyan Ophiolite occurrences and their age of formation (white).
6. **Fig. 1.5.1:** The belt of the main Ophiolite Suite of Manipur.
7. **Fig. 1.7.1:** Map showing different Districts of Manipur.
8. **Fig. 1.7.2 A:** Nong-in, State Bird of Manipur.
9. **Fig. 1.7.2 B:** Sangai, State Animal of Manipur.
10. **Fig. 1.7.2 C:** Sirui Lily, State flower of Manipur.
11. **Fig. 1.7.2 D:** Uningthou, State tree of Manipur.
12. **Fig. 1.7.2 E:** Kangla-Sha, State emblem of Manipur.
13. **Fig. 1.7.1.1A:** View of Imphal Valley from the top of Cheirao Ching.
14. **Fig. 1.7.1.1B:** View of Loktak Lake.
15. **Fig. 1.7.2.1:** Drainage Map of Manipur (after Soibam, 1998).
16. **Fig. 2.1.1A:** Geological map of Manipur showing study area.
17. **Fig. 2.1.1A B:** Study area within the Manipur Ophiolite Belt.
18. **Fig. 2.1.2:** Normal fault on Disang shale.
19. **Fig. 2.1.3:** Disang rocks showing turbidity and character.
20. **Fig. 2.1.4:** Disang shale intercalated with thin flaggy sandstone.
21. **Fig. 2.1.5:** Trace Fossil in Disang shale.
22. **Fig. 2.1.6:** Barail Sandstone Showing typical turbidite character.

23. **Fig. 2.1.7:** Thickly bedded Barail sandstone intercalated with thin layer of shale.
24. **Fig. 2.1.8:** Exposure of Surma group of rocks.
25. **Fig. 2.1.9:** Exposure of Tipam Sandstone.
26. **Fig. 2.1.10:** Conglomerate Horizon in between Surma and Tipam group of rocks.
27. **Fig. 2.2.1:** Dextral Shear Deformation mechanism of the IMR.
28. **Fig. 2.3.1.1:** Highly serpentinised Ultramafic exposed near Lunghar, Ukhrul Dist.
29. **Fig. 2.3.1.2:** Slickenside in serpentinised ultramafic near Khudengthabi.
30. **Fig. 2.3.1.3:** Fresh Ultramafic exposure near Lokchao river.
31. **Fig. 2.3.1.4:** Rodingite exposure at Kwatha.Tengnoupal Dist.
32. **Fig. 2.3.1.5:** Exposure of Hard & Compact Ultramafic boulders on the ridge of Sirui Hill.
33. **Fig. 2.3.1.6:** Less serpentinised Ultramafic exposednear Khudengthabi.
34. **Fig. 2.3.1.7:** Massive Ultramafic Blocks near Lunghar (Ukl Dist.)
35. **Fig. 2.3.1.8:** Exposure of dyke intruded into the ultramfics on the top of Sirui Hill, Ukhrul District.
36. **Fig.2.3.1.9:** Contact between Ultramafics and Shale.
37. **Fig. 2.3.1.10:** Litho contact between Chert And Ultramafic.
38. **Fig. 2.3.1.11:** Fibrous serpentine in host Ultramafic near Lokchao River, Moreh.
39. **Fig. 2.3.1.12:** Quartz veinlets in ultramafics.
40. **Fig. 2.3.1.13:** Chromite (massive) in closed view, Kwatha.Tengnoupal Dist.
41. **Fig. 2.3.1.14:** Chromite Blocks, Kwatha,Tengnoupal Dist.
42. **Fig. 2.3.1.15:** Chromite Exposure, Holenphai.
43. **Fig. 2.3.1.16:** Chromite along with host-rock Ultramafic, Holenphai.
44. **Fig. 2.3.1.17:** Chromite Exposure (with spotted & nodular mass), Phangrei.
45. **Fig. 2.3.1.18:** Gamnom Chromite, Ukhrul Dist.

46. **Fig. 2.3.1.19:** Host rock of chromite at Phangrei showing rugged surface, Ukhrul District
47. **Fig. 2.3.2.1:** Soil developed from Pelagic Shale.
48. **Fig. 2.3.2.2:** Typical Soil and Grass derived from the ultramafics.
49. **Fig. 2.3.2.3:** Exposure of chert in Lokchao river bank, Moreh, Tengenoupal District.
50. **Fig. 2.3.2.4:** Exposure of Limestone in pockets, Ukhrul District.
51. **Fig. 2.3.2.5:** Limestone Cavern at Kangkhui Village, Ukhrul District.
52. **Fig. 2.3.3.1:** Exposure of Exotic Sandstone near Kondong Lairembi, Moreh.
53. **Fig. 2.3.3.2:** Conglomerate exposure in the form of small Hillock near Pushing village, Ukhrul District.
54. **Fig. 2.3.3.3:** Pillow lava found near Ukhrul town.
55. **Fig. 2.3.3.4:** Pillow lava at Khudengthabi, Tengenoupal Dist.
56. **Fig. 2.3.3.5:** Pillow lava at Kwatha Lamkhai, Tengenoupal Dist.
57. **Fig. 2.3.3.6:** Pillow lava hill near Ukhrul town.
58. **Fig. 2.3.3.7:** Chert boulder in the Lokchao River Bed, near Moreh, Tengenoupal District.
59. **Fig. 2.3.3.8:** Quartz veins in Sandstone.
60. **Fig. 2.3.3.9:** Calcite veins in medium grain Exotic rocks.
61. **Fig. 3.1.1:** Presence of Opx, Cpx and Serpentine grains in ultramafic.
62. **Fig. 3.1.2A:** Primary spinel (width of 4mm) showing segregation and alignment in ultramafic.
63. **Fig. 3.1.2B:** Fractures developed in primary spinel.
64. **Fig. 3.1.3:** Orthopyroxene grain (width of 4mm) showing segregation and alignment in ultramafic
65. **Fig. 3.1.4:** Clinopyroxene grain (width of 4mm) showing aggregation and alignment in ultramafic.
66. **Fig. 3.1.5:** Mesh textured serpentine and relict of olivine.
67. **Fig. 3.1.6:** Elongated clinopyroxene (width of 4mm) grains having tapering ends.

68. **Fig. 3.1.7:** Olivine relict within serpentinitised Orthopyroxene.
69. **Fig. 3.1.8:** Secondary spinel grains which mimic the shape of the original fracture of olivine (polarized light).
70. **Fig. 3.1.9:** Xenoblastic orthopyroxene showing Corrosive structure at outer margin.
71. **Fig. 3.1.10:** Exsolution lamellae of Orthopyroxene in clinopyroxene host.
72. **Fig. 3.1.11:** Growth of serpentine into asbestiform chrysotile in extremely serpentinitised ultramafic.
73. **Fig. 3.1.12:** Ternary diagram of Ol-En-Di.
74. **Fig. 3.1.13-AB C:** Different Stages of partial melting and development of residue.
75. **Fig. 3.1.1.1:** Triangular plot of the ultramafic rocks of Manipur Ophiolite on the basis of modal minerals of olivine (Ol)-orthopyroxene (Opx)-clinopyroxene (Cpx).
76. **Fig. 3.2.1.1A.** Histogram showing ranges in Composition of Olivine from Ophiolite Metamorphic Peridotite.
77. **Fig. 3.2.1.1B.** Histogram showing ranges in Al_2O_3 contents of Orthopyroxene from Ophiolite Metamorphic Peridotite.
78. **Fig. 3.2.1.1C.** Histogram showing ranges in Al_2O_3 contents of Clinopyroxene from Ophiolite Metamorphic Peridotite.
79. **Fig. 3.2.2.1:** Pyroxene quadrilateral showing compositions of coexisting ortho- and Clinopyroxenes of ultramafics of Manipur Ophiolite.
80. **Fig. 3.2.3.1:** $\text{Ca}/(\text{Ca}+\text{Mg})$ ratio of clinopyroxene from ophiolite metamorphic peridotite. Temperature points taken from diopside-enstatite solvus at 30 kbar from Boyd (1970).
81. **Fig. 3.2.4.1:** Plot of $100\text{Cr}/(\text{Cr} + \text{Al})$ ratio in primary spinels against wt.% Al_2O_3 in coexisting orthopyroxene from spinel lherzolite xenoliths (after Carswell, 1980). Stars are the plot of Manipur Ophiolite Ultramafics.
82. **Fig. 3.2.4.2:** Compositional fields of Spinel of host rocks constituting the Ophiolite suite (after Pober and Fauph, 1980).
83. **Fig. 3.3.1.1:** The plot of $(\text{Al}_2\text{O}_3 + \text{CaO} + \text{Na}_2\text{O} + \text{K}_2\text{O} + \text{TiO}_2)/\text{SiO}_2$ versus MgO/SiO_2 of the Ultramafics of Manipur Ophiolite (stars).
84. **Fig. 3.3.1.2:** AFM plot of Manipur Ophiolite ultramafics. $(\text{Na}_2\text{O}+\text{K}_2\text{O})\text{-FeO-MgO}$ plot shows that the ultramafics are pigeonholed within the field of ultramafic peridotite.

85. **Fig. 3.3.1.3:** ACM (Al_2O_3 -CaO-MgO) plot of Manipur Ophiolite ultramafics shows that the ultramafics are pigeonholed within the field of ultramafic peridotites.
86. **Fig. 3.3.2.5:** Comparison of REE pattern of ultramafics of Manipur Ophiolite Belt with that of normal ophiolite sequences.
87. **Fig. 4.1.1:** Minerals present in the system MgO - SiO_2 - H_2O + CO_2 .
88. **Fig. 4.1.2 A:** X-ray diffraction (XRD) patterns of 3 (three) representative serpentinite samples from Manipur Ophiolite Belt.
89. **Fig. 4.1.2 B:** X-ray diffraction (XRD) patterns of 3 (three) representative serpentinite samples from Manipur Ophiolite Belt.
90. **Fig. 4.1.3:** SiO_2 vs. MgO plot for the analysed serpentine minerals in serpentinites from Manipur Ophiolite Belt.
91. **Fig. 5.1.1(A, B):** Photomicrograph showing chromite with secondarily filled silicates in the fracture spaces (polarised light).
92. **Fig. 5.1.2:** Photomicrograph showing highly brecciated chromite.
93. **Figs. 5.1.3 and 5.1.4:** BSE images showing inclusion of magnetite in chromites.
94. **Fig. 5.1.5:** BSE image showing chromite grain in pyroxene in the body of massive chromite.
95. **Fig. 5.1.6:** BSE image showing orthopyroxene and chrome-diopside in chromite.
96. **Fig. 5.1.7A:** BSE image showing fractured chromite with serpentine.
97. **Fig. 5.1.7B:** BSE image showing presence of nickel mineral, nepouite.
98. **Figs. 5.1.8A and 5.1.8B:** BSE images showing relicts of olivine surrounded by serpentine.
99. **Fig. 5.1.9:** BSE image showing orthopyroxene and serpentine.
100. **Fig. 5.2.1:** Plot of trivalent cations. The MOB chromites fall in the field of Al-chromite being pigeonholed mostly in ophiolite chromite.
101. **Fig. 5.2.2:** Compositional field of chromites from Manipur Ophiolite Belt.
102. **Fig. 5.2.3 :** Plot of Cr_2O_3 Wt % versus Al_2O_3 Wt % showing the chemical composition of chromite from Manipur Ophiolite Belt with a comparison of podiform and stratiform chromitites.
103. **Fig. 5.2.4:** Plot of Cr_2O_3 Wt % versus TiO_2 Wt % showing the chemical composition of chromite from Manipur Ophiolite Belt with comparison of podiform and stratiform chromitites.

Chapter 1

INTRODUCTION

1.1 General Idea about the Research Work

Petrology, an important branch of geology is the scientific study of rocks that deals with the composition, texture, structure, occurrence, distribution and their origin in relation to physicochemical conditions and other geologic processes. The word petrology is rooted from the ancient Greek words “petros” and “logos” meaning respectively rocks and study. The study of this core branch of geology also provides source of ideas about some of the events occurred during various episodes of the evolutionary history of the earth. The details of change of conditions occurred during the different stages of the earth's evolutionary history are well recorded in the rocks. Hence, the study of the different parameters of rocks such as their composition, mineralogy, texture and structure, occurrence and distribution etc. are used as important tools to solve a wide variety of geologic related problems.

Geochemistry is a science that uses the tools and principles of chemistry for explaining the compositions of the components of the earth and that of the earth as a whole. It also deals with the distribution and migration of the chemical elements in rocks and minerals within the earth in space and time, as well as the movement of these elements into the soil and water systems. The realm of geochemistry even extends beyond the earth, encompassing the entire solar system. The term geochemistry was first used by the Swiss-German chemist Christian Friedrich Schonbein in 1838. But Norwegian mineralogist Victor Moritz Goldschmidt has made commendable contributions in the field of geochemistry and hence he has been named as the father of geochemistry. According to him the primary purpose of geochemistry is to determine quantitatively the composition of the earth and its parts and on the other hand to discover the laws which control the distribution of the individual elements. The science of geochemistry has made important contributions in the understanding of a number of processes including mantle convection, the formation of planets and the origin of a number of rocks. Thus, the application of this branch of science is inevitable for a number of studies concerned with various

areas of geology and allied fields. Therefore, the study of geochemistry is considered as an important tool in finding clues about petrotectonic significance vis-à-vis origin, distribution, evolution, etc. of a type of a rock as well as that of the constituent minerals.

The term Lithosphere was coined by R.A. Daly meaning rock layer. This is the rigid, rocky outer layer of the earth, consisting of the crust and the solid outermost layer of the upper mantle (mainly composed of ultramafic peridotite) resting over the partially melted zone known as asthenosphere. It extends to a depth of about 30 to 60 miles (50 to 100 km). This rigid outermost shell of the planet earth (crust and upper mantle) has been broken up into seven or eight (depending on how they are defined) major and many minor blocks, which are in relative motion to each other. Such moving blocks are known as lithospheric plates.

The position as well as the relationship of lithosphere and asthenosphere with respect to the compositional as well as rheological layering of the Earth is as shown in **figure 1.1.1**. The idea of sea floor spreading was originally proposed by Harry Hess from Princeton University in 1960. According to him, the lateral movement was believed to be driven by convection currents in the upper mantle in the fashion of a conveyor belt. The continents (continental crusts, which are formed during the differentiation of the earth and evolved through ages) moved in response to the growth of ocean basins between them. It was suggested that oceanic crust is created from the uprising of materials from earth's mantle at the crest of the mid-ocean ridge system, a volcanic submarine swell (or rise) which occupies a median position in many of the world's oceans (**Fig. 1.1.2**). The oceanic crust, much thinner than the continental crust (simply continent), having a mean thickness of about 7 km, compared with the average continental thickness of about 35 km; is chemically different, and is structurally far less complex. In contrast to the continents the present-day oceanic crust is very young, probably not greater than 200 Ma in age. The fragments of the young oceanic crust (<35 Ma) including the associated sediments, when brought tectonically to the sub-surface along the margins of the continents or the oceanic island arcs, in due course of the subsequent tectonic inversion, are known as the ophiolites.

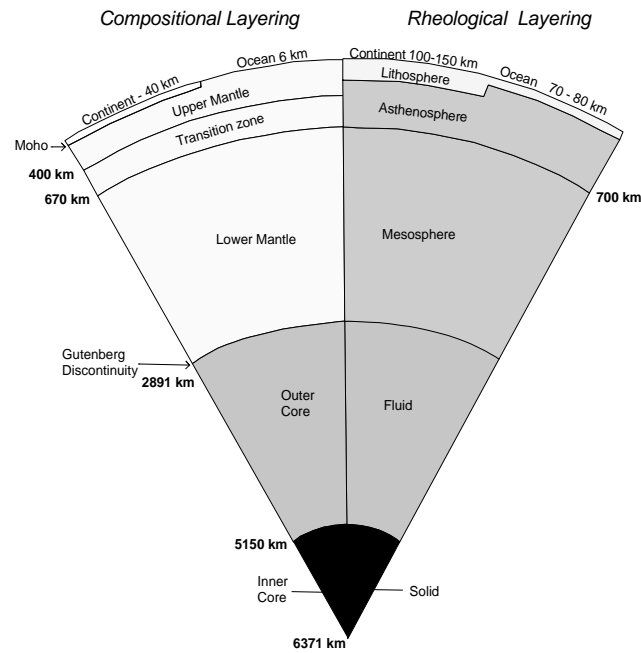


Fig. 1.1.1:
Layerings of the Earth.

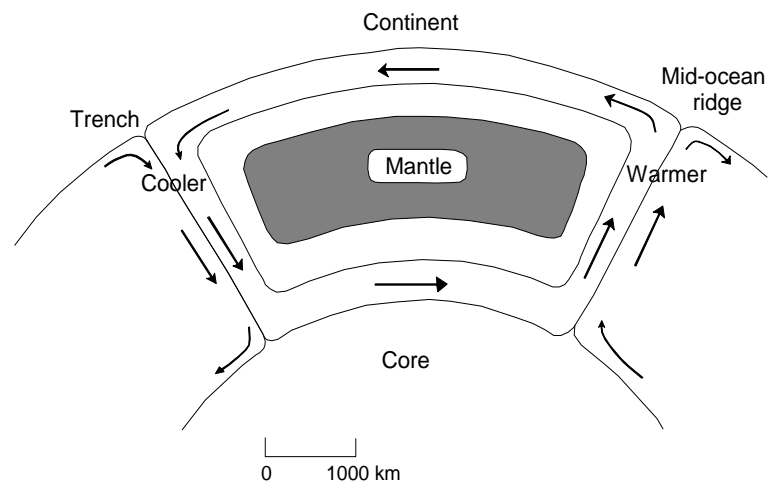


Fig. 1.1.2:
Diagrammatic representation of the concept of sea floor spreading
(after Hess, 1962).

It is mention-worthy that ophiolites of the Indo-Myanmar orogenic belt are comparatively less documented and less explored on account of various geographical and political factors. Very little about the tectonic setting of

generation, magma genesis and evolution, how and when these ophiolitic rocks were formed, etc. have not been agreeably established beyond doubt. Many other key questions are yet to be answered fully. Hence, critical analyses from different angles about the distinguishing characteristics of this part of ophiolite belt particularly about chromite mineralization and occurrences are considered as an important area where some innovative researches are called for.

Ultramafic rocks are usually defined by their modal mineralogy. They have more than 90% mafic minerals, less than 45% SiO₂, more than 18% MgO, high FeO and low potassium. Although the term ultrabasic (compositional use) is related to ultramafics (mineralogical use), they are not wholly equivalent. The Ultrabasic is a more inclusive term that includes igneous rocks with low silica content (< 45% SiO₂) that may not be extremely enriched in Fe and Mg. The ultramafic rocks are igneous and meta-igneous in origin. The earth's mantle is mainly composed of ultramafic rocks. The studies of ultramafic rocks formed in diverse tectonics environments are of great significance to decipher the mantle geodynamics and crust-mantle interaction processes. The ultramafic rocks are also present in ophiolite complexes/dismembered ophiolite fragments, formed in various petrogenetic and tectonic environments emplaced within continental masses. The geodynamic processes of ultramafic rocks have similarly been applied in many instances for the reconstruction of continental landmasses. The ultramafic rocks of the study area are closely associated with spreading regime during which ocean floor rocks have been generated owing to diapirism of upper mantle rocks and subsequent orogenesis of the Indo-Myanmar Ranges in due course of tectonic reversal thereby leading to the subduction of the Indian plate below the Myanmar micro-plate.

Chromite is an oxide mineral belonging to the spinel group. It is a complex mineral containing magnesium, iron, aluminium, and chromium in varying proportions depending on the type and environment of mineralisation, the composition of which can be represented as FeCr₂O₄ or (Fe⁺², Mg) (Cr, Al, Fe⁺³)₂O₄. It is iron-black or brown black in colour with brown streak, faint sub-metallic lustre, and uneven brittle fracture and is having hardness of 5.5 and specific gravity of 4.5 to 4.8. It is the only source of chromium metal. The chromite minerals are found in

two main deposits, which are stratiform deposits and podiform deposits. Stratiform deposits in layered forms are the main source of chromite resources and are seen in huge igneous intrusions like those of the countries of South Africa, Canada and Finland. Chromite resources from podiform deposits are mainly found in the ophiolite complexes like those of the countries of Kazakhstan, Turkey, Albania and Zimbabwe. Podiform chromite resource of the ophiolite complex of the Indo-Myanmar Ranges of northeast India is also mention-worthy. Podiform deposits are irregular in shape. "Pod" is a term given by geologists to express the uncertain morphology of this deposit.

The aim of the present work entitled “*Petrology and Geochemistry of Ultramafic rocks from parts of Manipur Ophiolite Belt with Reference to Chromite Mineralisation*” encompasses a wide spectrum of observations of the various aspects of the aforesaid interdisciplinary areas of study. The study aims to provide logical explanation through the analytical interpretations of the various data generated in this piece of research work so as to decipher a picture how the studies of petrology and geochemistry of the ultramafic rocks lead to reveal the processes of mineralization and occurrence of chromites in the ophiolite belt in Manipur. It is also tried to examine whether the petrotectonic conditions of serpentinization of the ultramafic rocks are playing an important role in chromite mineralization.

1.2 Ophiolite: Development and Evolution of Concept

The generally agreed concept of an Ophiolite is – it is a section of the earth’s oceanic crust and the underlying upper mantle that has been thrust and exposed above sea level and often emplaced onto continental crust rocks. The word is derived from the Greek word “*Ophio*” that means snake or serpent. It was first introduced by Brongniart (1827) to describe serpentinites because of serpent like greenish appearance of such rocks. The name *serpentinite* (rock composed mainly of serpentine minerals) is attributed to the greenish, mottled and shining appearance resembling a serpent. Therefore, ophiolite could have been used as a Greek equivalent of the word serpentinite (Khuman, 2009).

Steinman (1926) further expanded the term ophiolite to include set of rocks - peridotites (serpentinites), diabase, gabbro, spilites and other related rocks into a kindred relationship in the Mediterranean mountains, and interpreted their origin as differentiated ocean floor magmatic units. He later pointed out its close relation with associated deep-sea sediments such as radiolarian cherts and clays. From this point he transformed ophiolite from a rock term to a rock association term. Steinmann in his language said "As ophiolites, one must characterize only the consanguineous association of predominantly ultrabasic rocks of which the principal one is always peridotite (serpentinite) with subordinate gabbro, diabase, spilite or norite and related abyssal sediments. These abyssal sediments were predominantly cherts (radiolarite), pelagic clays and Calpionella- bearing limestones. Thus "Steinmann Trinity" consisting of serpentinite, diabase-spilite and chert was gradually combined into ophiolite and so ophiolite was to grow into a genetic rock assemblage. This led to the general concept that the ophiolites represented thick submarine magmatic extrusions emplaced in the early stages of eugeosyncline development. Steinmann's concept was accepted in Europe because it could explain the mafic and ultramafic association within alpine orogenic zones. But, Benson (1926) considered peridotites and serpentinites to be plutonic in nature and intrusive into folded geosynclinal sediments within orogenic belts and called them 'alpine type'. Meanwhile in America, Bowen (1927), putting forward his concept of fractional crystallization, challenged the generation of peridotites in the crust.

During 1930-1960, few researchers focused their attention on the ophiolites, during which studies were concentrated mainly on granites and volcanic rocks. Among them Hess (1938, 1955a, b) were notable exceptions. He could not reconcile the findings of Bowen's experiments with the field observations he had made on numerous mafic and ultramafic occurrences. So, he proposed a low temperature primary peridotite magma containing 5 to 10 percent of water based on the lack of high temperature contact aureoles and almost universal partial conversion to serpentinite. This concept of hydrous peridotite magma suffered a drawback after Bowen and Tuttle (1949) had shown that experimentally it was not possible for a peridotite magma containing water to exist below 1000°C. It was obvious that neither the field observations nor their interpretations could be reconciled with the

experimental work on the formation of peridotites. Brunn (1960, 1961), considered the ophiolites as the basaltic outpourings along rift structures at the boundaries of geosynclinal basins (from the findings of his studies in Greece). Differentiation of basaltic magma after emplacement was considered to have been responsible for the apparent stratigraphic sequence from peridotite upwards into gabbro and finally into basalts. However, the ratio of peridotites to mafic rocks (approximately 3:1) could not be explained by normal differentiation of basaltic magma. Thus, origin of ophiolites could not be satisfactorily explained for long.

During 1965 to 1975, a convergence of opinion concerning the origin of ophiolites has resulted from greatly expanded geological exchange and increased intensive study of these rocks. This, combined with the new concepts of global plate tectonics, has achieved a radical departure from previously held concepts. The early phase of convergence of researchers was marked by the publication of a collection of papers by 33 authors (Wyllie, 1967), which provided new and interesting facts on ultramafic and related rocks. In that publication, different associations of ultramafic rocks were distinguished. The alpine-type peridotite-serpentinite associations (ophiolites) like that of Papua, Newfoundland, Cyprus, Oman, etc. was taken as a separate entity separating from other mafic-ultramafic occurrences, which in the past had been mixed together creating more complications. From the analysis of various hypotheses regarding the origin of ultramafic rocks it is learnt that a mantle origin was favored by most investigators, but there was a wide divergence of opinion on what mantle processes were involved. Essentially, at least two magmatic processes were invoked: (1) differentiation of a basic liquid to form an ultramafic 'mush' which either forms a cumulate sequence or invades as lubricated 'mush', and (2) formation of primary peridotite magma within the mantle which is then intruded into the crust as mush or emplaced as a solid. But the basic problem of plutonic peridotites exhibiting only extremely slight contact metamorphism or none at all had not been resolved. As well, mechanism for the emplacement of the solid peridotite remained unresolved. The concept of plate tectonics provided a new framework through which emplacement of alpine-type peridotites could be explained thereby resolving a long pending petrotectonic problem. A number of papers (Coleman, 1971a; Dewey and Bird, 1971; Davies, 1971, Moores and Vine,

1971; Church, 1972) advocated that fragments of the oceanic lithosphere had been thrust over or into continental margins (obducted) at consuming plate margins.

In 1972, during the Penrose Conference (an international conference) of the Geological Society of America, the participants finally accepted the definition of the term ophiolite as - distinctive assemblage of mafic to ultramafic rocks and associated deep-sea sediments. Now, it is generally accepted that ophiolites represent fragments of upper mantle and oceanic crust (Dewey and Bird, 1971; Coleman, 1977; Nicolas, 1989) that were incorporated into continental margins during continent-continent and arc-continent collisions (Dilek and Flower, 2003), ridge trench inter-actions (Cloos, 1993; Lagabriele *et al.*, 2000), and/or subduction-accretion events (Cawood *et al.*, 2009). They are generally found along suture zones in both collisional-type (i.e., Alpine, Himalayan, Appalachian) and accretionary-type (i.e., North American Cordilleran, Indo-Myanmar Ranges) orogenic belts.

Moore (1969) and later Moore and Vine (1971) in Vourinos and Troodos ophiolites respectively, recognized the similarity of the ophiolite stratigraphy they were observing to the oceanic lithosphere. Miyashiro in 1973 reported that there were rocks in the Troodos that have silica content that is more than 52.5% and geochemically belong to the calc-alkaline series, suggesting that the Troodos Massif was probably formed in an island arc. This observation was followed by an answer of Moore (1975) that the calc-alkaline chemical characteristics that Miyashiro describes could have been the result of metasomatic alteration and by Gass (1975) who suggests that the 120 km continuous sheeted dykes complex was not compatible to the arc theory of Miyashiro. Pearce and Cann (1973) collected analyses from basalts that erupted in different tectonic settings and observed a chemical variability between many of them and basalts that have erupted in mid-ocean ridges (MOR). Robinson and Malpas (1990) studied the chemistry of glasses from Troodos and suggested a subduction-related origin. Pearce *et al.*, (1984) suggested that most of the up to then studied ophiolites have been formed in a supra-subduction zone setting (SSZ). According to the new emerging trend of the concept of ophiolites, many of them are the fragments of newly created young ocean floor rocks ($<<30\text{Ma}$) of generally small basins formed principally in the ocean-continent-transition (OCT) zones of hyper-extended continental margin environments that had been thrust over the continents or island arcs or along their

margins (Moore, 2002; Desmurs *et al.*, 2002; Manatschal and Muntener, 2009; Mohn *et al.*, 2012; Piccardo, 2015; Soibam *et al.*, 2015). Passive continental margin rifting at a very slow rate appears to have been the principal mechanism by which crustal stretching and basin formation occurred and was accompanied by lithospheric thinning and tectonic exhumation of sub-continental mantle (cf. Lemoine *et al.*, 1987; Froitzheim and Manatschal, 1996; Sutra and Manatschal, 2012). Generally, the sequence of an ophiolite comprises of mantle part, transition zone and crustal part, which are as enumerated below.

	Lithology	Layers	Typical Ophiolite	Normal Ocean Crust	
			Thickness (km)	Thickness (km)	P-wave vel. (km/s)
Crust	Deep-Sea Sediment	1	~0.3	0.5	1.7 - 2.0
	Basaltic Pillow Lavas	2A & 2B	0.5	0.5	2 - 5.6
	Sheeted dike complex	2C	1- 1.5	1.5	6.7
	Isotropic Gabbro Plagiogranite Layered Gabbro Wehrlite	3A	2-5	4.7	7.1
Transition zone	cumulate pyroxenite/dunite	3B			
Mantle	Chromitite pod Harzburgite/Lherzolite	4	up to 7		8.1

Fig. 1.2.1:
Lithology and thickness of a typical ophiolite sequence, based on Semail Ophiolite in Oman (after Brown and Mussett, 1993; Boudier and Nicolas, 1985).

Mantle part: it is bottom part of an ophiolite sequence which represents the upper mantle section. Harzburgite/Lherzolite and dunite, usually with a metamorphic tectonic fabric (more or less serpentinitised) are dominant rock types in this section, depending upon the amount of melt extracted from the mantle, and nature of the tectonic setting.

Transition zone: this zone lies just above the mantle part, where cumulate rocks of peridotite, pyroxenites and dunites with some amount of chromitite pods are found. Pyroxenites are generally considered as fractionated rocks derived from basaltic melt at the bottom of lower crust. Dunites might have formed in a similar condition when olivine is differentiated from the basaltic melt, but it may also be found as residual material after extraction of basaltic melt from the upper mantle. This transition zone is also sometimes considered as serpentinitisation front.

Crustal part: it is the section comprising of deep-sea pelagic sediment, volcanic complex both mafic sheeted dyke and mafic volcanic complex (commonly pillowed) just below the sheeted dyke. There is also isotropic gabbro, plagiogranite, and layered gabbro and wherlite. This sequence of lithology is shown as Layer-1 to Layer-3A in **figure 1.2.1**.

And, associated rock types include (i) an overlying sedimentary section typically comprise of ribbon chert, thin shale interbeds, and minor limestones; (ii) podiform bodies of chromite generally associated with harzburgite and/or dunite depending upon the tectonic setting; and (iii) sodic felsic intrusive and extrusive rocks.

Faulted contacts between mappable units are common. An ophiolite may be incomplete, disseminated or metamorphosed. Although ophiolite generally is interpreted to be of oceanic crust and upper mantle, the use of the term should be independent of its supposed origin.

The analogy of complete ophiolite sequence (**Table 1.2.1**) with oceanic lithosphere is supported by the gross similarity in chemistry, although there is considerable difference in detail like metamorphic grades corresponding to temperature gradients existing under spreading centers, and the presence of similar

ore minerals and deep-water sediments (Moore, 1982). Salisbury and Chistensen (1978) have compared the velocity structure of the oceanic lithosphere with the seismic velocities measured in samples from the Bay of Islands ophiolite complex in Newfoundland and concluded that the determined velocity stratigraphies are identical.

Table 1.2.1: Correlation of ophiolite stratigraphy with oceanic lithosphere (modified after Gass, 1980).

Complete ophiolite sequence	Oceanic correlation
	Layer 1
Sediments	About 0.4 km thick, comprising of unconsolidated turbidity current carried terrigenous sediments, pelagic clays, calcareous and silicic oozes and manganese nodules.
	Layer 2
Basic volcanics, commonly Pillowed, merging into Basic sheeted dyke complex	1.0 - 2.5 km thick (Olivine tholeite basalt with dykes). Uppermost sub-layer (0-1 km) is porous, and present only near the eruptive centre. Away from the ridge where porous layer is not developed this sub-layer infilled by the secondary minerals like calcite, quartz and zeolite-forms acoustic basement the lowermost is intrusive basic rocks rich sub-layer.
	Layer 3
High level intrusives Trondhjemites Gabbros	About 4.0 km thick, main plutonic foundation of oceanic crust comprising of upper mantle derived material whose olivine had reacted with water to produce serpentinised peridotite, which has an upper sub-layer of gabbro with pocket of plagiogranite. The lower sub-layer consists of cumulate gabbro and pocket of cumulate ultramafics
Layered cumulates (peridotite) Olivine gabbros Pyroxenites Peridotites Moho Layer 4 (This layer has a thickness up to about 7 km)
	Upper mantle
Harzburgite, commonly Serpentinised \pm lherzolite. dunite, chromitite	

At one time it seemed that investigations of the petrology and structure of the oceanic lithosphere could conveniently be accomplished by the study of ophiolite sequences on land. Though this sequence has been thought to represent an analogue for the oceanic crust formed at the spreading centers, there are problems

with this analogue. First, the average thickness of the oceanic crust is about 7 km; but most ophiolite magmatic sections range from about 3 to 5 km thick (White *et al.*, 1992; Cloos, 1993). Second, many complexes do not display the complete sequence. These observations have led to much misunderstanding and hampered full use of ophiolites as a tool in historical geology. Recent recognition of incomplete magmatic sequences in the oceanic crust studied during the Ocean Drilling Program (ODP) and other investigations has led to a partial resolution of this dilemma. Fast spreading centers or magma rich centers, such as the East Pacific Rise generally display a complete “Penrose Conference type” sequence (Karson, 1998, 2001; Macdonald, 1998), whereas slow spreading centers with variable magma supply, such as the Mid Atlantic Ridge or the Southwest Indian Ridge may be incomplete (Lagabriele and Cannat, 1990; Lagabriele *et al.*, 1998; Karson, 1998). On the other hand, geochemical evidence (Pearce, 1980; Elthon, 1991) suggests that original sites of ophiolite were marginal seas or Red sea-type oceans on the ground that many ophiolites display compositions more reflective of modern arc and back arc environments than that of most mid-oceanic ridges. Recently, however, it has been reported that oceanic ridge sites contain the chemical fingerprints of subduction related sources or inferred continental lithosphere in the mid-oceanic ridge lavas. In addition, some modern arc complexes contain lavas reminiscent of mid-oceanic ridge basalts (MORBs) and oceanic island basalts (OIBs) (Leeman *et al.*, 1990). Thus, mantle heterogeneity seems to be an important factor in both modern spreading centers and island arcs. Many ophiolites with so-called subduction-related or ‘supra-subduction zone’ (SSZ) sources lack any evidence of the existence of a well-developed arc edifice.

1.3 Ophiolite: Global Distribution

Ophiolites occur along the seismic orogenic belts along the suture zones of convergent plate boundaries. The distribution of certain ophiolite types during particular time periods coincides with major tectonic and magmatic events in earth's history. For example, the formation of the late Palaeozoic and Jurassic ophiolites was coeval with the dismantling and rifting of the northern edge of western

Gondwana. Most of the ophiolites were obducted during Jurassic-Cretaceous period. The development of the Jurassic–Cretaceous ophiolites overlapped in time with the emplacement of giant dike swarms and the formation of large igneous provinces (LIPs) (Kerr *et al.*, 1998; Vaughan and Scarrow, 2003) and with the breakup of Pangea through discrete episodes of continental rifting (Dalziel *et al.*, 2000). The main ophiolite pulses that are the peak times of ophiolite genesis and emplacement could be in the early Palaeozoic, the late Jurassic and the Cretaceous, which are contemporaneous with the closure of some ocean basins and major orogenic events (Dilek and Furnes, 2011).

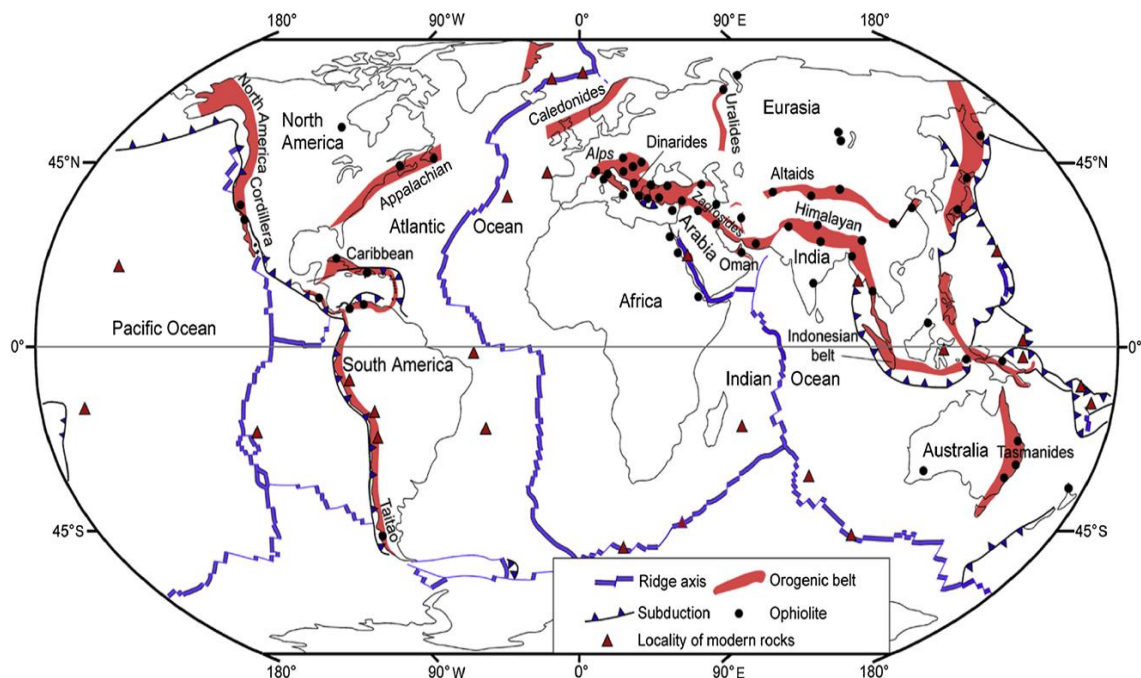


Fig. 1.3.1:
Global distribution of major Mesozoic and Cenozoic ophiolite belts
(after Emilio Saccani, 2014).

Mesozoic and Cenozoic ophiolites (**Fig. 1.3.1**) are much more abundant and constitute most of the important large exposures of ophiolite. The Tethyan belt extends from the Baltic Cordillera and Rif of Spain and Africa eastward through the Alps, the Dinarides in Yugoslavia, through Greece, Turkey, Iran, Oman, Pakistan, the Himalayas, the Indo-Myanmar Ranges and Indonesia. Within the Pacific area, ophiolite belts of Mesozoic and Cenozoic age extend from New Zealand north-

westerly to New Caledonia, New Guinea, Celebes, Borneo, Philippine Islands, Japan, Sakhalin, Kamchatka, and the Koryak-Chukotka region and from Alaska southward along the Western Cordillera of North America. Eastward from Guatemala, the ophiolite trends through the Greater Antilles, Cuba and Puerto Rico and loops into the Caribbean Andes of Venezuela southward through Western Columbia and terminating in Ecuador.

The early Palaeozoic ophiolites in the Appalachian and Caledonian orogenic belts evolved in the Iapetus Ocean and its seaways between North America, Greenland, and Baltica-Avalonia as they were closing. The Palaeozoic ophiolites in Iberia, central Europe, north-western Africa, and northern Anatolia developed in the Rheic Ocean between the Baltica-Avalonia, Laurasia, and Gondwana continental masses. The Palaeozoic ophiolites in the Urals developed in the Uralian Ocean, which separated the Baltica-Eastern Europe and Kazakhstan-Siberian continental masses (Windley *et al.*, 2007). The late Jurassic to late Cretaceous ophiolites in the Alpine–Himalayan orogenic belt formed in various seaways of the Tethyan oceanic realm, preceding the collisions of Apulia, Arabia, India, and other Gondwana derived microcontinents with Eurasia.

1.4 Ophiolites around the Indian Plate

The ophiolites around the Indian plate are known as the Tethyan ophiolites. Tethyan ophiolites (**Fig. 1.4.1**) developed as a result of collision of the Indian plate with Asian continental block (Gansser, 1964) and the Myanmar continental block to the east (Mitchell 1993; Khuman and Soibam, 2010; Soibam *et al.*, 2015) during Mesozoic and early Tertiary. A good amount of ophiolitic rocks is also found along the western, northern and eastern margins of the Indian plate. *The Bela Ophiolite, Muslim Bagh Ophiolite, and Waziristan-Khost ophiolites* are found in Pakistan and bordering Afghanistan (Alleman, 1979; Gnos *et al.*, 1997) along the western margin of the Indian plate; and the related ophiolite belts are further extended along the south-eastern coast of Oman, which emplaced around the Cretaceous/Tertiary boundary. According to the present understanding, ophiolitic rocks at the northern margin of the Indian plate originated between Jurassic and Early Cretaceous

(Aitchison *et al.*, 2003; Aitchison and Davis, 2004). Geochemical data indicate that the ophiolitic rocks are formed in fore-arc, arc and back-arc, continental margin settings (Hebart *et al.*, 2012; Khuman and Soibam, 2010; Soibam *et al.*, 2015). These rocks were obducted southwards onto the Indian plate margin or accreted within the Indus-Yarlung-Tsangpo Suture Zone (ITSZ) (Thakur, 1981) as the Indian continental block collided with the intra-oceanic arc in Late Cretaceous and with the Asian continent in Palaeocene-Eocene as the Neo-tethys closed (Tapponnier *et al.*, 1981; Allègre *et al.*, 1984; White and Lister, 2012). The ophiolites along the suture zone were emplaced as thrust sheets on the Indian continental margin and presently occur as klippen on deep-water marine sedimentary sequences of the Indian passive margin, whereas others occur as well preserved or dismembered sections and mélanges within the ITSZ (Gansser, 1964; 1980).



Fig. 1.4.1:
Regional tectonic setting of the Himalaya showing Tethyan ophiolite occurrences and their age of formation (white). Base map sourced from GeoMapApp software.

Some of the major ophiolites occurring along the ITSZ are *Spontang, Nidar, Yungbwa, Saga, Sangsang, Xigaze, Zedong, Loubusa from west to east, and Tidding ophiolite of Arunachal Pradesh at the eastern syntaxis*. The ITSZ suddenly changes its form from east-west extension to north-south extension at the eastern syntaxial bent in Arunachal Pradesh. This suture giving rise to the Indo-Myanmar Ranges (IMR) is convex towards the west in Nagaland and Manipur sector of the north-eastern part India and further extended south to the Andaman and Nicobar Islands, where the suture is convex towards the east. The prominent ophiolites of this suture zone are Nagaland-Manipur ophiolite, Chin hill ophiolite and Andaman ophiolite. The Tethyan ophiolites are important because many new ideas on the “ophiolite concept” could be emerged from the systematic structural, petrological, geochemical, geochronological, and tectonic studies of these ophiolites, as the ophiolites occur comparatively fresh and preserved well. Tethyan ophiolites are highly diverse in terms of their structural architecture, geochemical features, isotopic fingerprints, and emplacement ages and mechanisms (Dilek, 2003).

i). The Bela Ophiolite: This ophiolite in Baluchistan province of Pakistan is a dismembered sequence that presumably once formed in a single thrust sheet. It consists of serpentinised mantle harzburgite overlain by layered peridotite and gabbro, foliated and isotropic gabbro, sheeted dikes and extrusive rocks (Gnos *et al.*, 1998). Chemical composition of the plagiogranite is consistent with its origin from fractional crystallisation of basaltic magma, and U–Pb zircon dating of trondhjemite and granite yielded an age of 68 ± 3 Ma (Ahmed, 1993). These ages constrain the age of origin and emplacement of the ophiolite.

ii). The Muslim Bagh Ophiolite: The Muslim Bagh ophiolite (earlier called Hindu Bagh) is a well exposed ophiolite in Pakistan. It is a part of western ophiolite belt (Bela-Muslim Bagh-Zhob-Waziristan) that separates the Indian plate from the adjacent continental block (Luth and Afghan block). The Muslim Bagh ophiolite was first reported on maps by Vredenburg (1901). The plagiogranite of sheeted dikes in the Muslim Bagh ophiolite yield U-Pb age of 80.2 ± 1.5 Ma (Kakar *et al.*, 2012). It is believed that this ophiolite formation was coeval with the Spongtag Arc in a

similar tectonic environment that formed in an ocean-ocean subduction setting ~15 Ma before they were obducted on the Indian passive margin.

iii). The Waziristan Ophiolite: It is located to the north of the Muslim Bagh ophiolite, along the suture zone between the Indian Plate to the east and Afghan Block to the west. It occupies about 500 sq. km. It occurs as dismembered thrust slices overriding Jurassic-Cretaceous calcareous sediments deposited above the Indian plate. It is a typical ophiolite consisting of ultramafic rocks, gabbros, sheeted dykes, and pelagic sediments. Faunal evidence in the associated sediments suggests that the ophiolite is of Tithonian-Valanginian age of ~142 Ma (Khan, 1995 and 1999). The sheeted dikes show chilled margins. Several geochemical parameters suggest that the dykes of Waziristan Ophiolite have transitional characteristics between mid-ocean ridge basalt and island-arc tholeiite. It is therefore proposed that this ophiolite may have been originated in a back-arc basin tectonic setting (Khan *et al.*, 2007).

iv). The Spontang Ophiolite: The Spontang Ophiolite in the Ladakh Himalaya is believed one of the few remnants of oceanic crust and upper mantle from the neo-Tethyan ocean, which once separated India and the Asia along the present-day Himalayas. It consists of thrust sheets of upper mantle and oceanic crustal rocks obducted onto the northern passive continental margin of India during the late Cretaceous. U–Pb dating of zircons from a dioritic segregation in the high-level gabbros of the Spontang ophiolite shows that the complex formed at 177 ± 1 Ma (mid-Jurassic) which represents a fragment of Neo-Tethyan oceanic crust (Pederson *et al.*, 2001).

v). The Nidar Ophiolite: This is about 10 km thick ophiolite suite in the northwest part of Himalaya, India. This complex is exposed within the ITSZ in Ladakh. This ophiolite complex comprises a sequence of ultra-mafic rocks at the base, gabbroic rocks in the middle and volcano-sedimentary assemblage on the top. Mineral and whole rock geochemical and isotopic data indicate their generation and emplacement in an intra-oceanic subduction environment, with no influence of continental contamination. Whole rock Sm–Nd isochron corresponds to an age of 140 ± 32 Ma (Ahmad *et al.*, 2008).

vi). The Yungbwa Ophiolite: This is a thrust sheeted ophiolite occupying about 800 sq.km. and tectonically exposed as klippe and located in SW Tibet, about 20 km south of the ITSZ and Mount Kailas. It is a large peridotitic complex tectonically overlying a mélangé that contains blocks of Permian reef limestone. Based on dating of diabase and tholeiite (U–Pb zircon), the age of Yungbwa ophiolite is 123.4 ± 0.9 Ma (Chan *et al.*, 2007).

vii). The Saga, Sangsang and Xigaze Ophiolites: These ophiolites are located in the central part of the 2000 km long East-West trending ITSZ as a remnant of Neo-Tethys paleo ocean (Aitchison *et al.*, 2011). U–Pb zircon dating in diorite, gabbro and diabase yielded ages of 130 Ma for Saga and 125.2 ± 3.4 Ma for the Sangsang massif (Xia *et al.*, 2008). Pegmatitic gabbro from the Xigaze Ophiolitic crust yielded an age of 132.0 ± 2.9 Ma (Chan *et al.*, 2007). The Saga and Sangsang Ophiolites are located about 200–350 km west of Xigaze. They consist of mantle peridotites overlain by leuco- and melano-gabbros, and a mafic crust.

viii). The Zedang and Luobusa Ophiolites: They lie in the eastern part of the ITSZ. There are no complete ophiolite assemblages in the Zedang Ophiolite. It is mainly composed of mantle peridotite and a suite of volcanic rocks as well as siliceous rocks with some blocks of olivine-pyroxenites and has been dated at 161 ± 2.3 Ma by the U–Pb zircon method in dacite, and 152.2 ± 3.3 Ma by $^{40}\text{Ar}/^{39}\text{Ar}$ step heating of hornblende in andesitic dike (McDermid *et al.*, 2002). U–Pb dating of zircon in diabase yielded ages of 149.7 ± 3.4 Ma, 150.0 ± 5.0 Ma (Chan *et al.*, 2007) for the Luobusa massif.

ix). Nagaland-Manipur Ophiolite: It occurs in the northern part of the 1200 km long narrow sigmoidal belt of the Indo-Myanmar Ranges (IMR). The IMR has three distinct segments from south to north viz ArakanYoma, Chin Hill and Manipur-Naga Hill, each 400 km length (Brunnschweiler, 1966). The total length of the Nagaland-Manipur Ophiolite (NMO) in the IMR is about 200 km and breadth varies from 2 km to 20 km and covering an area of 2000 sq. km. It starts from Phokphur of Phek district of Nagaland in the north and extends beyond Moreh of Tengnoupal district of Manipur in the south. The NMO has been interpreted as an accretion prism resulting from the convergence between the Indian and Myanmar

plates (Khuman and Soibam, 2010; Soibam *et al.*, 2015). The works carried out in the Nagaland sector of the ophiolite belt (Chisoi, 2010; Meirangsoba, 2011; Rao and Nayak, 2016) revealed that the ophiolite in the southern sector (in the territory of Manipur) is the further continuation and belong to the same belt as characterised by similar geological, petrological and geochemical characteristics. The Ophiolite Belt consists predominantly of the main ophiolitic body (ultramafic suite), pelagic sediments and various blocks of exotic rocks. The associated exotic rocks in the host of mostly of pelagic shale and ultramafic rocks include a number of blocks of variable dimensions of diabasic dyke, pillow lava, conglomerate, limestone, gritty sandstone and rocks kindred with lava extrusion (Soibam *et al.*, 2015). The presence of radiolarian and coccoliths in pelagic sediments the NMO establishes to be Maestrichtian to Eocene (Chattopadhyaya *et al.*, 1983).

1.5 Manipur Ophiolite

This is the southern part of Nagaland-Manipur Ophiolite of the Indo-Myanmar Ranges (IMR). It is about 110 km long and 2-20 km in breath. It starts from Ukhrul district, bordering Nagaland in the north and extends beyond Moreh of Tengenoupal district of the state. The Manipur ophiolite belt consists predominantly of tectonic slices representing various units of the sequence of ancient oceanic lithosphere that include the ultramafic suite (**Fig. 1.5.1**), mafic dykes and sills, pillow lavas, pelagic sediments like chert and limestone, etc. in a jumbled manner (Khuman and Soibam, 2010; and Soibam *et al.*, 2015). The peridotites (ultramafic suite) are mainly of metamorphic harzburgite and lherzolite with sporadic podiform chromite occurrences. The ultramafics having sporadic diabasic dykes cutting across them are found to have been sandwiched with pelagic shale and generally occupies the central portion of the belt where very few of the exotic rocks are found.

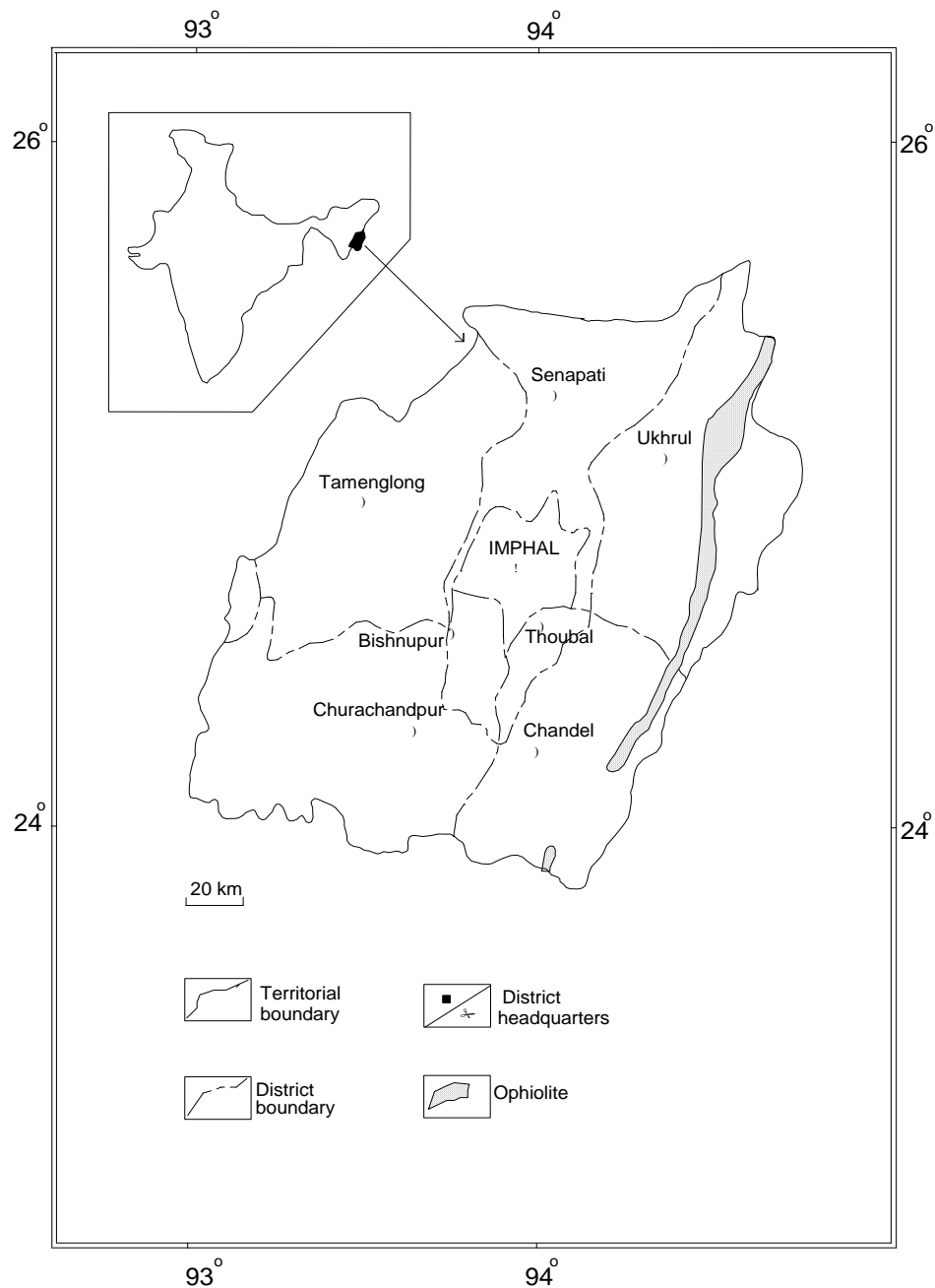


Fig. 1.5.1:
The belt of the main Ophiolite Suite of Manipur (after Soibam, 1998).
The actual Ophiolite Melange Zone is considerably wider (Fig. 2.1.1).

Not only the ultramafics have sporadic diabasic dykes the pelagic sediments also have occasional diabasic dykes and sills. The horizon of the ultramafic suite is flanked at the western and eastern margins by the exposure of the mixture of pelagic

sediments – shale, chert and limestone and associated exotic rocks. Out of the pelagic sediments, shale is exceedingly predominant and sometimes mixed with flysch like sediments. The associated exotic rocks in the host of mostly of pelagic shale and ultramafics in the lesser extent, include a number of blocks of variable dimensions of diabasic dyke, pillow lava, conglomerate, limestone, gritty sandstone and rocks kindred with lava extrusion. The assembly of the different tectonic blocks of the whole range of the litho-units comprising of the ultramafic suite, pelagic sediments and exotic rocks of various kinds constitute the Ophiolite Mélange Zone (**Fig. 2.1.1**).

The ultramafic rocks (serpentinites) are principally composed of serpentines derived from olivine, bastites (pseudomorphs of serpentine after pyroxenes showing bronze like metallic luster or schiller), relics of olivine, orthopyroxene, clinopyroxene (in samples with protoliths) and primary and secondary spinels. The rocks generally show xenoblastic granular texture and the grain size is quite variable. No sample having indications of original euhedral crystal faces that have not suffered partial melting could be found.

The dyke and sill rocks are fine (<1mm) to medium (1-5mm) grained. These rocks are composed of euhedral phenocrysts of olivine, orthopyroxene and clinopyroxene and the sub-hedral phases of larger plagioclase laths and intergranular uraltised pyroxene grains and patches of uraltites (Khuman and Soibam, 2010). The subhedral plagioclase grains are cloudy or dirty albite and consist of myriad of minute crystals of epidote. In some samples, the earlier formed euhedral pyroxenes are partially uraltised. There are limited magnetite grains as pseudomorphs after the earlier formed crystals most probably olivine. The basic rocks commonly show idiomorphic inequigranular texture with intergranular diabasic or sub-ophitic fabric. The plagioclase grains are mostly prismatic. In some samples there are vesicles mostly ranging 0.02-0.03 mm diameters, which are filled in by secondary calcite indicating sub ocean floor intrusion. The dyke and sill rocks have undergone greenschists facies metamorphism and hence become spilites (Soibam and Khuman, 2011).

The slender plagioclase crystallites of the pillow lavas have random to radial orientation giving rise to typical variolitic texture. There are also larger grains of euhedral (earlier formed) pyroxenes, major portion of which are uralitized. In some of the samples, there are phenocrysts of un-zoned olivine, orthopyroxene and clinopyroxene, all of which are partially or almost wholly uralitised. The plagioclase crystallites are of albitic composition with myriad of tiny epidote crystals. The numerous vesicles (filled by secondary calcite) ranges approximately between 0.2 - 0.4 mm diameter, the average being about 0.3mm diameter. The pillow lavas have undergone greenschists facies metamorphism and hence become spilites (Soibam and Khuman, 2011).

1.6 Chromite and Its Occurrence in Ophiolites

Chromite is an oxide mineral belonging to spinel group. It is the only source of chromium metal. Chromite deposits are characterized by its closed relationship with ultrabasic rocks commonly in the peridotites and therefore in the ophiolites and have originated from concentration of early magmatic crystallisation (magmatic segregation). It is also reported that chromites are also formed during late magmatic or even hydrothermal process. The chromite minerals are found in two main deposits, which are stratiform deposits and podiform deposits. Stratiform deposits in layered forms are the main source of chromite resources found in the igneous intrusions. Chromite resources from podiform deposits are mainly found in the ophiolite complexes. Chromites found in large mafic igneous intrusions of the Bushveld Complex of South Africa contain about 90% of chromite bearing rock called chromitite. They are also found as orthocumulate lenses of chromite in peridotite from the earth's mantle. In addition, they are found in metamorphic rocks such as serpentinites. Usually chromites are associated with olivine, magnetite, and serpentine. Ore deposits of chromites form as early magmatic differentiation. In stratiform deposit, bands and layers indicate gravitative settling. Chromites found in South Africa, Canada, Finland and Madagascar are of stratiform deposits. Podiform chromites occur mostly in nodular form or pods and are usually associated with

dunite/harzburgite/lherzolite. Chromite deposits found in Kazakhstan, Turkey and Albania are of podiform types.

1.7 General Account of Manipur

Manipur is a small picturesque hilly state located in the extreme north eastern border of the union of India, having a unique entity with a beautiful oval shaped valley at the centre and a freshwater lake at the south-western corner of the valley. The hill ranges orient roughly north-south. Manipur lies approximately between $23^{\circ}15'$ N and $25^{\circ}41'$ N latitudes and $93^{\circ}2'$ E and $94^{\circ}47'$ E longitudes. The Tropic of Cancer runs very close to the southern boundary of the state. The state is bordering with the Union of Socialist Republic of Myanmar (Burma), and shares almost a half of the borderline with this country along the eastern and south eastern flank. The remaining half of the borderline is shared with the Indian states of Nagaland, Assam and Mizoram, on the northern, western and south western sides respectively.

Manipur is small state having an area of about 22,327 km². The oval shaped Imphal valley, in the central part of the state shares approximately 1843 km² of the total area and the surrounding hills cover the remaining area of about 20484 km². So, the hills constitute more than nine-tenths of the total area of the state. The state is endowed with excellent natural beauty. The glory of the valley is further enhanced by the enclosing luxuriant blue hill ranges. There are a number of isolated chains of hillocks within the valley protruding above the flat alluviums. The valley surrounded by hill ranges in all the sides, has a fresh water lake known as the Loktak Lake, the biggest of its kind in the entire Northeast India. The soldiers of the World War II described this part of the globe as the “Switzerland of the East”. Because of its natural beauty and rich cultural heritage this land is also known as the “Little Paradise on Earth”. The first and foremost prime minister of India, late Pandit Jawaharlal Nehru called this land of the God as the “Jewel of India”.

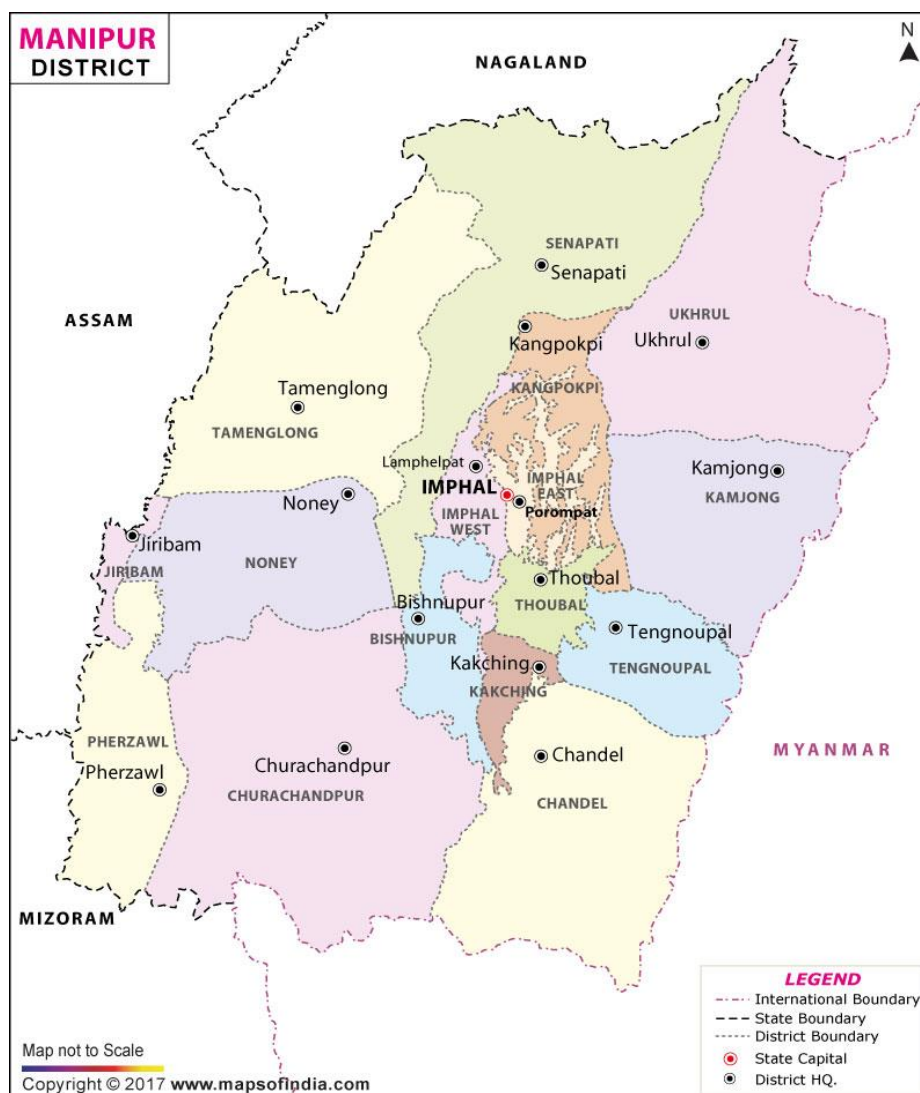


Fig. 1.7.1:
Map showing different Districts of Manipur.

The state has 16 districts of which six are in valley and eleven are in hills. The districts are – 1) Imphal West, 2) Imphal East, 3) Thoubal, 4) Kakching, 5) Bishnupur, 6) Jiribam, 7) Ukhul, 8) Kamjong, 9) Chandel, 10) Tengnoupal, 11) Tamenglong, 12) Noney, 13) Churchandpur, 14) Pherzawl, 15) Senapati and 16) Kangpokpi (**Fig. 1.7.1**). Imphal is the capital of the state. It is well connected by air as well as surface transport systems with the rest of the country and some parts of the globe as well.

Manipur is inhabited by three major ethnic groups of people. The Meiteis, forming the largest group of people are mainly concentrated in the valley and speak a common language. The other two ethnic groups – Nagas and Kukis are settled mostly in the hill areas. The classification of these ethnic groups is made by the British anthropologists in later part of nineteenth century after their arrival in the region. Nagas and Kukis are respectively conglomerations of different smaller sub-tribes having some affinities but speak different dialects (Khuman, 2009). Anal, Kabui, Mao, Maram, Maring, Tangkhul, etc. are some of the sub-tribes that belong to the Nagas; while Aimol, Gangte, Hmar, Paite, Ralte, Simte, Thadou, etc. belong to the Kukis (Kabui, 1990; Deva Singh, 1993). There are other tribes in the hills like the Chirus, Koirengs, Koms, etc. which are neither belonging to the Nagas nor the Kukis. The other main indigenous ethnic groups of people including those neither belonging to the Nagas nor the Kukis, are Mongoloids. Besides, there are also a numbers of non-mongoloid minority communities who have settled in the state at the later times. Amongst them, the Pangals (Manipuri Muslims) are one having a long association in the historical background of the state.

The State bird, state flower, state tree and state animal and state Emblem of the state of Manipur (**Figs. 1.7.2 A, B, C, D, E**) are respectively Nong-in (*Syrmaticus humiae humia*), Sangai (*Cervus eldi*), Shirui Lily (*Lilium mackliniae*), Uningthou/Bonsum (*Phoebe hainesiana hainesiana brandis*) and Kanglasha.

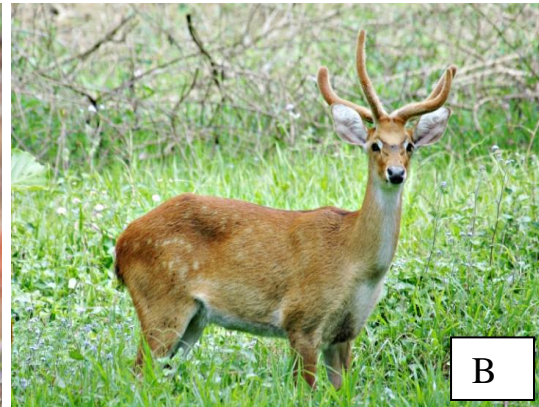


Fig. 1.7.2 A:
Nong-in,
State Bird of Manipur.
Fig. 1.7.2 B:
Sangai,
State Animal of Manipur.
Fig.1.7.2 C:
Shirui Lily,
State Flower of Manipur.
Fig. 1.7.2 D:
Uningthou,
State Tree of Manipur.
Fig. 1.7.2 E:
Kangla-Sha,
State Emblem of Manipur.

1.7.1 Relief and Topography

According to relief or surface feature, Manipur may be broadly divided into three physiographic divisions viz., 1). Central valley or Imphal valley or Manipur valley, 2). Hills surrounding the Central valley and 3). Peripheral plain areas.

1). Imphal Valley or Manipur Valley

This valley is located in the central part of the state and is almost flat. There are a number of isolated hills and low winding ridges scattered here and there throughout the valley. It is also known as the Imphal valley because the Imphal River runs through the middle of it and the capital city of Imphal is located in it (**Fig. 1.7.1.1A**). It is an irregular oval-shaped depression with the longer axis is along the N-S extent. Its north-south stretch is about 60 km long whereas the east-west extent is about 30 km wide. The general slope of this valley is north to south, as a result of which the rivers in the valley flow towards the south. The average elevation of the valley is about 780 m above mean sea level (m.s.l.). This valley was formed by the filling up (silting) of an ancient lake (fluvio-lacustrine origin) which was once covered the whole valley. Some of the isolated hillocks rising above the flat alluviums reach a considerably high altitude of about 1583 m (Nongmai Ching) while others mainly have an average elevation of about 900 m above m.s.l. The hillocks are principally made up of Disang sediments with occasional Barail sediment capping as outliers in some of them. As the valley is covered by alluviums brought down by rivers and consequent accumulation, it is very fertile. So, most of the people live in this valley where farming and transport of goods are much easier. The Loktak Lake (**Fig. 1.7.1.1B**) located at the southern part of the Imphal valley is the largest fresh water lake not only of the state but also of the entire NE India. The world-famous endangered species (**Fig. 1.7.2B**) Sangai (*Cervus eldi*) is inhabited in the Keibul Lamjao National Park (made up of floating biomass) located in this large fresh water lake.



Fig. 1.7.1.1A:
View of Imphal Valley from the top of Cheirao Ching.



Fig. 1.7.1.1B:
View of Loktak Lake.

2). Hills surrounding the Central Valley

The hills of Manipur are the southward extension of Naga Hills. They consist of a series of parallel ranges and extend up to the southern part of the state. The oval shaped central valley divides the hills of Manipur into two groups- i). Eastern Hills - those hills ranges that lie to the east of the central valley and ii). Western Hills- those to the west of the central valley.

i). Eastern Hills

The Eastern Hills run as a continuous chain along the eastern border of Manipur. They are about 200 km long and 30-50 km wide. The important ranges are running in NNE-SSW direction and include the hills like the Mapithel, the Chingai, the Mulain, etc. The average height of these ranges is about 1,500 m above the m.s.l. The Khayangbung (2833 m), the Shirui (2568 m) and the Kachabung (2498 m) are the important higher peaks belonging to the Eastern Hills. The lowest elevation is represented by the eastern foothill plain region of Moreh area having an altitude of about 180 m above m.s.l.

In general, eastern slope of the Eastern Hills are steeper than the western slopes. The Eastern Hills are principally composed of Disang sediments (mainly shale) and ophiolitic rocks with isolated blocks of Barails as outliers. Major rivers rising from this hill ranges are- Thoubal River, Iril River, Chingai River, Lokchao River, Sekmai Rivers, Maklang River, Tuyungbi River. Most of these rivers fall in Yu and Chindwin rivers.

ii). Western Hills

The Western Hills cover the entire western part of the central valley. They comprise of parallel ranges and few isolated small valleys are found within the hill ranges. Their total length is about 180 km and their wide varies from 50-70 km from north to south. Important ranges include the Yangpujilong, the Daimikilong, the Uningthou, the Koubru, the Khoupum, the Nungba and the Kalanaga. The mount Iso also known as Tenipu (2994 m) is the highest peak of the entire state of Manipur which is located in the north-western part of Mao. Other important peaks of the

Western Hills are Leikot (2831 m), Tampaba (2564 m) and Koubru (2562 m). The hills of this unit trend N-S to NNE-SSW. Among the valleys of the Western Hills, the Khoupum valley is the most important one. The Dzuko valley where the famous Dzuko Lily grows, is located at the foot of Mt. Iso. These hill ranges are principally made up of Barail and Surma sediments of Tertiary age, and are the continuation of the hill ranges in Assam and Nagaland states on the north western side of Manipur. Important rivers originated from these Western Hill include- the Barak River, the Imphal River, the Irang River and the Leimatak River.

3. Peripheral Plain Areas

There are some plain areas in the state beyond the hill ranges. Two important peripheral plain areas are the Jiribam plain area in the west and the Moreh area plain in the east. These plain areas occur where the hill ranges end. Jiribam plain is the extension of the Cachhar plain of lower Assam. The plain area in and around Moreh starts just after the end of the hill ranges of the Eastern Hills and continues further to extend towards the east by the plain of Kabaw valley of Myanmar.

The Jiribam plain is also called the Manipur Western Plain. It is mainly made up of old alluvium. The plains coexist with the low-lying hills made up of Tipam and Surma sediments. The average elevation of Manipur Western Plain may be about 100 m. In some of the areas of this unit, the elevation is as low as 40 m, while the hill peaks have average altitude of about 180 m above mean sea level. In the central portion of the plains area as well as near the stream/river channels, the alluviums are mainly composed of sand, silt and clay; while near the foothills cobbly to pebbly deposits are common.

The Moreh area plain is having an average elevation of about 100 m above the m.s.l. This plain also coexists with low lying hills made up of ultramafics, pelagic shale and exotic sandstones of the ophiolite belt. The hill peaks have an average altitude of about 500 m above the m.s.l. Some area of the plain is covered by thin layer of alluvium. The stream channels are mainly composed of sand, silt, cobble and boulder.

1.7.2 Drainage

Manipur has two important drainage systems, one is the *Imphal river system* and another is the *Barak river system*. The general trend of the drainage in the state (**Fig. 1.7.2.1**) is NNE-SSW although there are oblique to transverse exceptions. The Imphal River and its tributaries which drain in the central part of the state constitute the Imphal river system. The Imphal river system is a part of the Chindwin-Irawaddy river system in the east. In the western part of the state the Barak River and its tributaries make the Barak river system, which finally belongs to the Brahmaputra river system. The eastern ridge line of the Western hill forms the water divide between the Barak and the Imphal river basins.

1. Imphal River System

The central plain area of Imphal valley is mainly drained by the Imphal River and its tributaries. The Imphal River, one of the longest rivers of Manipur, originates from the highlands to the west of Kangpokpi and flows towards the south. In its course in the valley it is joined by many tributaries such as the Sekmai, the Khuga, the Kongba, the Iril, the Thoubal, the Chakpi, etc. Among the tributaries, the Iril and the Thoubal are the most important ones. At Lilong the Iril river joins the Imphal river. The Iril River rises from north-eastern part of Mao and flows southward. The Thoubal river originates from the Huimi hill of Ukhrul and flows south-westward and join the Imphal river at Irong-Chesaba (Near Mayang Imphal). Although Imphal river flows through the Manipur Central Valley, it does not fall into the Loktak Lake, the most depressed part of the valley, rather it flows passing through the eastern part of the lake. A river called the Khordak drains the water of the Loktak to the Imphal river. To the south of the Loktak, the Imphal River is known as the Manipur River. Finally, the Manipur River crosses the southern boundary through narrow gorges called Sugnu hump (possibly structure controlled sandstone predominant riffle like river bed projection at the southern margin of Manipur valley) and enter the Chin hills of Myanmar. In the Chin Hills it is joined by a north flowing river called the Myitha and falls into the Chindwin river of Myanmar.

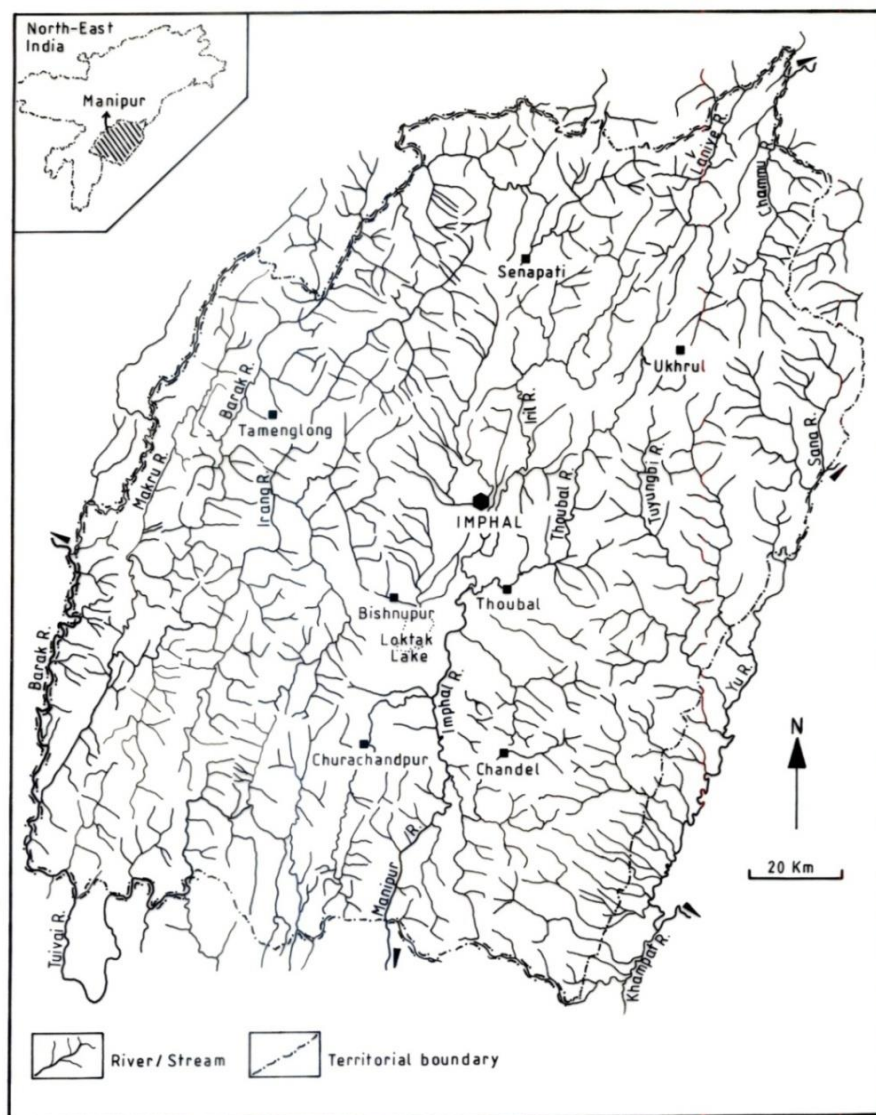


Fig. 1.7.2.1:
Drainage Map of Manipur (after Soibam, 1998).

In the eastern side of the state, a number of small rivers rise from the eastern slope of the Eastern Hills. They also belong to the Chindwin river system. The Chingai and the Chalou drain the northern parts of the Eastern Hills. They flow to the north-east and later on to the south-east to join the Chindwin river. In the south, the Maklang and the Tuyungbi join to form the Yu river in Kabow valley of Myanmar. Further south, the Lokchao and the Taret flow south-eastwards to join the Yu-river. The Yu-river finally falls into the Chindwin river.

2. Barak river system

The Barak River and its tributaries make the Barak river system which is again a part of the Brahmaputra river system. This system lies on the western side of the state and occupies nearly 40% of the total catchment area of the state. The Barak is the largest river system of the state and it rises in the northern highland areas belonging to Senapati area. Near the source, it follows a south-westerly direction. Major tributaries of the Barak river are the Irang, the Tuivai, the Makru, the Jiri, and the Leimatak. Almost all the rivers/streams of the Barak drainage system follow the regional strike (NNE-SSW) occupying antiformal and synformal axes as well as faults and fractures in certain sections. At Karong, the Barak river take a sharp bent towards the north and then flows westward to form a short boundary between Manipur and Nagaland. On its way to the south, it is joined by the Makru and the Irang (two most important tributaries). Further south at Tipaimuk area, the Barak is joined by a north flowing river called the Tuivai. Here, the river runs north and forms the natural boundary between Manipur and Assam. The river is again joined by the Jiri river at Jirimukh. It then flows westward toward Cachhar and Sylhet plain where it is known as the Surma. It finally falls to the mighty Brahmaputra in Bangladesh.

1.7.3 Climate

Manipur state is located entirely in the north of the Tropic of Cancer ($23^{\circ}30'N$) and enjoys a sub-tropical monsoon type of climate. Many factors influence the climate of Manipur. These include elevation, topography, proximity to the Himalaya and the Bay of Bengal. The elevation above sea level varies from 200 m in Barak basin of the south-west to about 3000 m in the northern highlands near Mao. Temperature varies considerably since altitudes are widely variable in different parts of the state. The usual range of temperature is $0^{\circ}C$ to $35^{\circ}C$. But, in some places, like the Jiribam and Moreh areas, the elevations of which are respectively 40 m and 100 m approximately above the mean sea level, reach a maximum temperature of about $40^{\circ}C$. The central valley has an average maximum temperature of about $33^{\circ}C$ and average minimum temperature of about $2^{\circ}C$ though

occasionally the mercury shrinks to 0°C. In higher places like Tamenglong, Tengnoupal, Ukhrul, etc. the mercury sometimes drops below 0°C.

The state is very near to the Himalaya as well as to the Bay of Bengal. So, the climate of the state is influenced by the western disturbances in winter and tropical cyclone in summer. The state has an average annual rainfall of about 1518.36 mm (source ENVIS Hub Manipur, 2017)). However, the annual rainfall is highly variable from place to place depending on the position and altitude of the respective places. Generally, the western half of the state comprising of higher hill ranges has relatively higher rainfall ranging between 2600-3200 mm, because these ranges might have acted as rain barriers of the South West Monsoon. Tamenglong area located at the western higher hill ranges, experiences maximum annual rainfall recording an average value of about 3400 mm, which sometimes far exceeds 4000 mm. The eastern half of the state including the Imphal valley, with the exception of few stations of high altitude, has relatively low rainfall ranging between 1400-1800 mm per year. Possibly these parts of the state become slightly rain shadowed due to the western higher ranges. Humidity in the state is relatively high, the average relative humidity ranging between 90 to 100% during the wet seasons. But the relative humidity in the dry seasons is widely variable which is sometimes as low as 12%.

Base on temperature and rainfall, a year in Manipur is divided into four different seasons. They are

- i). *The Cold season* (December to February called locally as Ningthamtha),
- ii). *The Hot and Dry season* (March to May called locally as Kalentha),
- iii). *The Rainy season/ Monsoon season* (June to September called locally as Nongjutha), and
- iv). *The retreating monsoon season* (October and November called locally as Olangtha).

As November to March is usually dry, even though there may be occasional winter rains. So, this period is the most ideal time for geological field trips in Manipur.

1.8 Objectives of the Present Work

The scope for solution of any problem requires setting of some well-defined objectives. The general objective of the present study is to investigate the detailed petrographical, mineralogical and geochemical studies of the different rock types of the ultramafics of Manipur Ophiolite vis a vis petrogenesis, evolution and chromite mineralization. The objectives are to be materialized through some systematic and rational ways which are known as the methodologies (for solving the challenges in question). For this piece of research work so as to achieve solutions of the challenges, concentrations are made in the following areas, which have been set as desired objectives.

The objectives set for this piece of research work are summarized as follows:

- ❖ *To work out Petrogenetic history and the Physico-chemical conditions responsible for the evolution and Serpentinisation of the Ultramafic rocks.*
- ❖ *To Study the detailed petrography and geochemistry of the Ultramafic rocks of the Manipur Ophiolite Belt to reveal the occurrence of chromites.*
- ❖ *To study bulk rock geochemistry of major oxides (XRF) and trace and REE (ICP-MS) data of the different ophiolitic rocks to decipher processes of chromite mineralization.*
- ❖ *To work out the Geodynamic processes of Chromite Mineralisation in the host Ultramafics.*

1.9 Methodology

To achieve the goal of above objectives through a systematic field investigation and laboratory studies, the following research methodologies are targeted.

1.9.1 Field Studies

- * *Collection of geological and structural data across some selected sections of the Ophiolite Mélange Zone. The field data will be used in establishing the field setting of the different litho units of the MOMZ.*
- * *Collection of representative samples for each of the various rock types of ultramafic rocks and chromites along some selected traverses for studying their petrography, mineralogy and bulk rock geochemistry.*

. 1.9.2 Laboratory Studies

- * *Preparation of representative thin sections for petrographic studies as well as EPMA analysis.*
- * *Carrying out studies pertaining to petrography and mineral chemistry (EPMA data).*
- * *Pulverization of representative samples and analysis for XRF, XRD and ICP (MS).*
- * *Statistical analysis of the variability of the data generated from EPMA, XRF, XRD, ICP-MS, etc. for comparing and identifying the information of both field and laboratory findings with an emphasis to decipher conditions of serpentinisation and chromite mineralization.*

Chapter 2

GEOLOGICAL AND TECTONIC SETTING

The area under investigation of the piece of research work entitled "Petrology and Geochemistry of the Ultramafic Rocks from parts of the Manipur Ophiolite Belt with reference to Chromite Mineralisation", lies within the Nagaland Manipur-Chin Hill Ophiolite (NAMCHO) Belt, which is a part of the westerly arcuate Indo-Myanmar Hill Ranges (IMR). The ophiolite belt exposed within the Indo Myanmar Hill Ranges was part of an ancient oceanic floor created at the time of spreading. Then, the consequent tectonic inversion led to the subduction of the Indian plate beneath the Myanmar micro plate, which ultimately caused the consequent orogenesis of the hill ranges. In due course of the orogenesis of the IMR the Ophiolite Belt was also obducted. Soibam *et al.*, (2015) are of the opinion that the Nagaland-Manipur Ophiolite Belt (NMOB) is the remnants of the ocean floor rocks created on account of slow rifting of continental margin of South East Asia (Myanmar), fragments of which are obducted in due course of tectonic inversion and orogenesis of the Indo-Myanmar Ranges. The present chapter deals with the broad geological set up of the eastern flank of the Indo Myanmar Hill Range and neighbouring regions in which the study area belongs to.

2.1 General geological setting

While considering the history of the geological account of the state of Manipur one has to start from the works carried out by the pioneer workers of the region particularly those who have extensively worked in Assam and adjoining region in connection with exploration of oil and natural gas. Evan (1932) gave most comprehensive stratigraphic succession of Assam province. The stratigraphic succession of Assam was further extended to the adjoining areas including Manipur with the incorporation of data of other workers. Significant pioneering geological works of this region were carried out by Medlicott (1865) and Mallet (1876). Later on, Mathur and Evans (1964) and Bhandari *et al.* (1973) gave the Tertiary

stratigraphy of Assam incorporating all the new data at that time especially from oil exploration in Assam. A generalized stratigraphic succession of the Northeast India in general and that of Assam in particular was also provided by Anonymous (1974). In case of Manipur, it was Soibam (1993, 1998), who first established a complete stratigraphic succession of Manipur by compiling and modifying the available literatures as well as incorporating all new primary geologic data. The stratigraphic succession of the state is given in **table 2.1.1**. Geologically Manipur is made up of the rocks of Tertiary and Cretaceous sediments with minor igneous and metamorphic rocks. The flysch sediments of Tertiary age constitute nearly 65% of the total area of the state (Khuman and Soibam, 2010). The different litho-units in this region are intensely deformed and juxtaposed against each other as an imbricate thrust system having NNE-SSW trend in this part of the IMR, in such a way that the younger ones are on the west while the older ones are on the eastern side (Soibam, 2000; Soibam and Pradipchandra, 2006; Khuman and Soibam, 2010). The general geological and structural map of Manipur is shown in **figure 2.1.1A**

In Manipur as well in other parts of the IMR the oldest groups of rocks are exposed in the easternmost part. This oldest group of rocks is comprised of a metamorphic complex. The Metamorphics exposed on the eastern part of the state is assigned as Naga Metamorphics. This part comprised of intensely thrust group of metasediments, which is predominantly made up of low to medium grade phyllitic schists, hornblende schists, quartzite, quartz-sericite schist, mylonite, etc. The term Naga Metamorphics was first introduced in the geology of Northeast India by Brunnschweiler (1966) and its age was assigned as Pre-Mesozoic age or older. But on the basis of faunal assemblage, other workers assigned its age as Proterozoic (Acharyya *et al.*, 1986; Chungkham and Jafar, 1998). These rocks occur as klippen thrusting westward over the younger Ophiolite Melange Zone.

Manipur Ophiolite Belt, a part of Nagaland-Manipur-Chin Hill Ophiolite (NAMCHO) Belt is bounded in the east by Cenozoic sediments of Central lowland of Myanmar (Mitchell and McKerrow, 1975), on the west by Assam shelf and Mikir Hill Massif, to the north by Eastern Himalayan Syntaxis and on the south by Chin-

Arakan-Yoma-Andaman-Nicobar extended further into the Mentawai Islands of the Sumatra coast (Mitchell and McKerrow, 1975).

The creation of new oceanic crust on account of continued rifting of continental margin and emplacement of fragments of which as a result of tectonic inversion during the subduction of Indian plate beneath the Myanmar micro-plate, make Manipur Ophiolite, an active continental margin ophiolite (Soibam and Khuman, 2008; Soibam *et al*, 2015). This ophiolite belt is found to be associated with different types of rocks in Manipur and found overthrust the Disang-Barail flysch sediments.

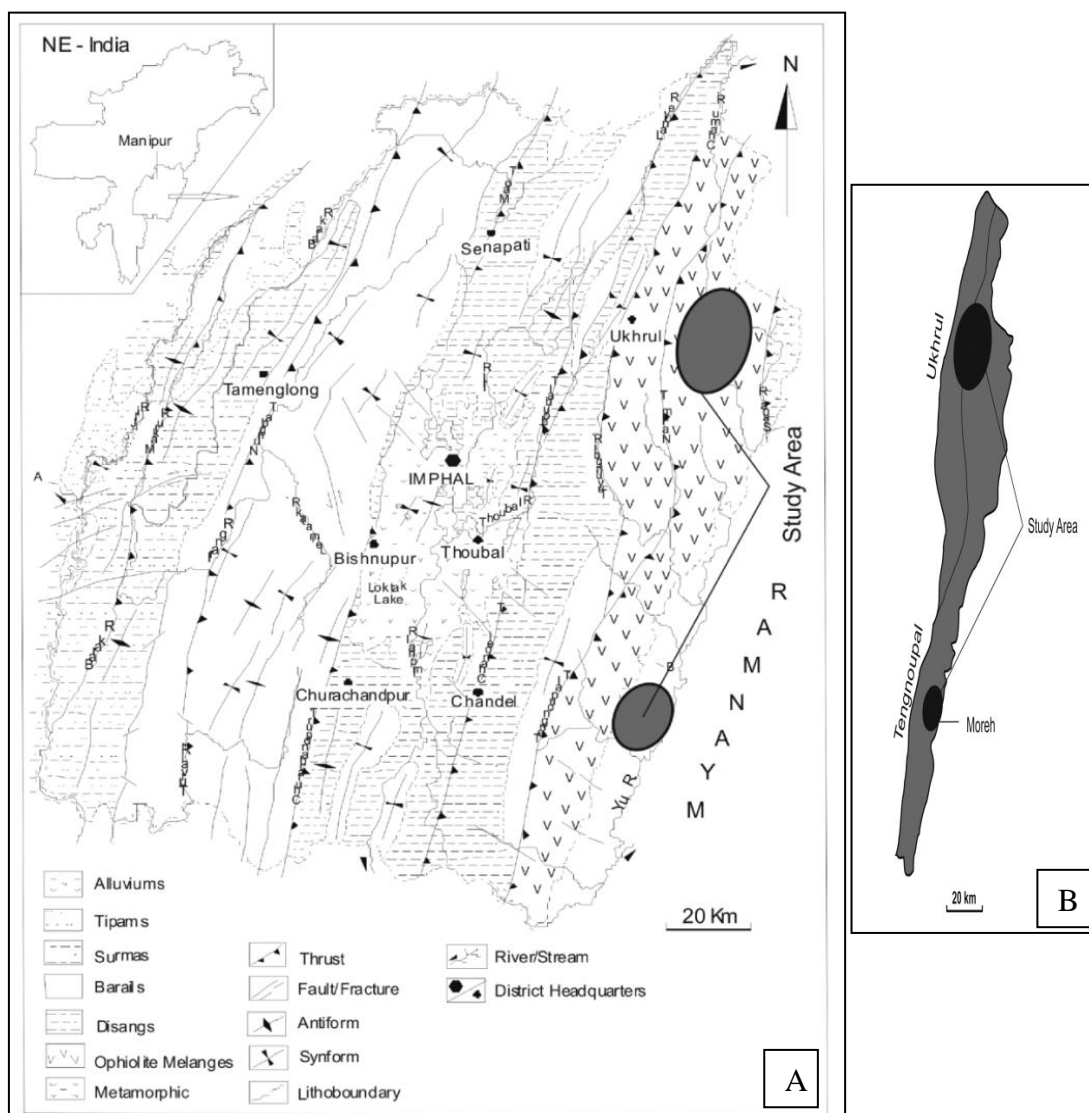


Fig. 2.1.1

A: Geological map of Manipur showing study area (modified after Soibam, 1998).

B: Study area within the ophiolite suite of Manipur Ophiolite Belt.

Table 2.1.1: Generalized stratigraphic succession of Manipur
(after Soibam, 1998 and Khuman, 2009)

Lithounits and age	Description of rocks
Alluviums { Quaternary - Holocene to Pleistocene (?) Older }	Dark grey to black clay, silt and sandy deposits of fluvio-lacustrine origin of the Imphal Valley. Fluvial alluviums in the Barak valley area of Western plains. Clay, sand, gravel, pebble, and boulder deposits of the foothills and old river terraces.
----- Stratigraphic break -----	
Tipams (Miocene)	Mottled clay, mottled sandy clay, sandy shale, clayey shale and sandstone. Greenish to blue, moderate to coarse ferruginous sandstones with sandy shale, clay. Often brown to orange due to weathering. Molasse type of deposits
Surmas (Miocene to Upper Oligocene)	Shale, sandy shale, siltstone, ferruginous sandstone, massive to false-bedded ferruginous sandstones. Alternations of sandstone and shale with more argillaceous horizons in the middle and minor conglomerates. Traditional characters from flysch to molasse sediments.
~~~~~ Unconformity ~~~~~	
Barails (Oligocene to Upper Eocene)	Massive to thickly bedded sandstones. Alternations of shale and sandstone with carbonaceous matters. Intercalation of bedded sandstones with shales. Flysch sediments of turbidite character.
Disangs (Eocene to Upper Cretaceous)	Dark grey to black, splintery shales and intercalation of shales siltstones and sandstones showing occasionally rhythmite character.
~~~~~ Unconformity (partly) ~~~~~	
Ophiolite Melange Zone (Lower Eocene to Upper Cretaceous)	Mostly of ultramafic rocks of harzburgite and lherzolite types with sporadic basic dykes and very thin layer of pillows with associated sediments such as pelagic-chert, shale, limestone, etc.
~~~~~ Unconformity ~~~~~	
Metamorphic Complex (Pre Mesozoic or Older)	Low to medium grade metamorphic rocks of various compositions - phyllitic schist, quartzite, micaceous quartzite, marble and quartz-chlorite-mica schist.
~~~~~ (?)Unconformity ~~~~~	
Basement Complex	Unseen. (?) Early Mesozoic/Palaeozoic rocks or Precambrian rocks.

The Manipur Ophiolite Belt (MOB) which is the southward extension of Ophiolite Belt in Nagaland is about 110 km in length and 2-20 Km in breadth. The MOB is found to have been exposed in the eastern part of the state. The general trends of the narrow strip of the main ophiolitic body (ophiolite suite) is NNE-SSW and occur from the border of Nagaland in the north to Moreh of Tengenoupal district in the south as a continuous strip. The ophiolite belt beyond it continues further south as discontinuous bodies extending upto the Myanmar territory, which could have ultimately reached the Andaman Islands. Ultramafics are the main litho-unit of this main ophiolite body and the ultramafic bodies are always sandwiched in between pelagic shale. More than 90% of the rock exposure of MOB is the ultramafics. The diabasic dykes are also generally found cutting across the ultramafics as well as the pelagic sediments particularly shale. The pillow lavas are generally found as exotic bodies/blocks on the western margins, in most of the cases, beyond the middle strip of shale sandwiched main ultramafic bodies. But, considerably larger pieces of pillows are also found in some of the river beds flowing on the eastern side of the main ophiolitic body indicating similar field setting on both the margins. The hosts of pelagic shale exposed on the western side of the main ophiolitic body, with which other exotic rocks are associated, are found to be intermingled with flysch sediments of Disang and such intermingling nature continues upto the Thoubal Thrust (**Fig. 2.1.1A**). The whole range of the mixture of the rocks, which are the fragments of the oceanic crust and the ocean floor sediments, and found exposed in a horizon where the ultramafic suite is occurred along with the host of pelagic shale intermingled with flysch sediments, with which the exotic rocks (of various dimensions) of diabasic dyke, pillow lava, chert, pelagic limestone, conglomerate, gritty sandstone and other kindred rocks are also associated, make up the Manipur Ophiolite Melange Zone (Khuman, 2009). Thus, the *mélange* zone is much wider than the strip of the main ophiolitic body (**Fig. 2.1.1A**). Exposures termed as exotic bodies are of huge dimensions – as big as hills and the floating nature is not directly observed, whereas the exposures termed as exotic blocks represent comparatively smaller ones usually less than 25 meters or so, in diameter and the floating nature is directly observable. The other less predominant exotic blocks of the *mélange* zone include a kind of rock comprising of calcite and quartz (spilitic carbonatite).

The Manipur Ophiolitic Mélange Zone is found to over thrust the younger flysch sediments known as the Disangs and the Barails (Mathur and Evan, 1964). Disang and Barail sediments occupy the major central part of the state. Mallet in 1876 first introduced the term Disang in the geological literature. The **Disang Group** comprises of monotonous sequence of dark grey to black splintery shales (**Figs. 2.1.2 and 2.1.3**). In most of the places it is intercalated with siltstones and fine to medium grained sandstones of light to brownish grey, occasionally giving rise to rhythmite character specially in the upper horizon. The sandstones sometimes form bands/lenses of few meters thick. Structurally the Disang sediments are intensely deformed. On the regional scale they are folded into antiforms and synforms running in NNE-SSW direction. Thrusting and reverse faulting of similar trend are also common. A number of joint sets and fractures characterize these rocks, some of which specially the E-W trending ones have secondary silicification. At many places, the Disang shales show incipient metamorphism displaying slaty cleavage. But in the northern part of the state, particularly in and around Jessami area, almost all of the shales are metamorphosed into slate considerably. The Disangs are divided into two units viz. Lower Disang and Upper Disang on the basis of degree of compaction. The Lower Disang is made up of Shale intercalated with thin flaggy sandstone (**Fig. 2.1.4**) and contains Cretaceous fauna while the Upper Disang has proportionately greater volume of sandstone and contains trace fossils (**Fig. 2.1.5**). The fossil content indicates Maestrichtian age. The Disang Group ranges in age from upper Cretaceous to upper Eocene (Pascoe, 1912). The Lower Disang Group is made up of dark grey shale, slate and phyllite interbedded with siltstone, mudstone and sandstone (Rang Rao, 1983). This can be seen in the eastern side of Manipur and mostly of argillaceous in nature. The gradual increase in thickness of sandstone marks the Barail-Upper Disang contact. The contact between the sediment of Disang and those of younger Barail run more or less parallel to the western margin of the central valley (Imphal Valley). They usually show gradational contact. At some locations, these contacts are marked by high angle reverse fault (Soibam, 1998).



Fig. 2.1.2:
Normal fault on Disang shale.



Fig. 2.1.3:
Disang rocks showing turbidite Character.



Fig. 2.1.4:
Disang shale intercalated with
thin flaggy sandstone.



Fig. 2.1.5:
Trace fossil in Disang shale.

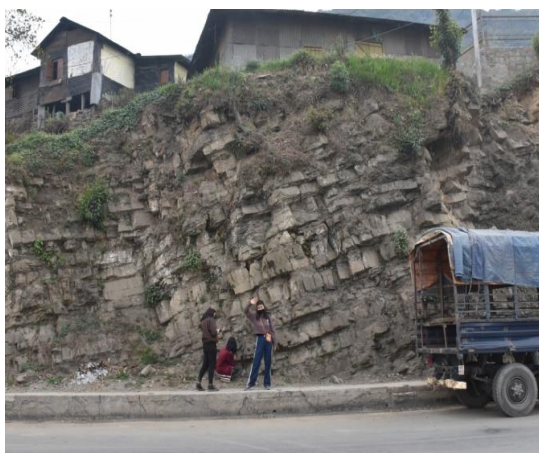


Fig. 2.1.6:
Barail sandstone showing
typical turbidite character.



Fig. 2.1.7:
Thickly bedded Barail sandstone
intercalated with thin layer of shale.



Fig. 2.1.8:
Exposure of Surma Group of rocks.



Fig. 2.1.9:
Exposure of Tipam sandstone.



Fig. 2.1.10:
Conglomerate horizon in between
Namshang Fm and Tipam Groups of rocks.

Barail Group was first introduced by Evans (1932) to describe a thick column of arenaceous beds interbedded with shales overlying the Disang Group. They are characterized by light grey to brown; fine to medium grained sandstones with minor to considerably thick interbeds of shale (**Figs. 2.1.6 and 2.1.7**). The name was adopted from a hill range known as Barail Range, which forms the backbone of the North Cachhar Hills and extending up to the north western part of Manipur. Sandstone of Barail groups is comparatively thicker than that of Disang group. Barail sediments are found on the western half of the state (**Fig. 2.1.1A**). The Barail Group of rocks are conformably underlined by Disang, which comprises of light to brownish grey, fine to medium grained thick sandstones often interbedded with brown to dark grey shales. They are also found occurring as outliers forming capping in the western part of the state. The Barails like the Disangs are deformed into regionally extended folds and faults, which follow N-S to NE-SW trend. The sandstone is intercalated with shale displaying typical turbidite character (**Fig. 2.1.6**). The Barails range in age from Upper Eocene to Oligocene (Evans, 1932; Anon, 1974). It has been reported that sediments of the Disang and Barail Groups contain ichno-assemblage represents the record of classical Skolithos and/or Cruziana ichnofacies, being characteristic of a shallow-marine environment, with occasional high energy conditions (Hemanta Singh *et al.*, 2008). The Disang-Barail flysch sediments are unconformably overlain by the younger molassic sediments characterised as the Surma Group and Tipam Group.

Surma Group unconformably overlies the Barail Group. The term was first introduced by Evans (1932) adopting the name from the type area of Surma valley, where it is best exposed. The Surma Group occupies the western part of the state (**Fig. 2.1.1A**). The Surmas comprise of a thick sequence of shale, sandy shale, mudstone, slaty sandstone, sandstone and a thin layer of conglomerate. The presence of conglomerate layer above the Barails Group, indicate an unconformity. The rocks of Surma Group are mainly grey to brownish grey in colour. When fresh they are usually light grey, and brown to yellowish brown when weathered. They are generally medium to coarse grained sandstones having occasional shale and silt/shale intercalation between massive to thickly bedded sandstone (**Fig. 2.1.8**). In

Some places turbidite like bedding characters are found. Primary structures such as cross bedding, ripple marks etc. are associated with Surma Group (Soibam, 1998).

The same features are also found in Barail Group. The rocks of Surma Group are also well characterized by folds and faults having regional trend similar to that of the Barails. This group of sediments is treated as of molassic nature. The sediments of the Surma Groups have been assigned Miocene age (Anon, 1974); and might have extended up to the uppermost part of Oligocene.

Earlier literatures claim that **Tipam Group** overlies the Surma group without any stratigraphic break. But while geological mapping along Dimapur-Kohima and Marapani-Wokha sections in Nagaland by a team of Department of Geology, Nagaland University led by Dr. Chabungbam Mangi Khuman it has been observed very recently that there is an unconformity between Namshang formation and Tipam Group. A photograph indicating a conglomerate horizon between these two molasses Groups is shown (**Fig. 2.1.10**). The term Tipam Group was first used by Mallet (1876) after Tipam Hill between Dihing River and Digboi in upper Assam, for a group of sediments which is moderately coarse grained ferruginous, massive, sometimes false bedded sandstones. Minor intercalation of fine sandstone-silt-mud can also be seen at places. There is a sudden change in the litho- characters one approach from the Surmas to the Tipams. The Group is well known over a vast area in northeast India, but better developed in Tripura, which is also a part of the Surma valley. In Manipur, Tipams do not occur over a large area. They usually occur as outliers on the western part of the state particularly in and around Jiribam area. The Tipam sandstones (**Fig. 2.1.9**) are often marked by partings of shales. At places, fossil wood is found and thin lignite bands are quite common. The rocks of the Tipam Group are also commonly folded and faulted. As in case of the Surmas, in Tipams also, river valleys usually follow synformal axes while antiformal axes roughly coincide with the ridges. These are quite different from the folds present in the Disangs and Barails where antiformal axes correspond to valleys and synforms to ridges. And, such topographic and drainage relationship might have been related to the evolution stages of the Indo-Myanmar Ranges as contended by Soibam and Pradipchandra, 2006. The age of Tipam sediments have been assigned Miocene

(Anon, 1974). In Manipur Alluvium deposit overlies the Tipam Group. But it is found in some parts of Assam. It is probably after the deposition of the Tipams, uplift of the region might have been above the depositional level by the end of Miocene or early Pliocene. Since then, erosion and denudation started in the region. Therefore, post Tipam period is represented only by a sequence of alluviums in the state.

Alluvium Deposits overlie the Tipam Group. It is because of the upliftment of the region above the depositional level after the deposition of Tipam. The major depositions of alluviums take place in the Imphal valley, which is likely to have been formed since Pleistocene times. The alluvium deposits of Manipur can be grouped into two – the Old Alluvium and the New Alluvium. The older Alluvium is found mainly in Barak valley of newly created Jiribam district, whereas the new alluvium occurs in the Imphal valley (central plain). According to Soibam, 1998, the higher part of Imphal valley is mainly composed of cobbles and boulders with considerable amount of clay, silt and sand and the lower part of Imphal valley, must have possibly comprised of the Older Alluvium. The Manipur valley (Imphal valley) has a column of alluviums of fluvio-lacustrine origin. It may have a thickness of about 150 to 350 m although, variable at places (Soibam, 1998; Soibam and Hemanta Singh, 2007). These are principally dark grey to black clay, silt and sand deposits. They are rich in carbonaceous matter characterizing swampy or marshy deposits. In Imphal valley, the Newer Alluviums are mainly found as recent alluvium deposits of streams and rivers.

2.2 General tectonic setting

The structural and tectonic pattern of Manipur is transitional between the NE-SW trend of Naga-Patkoi Hills in the north and northeast, and N-S trend of Mizoram and Chin Hills in the south and southwest. The general structural and lithological trend of the rock formations of the state is NNE-SSW (N15°E-S15°W). It frequently varies between N-S and NE-SW, although sometimes NNW-SSE trends are locally common. Almost all the major structural elements such as folds,

thrust and reverse faults follow this regional strike signifying the general tectonic extension direction. Majority of the extensional structures e.g., normal faults, tensile fractures have WNW-ESE (N75°WS75°E) trend indicating nearly E-W regional/tectonic compression. While the structures having neither compressional nor extensional affinities strike in the NW-SE and NE-SW quadrants. Dip of the litho-units varies between moderate to steep angles towards east or west. The geological and structural features suggest a typical deformation and tectonic evolutionary mechanism of the region. Analysis of plate kinematics in and around Manipur reveals that the structural and tectonic features of the IMR in general and that of Manipur Hills in particular have been evolved as a result of interaction between the Indian and Myanmar plates rather than Indian and Eurasian plates, and Myanmar (Burma) and Eurasian (China) plates (Soibam, 2006). Computation of plate motions by Soibam using rotation vectors given by various workers (e.g. De Mets *et al.*, 1990; Minster and Jordan, 1978; Curray *et al.*, 1978) and nature of plate interaction in and around Manipur are shown in **table 2.2.1**. From the analysis it is observed that relative motion of Indian plate with respect to

Table 2.2.1: Plate motion at various points in and around Manipur
(after Soibam, 2006)

Plate pairs	24°N, 93°E	22°N, 93°E	25°N, 94.5°E	26°N, 94°E
${}^E V_I$	5.45cm.yr ⁻¹ N17.7°E	5.47cm.yr ⁻¹ N18.6°E	5.49cm.yr ⁻¹ N17.9°E	5.46cm.yr ⁻¹ N17.3°E
${}^E V_M$	3.50cm.yr ⁻¹ N9°W	3.54cm.yr ⁻¹ N12.1°W	3.34cm.yr ⁻¹ N6.3°W	3.36cm.yr ⁻¹ N
${}_M V_I$	2.71cm.yr ⁻¹ N50°E	2.92cm.yr ⁻¹ N53°E	2.75cm.yr ⁻¹ N46°E	2.59cm.yr ⁻¹ N44°E

Note: I - India, E - Eurasia, M – Myanmar

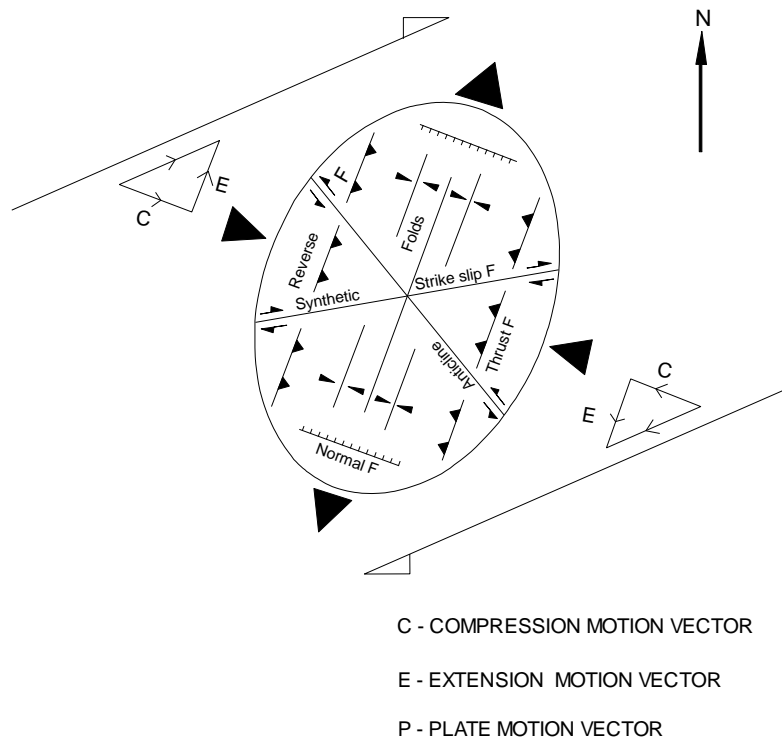


Fig. 2.2.1:
Dextral Shear Deformation mechanism of the IMR (after Soibam, 2006)

Eurasian plate (EV_I) is almost parallel to NNE, the tectonic strike of the region and therefore, such a motion cannot produce compression structures parallel to its motion. Similarly, the Myanmar plate motion relative to the China (Eurasian) plate (EV_M) is towards North making little different from the regional strike and so, may not be responsible for the evolution of structural and tectonic features of the state and its adjoining region. Thus, relative motion of Indian plate with respect to Myanmar plate (MV_I), which moves towards NE, induces a dextral shear couple deformation mechanism of the region lying between the two plates producing the tectonic features of the state. In the process, the rocks of the region have been compressed in the WNW-ESE (E-W) and extended in the NNE-SSW (N-S) directions (**Fig. 2.2.1**). And such a deformation mechanism is virtually related to the oblique subduction of then Indian plate below the Myanmar plate.

2.3 Ophiolite Melange Zone of Manipur

The Ophiolite Melange Zone is an elongated assemblage, mostly of igneous and sedimentary rocks, which form a mappable litho-unit but not a stratigraphic unit. In the field, the Ophiolite Melange Zone of Manipur comprises the following three important units.

The Ophiolite Suite – This unit of Ophiolite Melange Zone is made of mostly ultramafics having sporadic dibasic dykes cutting across them and constitute strip of the main ophiolite body. The ultramafics are found having been sandwiched with pelagic shale.

The Oceanic Pelagic Sediments (OPS) – These are mainly composed of shale, thick sequence of chert, variegated clay, limestone and diabasic dykes/sills in shale and chert. These sediments are usually intermingled with Disang and Barail sediments.

The Exotic Rocks – A number of exotic rocks/blocks of various rock types are found float over and/or intermingle with the hosts of ultramafics and pelagic shales in the ophiolite mélange zone, particularly at the outer margins. They include diabasic dyke, pillow lava, conglomerate, chert, limestone, gritty sandstone (mélange sandstone) and rocks kindred with lava extrusion. These exotic rocks/bodies have different sizes and dimensions.

2.3.1 The Ophiolite Suite

The ophiolite suite of Manipur is about 110 km long and 2 – 20 km in breadth. The main ophiolite suite is mainly composed of Peridotitic Ultramafics. Harzburgite and Lherzolite (Chapter 3) are the two important types of the peridotite of Manipur ophiolite with occurrence of some blocks of podiform chromite. There are two physically distinct ophiolitic peridotites found within the strip of the main ophiolitic body of the Manipur Ophiolite Mélange Zone (Khuman and Soibam, 2010).



Fig. 2.3.1.1:
Highly serpentinised ultramafics exposed
near Lunghar, Ukhrul Dist.

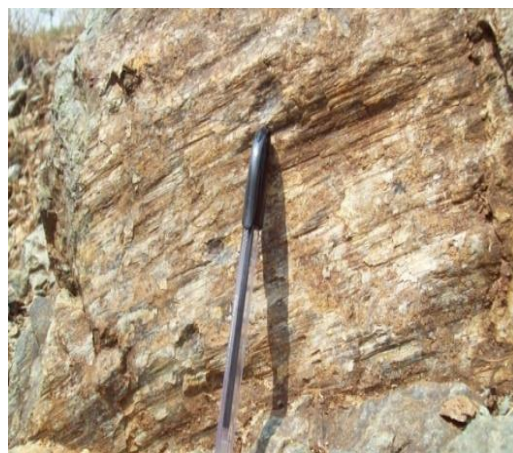


Fig. 2.3.1.2:
Slickenside in serpentinised Ultra-
mafics near Khudengthabi.



Fig. 2.3.1.3:
Fresh ultramafics exposure near
Lokchao river.



Fig. 2.3.1.4:
Rodingite exposure at
Kwatha, Tengnoupal District



Fig. 2.3.1.5:
Exposure of hard and compact Ultramafics
boulders on the ridge of Sirui Hill.



Fig. 2.3.1.6:
Less serpentinised ultramafics
exposed near Khudengthabi.



Fig. 2.3.1.7:
Massive ultramafic blocks near
Lunghar (Ukhrul District)

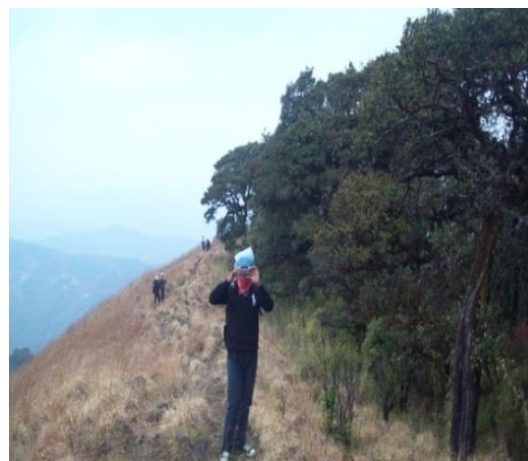


Fig. 2.3.1.8:
Exposure of dyke intruded into the ultra-
mafics exposed on the top of Sirui Hill,
Ukhrul District.



Fig. 2.3.1.9: Contact between
ultramafics and shales.



Fig. 2.3.1.10: Litho contact between
chert and ultramafics.

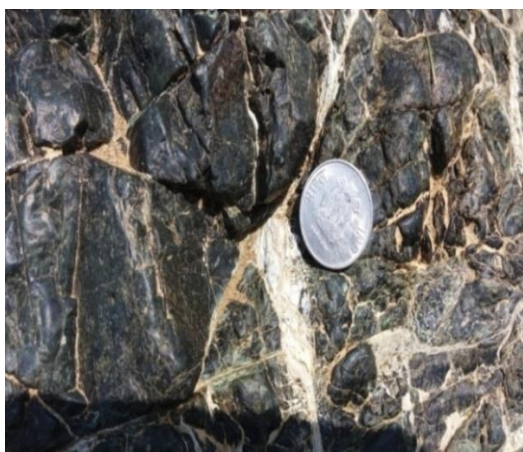


Fig. 2.3.1.11:
Fibrous serpentine in host Ultramafics
near Lokchao River, Moreh.



Fig. 2.3.1.12:
Quartz veinlets in ultramafics.



Fig. 2.3.1.13:
Chromite (massive) in closed view,
Kwatha, Tengenoupal District.



Fig. 2.3.1.14:
Chromite blocks, Kwatha,
Tengenoupal District.



Fig. 2.3.1.15:
Chromite exposure, Holenphai,
Tengenoupal District



Fig. 2.3.1.16:
Chromite along with host-Rock
ultramafics, Holenphai.



Fig. 2.3.1.17:
Chromite exposure (with spotted & nodular mass), Phangrei, Ukhul District



Fig. 2.3.1.18:
Chromite, Gamnom, Ukhul District



Fig. 2.3.1.19:
Host rock of chromite at Phangrei showing rugged surface, Ukhul District

One type is almost wholly serpentinised (degree of serpentinization ~ 90%) with very intense shearing along closely spaced fractures with slickensides (**Figs. 2.3.1.1 and 2.3.1.2**) which sometimes resemble serpentine schist (**Fig. 2.3.1.3**). Veins and lenses of rodingite (a leucocratic rock) are present in serpentinised ultramafics (**Fig. 2.3.1.4**). The other type is comparatively fresh and least serpentinised (degree of serpentinisation ~ 60%) and is found occurred as blocks embedded within the earlier type, which are generally found protruding above the exposed surface of extensively serpentinised ultramafics (**Figs. 2.3.1.5, 2.3.1.6 and 2.3.1.7**). More than 90% of the total exposure of Manipur ophiolite is the ultramafic rocks. They are found to have sporadic basaltic dykes (**Fig. 2.3.1.8**).

In the field, peridotitic ultramafics are juxtaposed against the pelagic sediments. In the Lokchao- Moreh section, a good exposure of juxtaposition of ultramafic against pelagic sediment (**Fig. 2.3.1.9**) is observed. Such kinds of exposures are common everywhere in the ophiolite belt in Manipur. Ophiolitic ultramafics are also observed juxtapose against radiolarian chert indicating a thrust contact (**Fig. 2.3.1.10**).

Along the western margin of the strip of the main ophiolitic body of Manipur Ophiolite Mélange Zone particularly in the northern sector where the ophiolitic body is thicker, schistose talc crystals are well developed. In the hand specimen the curvilinear columnar aggregate of acicular crystals of talc is almost black and shows shining appearance in reflected light. A wide horizon of talc schist in the host of extensively serpentinised ultramafic body has also been developed in the western margin of the main ophiolitic body of the Manipur Ophiolite Mélange Zone (Khuman, 2009). Fibrous serpentine minerals are well developed in the serpentinised ultramafics (**Fig. 2.3.1.11**). Besides, in the Lokchao river bed, the development of anastomosing quartz vein-lets are clearly seen in the ultramafics (**Fig. 2.3.1.12**).

In the field setting, normally two types of basaltic dyke rocks are found cutting across either the ultramafics or the pelagic sediments (mostly in shale); these dyke rocks are also found as exotic blocks. Similar basaltic rocks are also found as sills in pelagic chert. The dykes intruded into the ultramafics as well as the sills

within pelagic chert comprise of fine to medium grained earlier formed pyroxenes and olivine, and later formed larger grains of plagioclase and uralitised clinopyroxene. On the other hand the dykes in the pelagic shale, although have the same basaltic composition, the later formed clinopyroxene grains are serpentinised instead of uralitisation as in case of the dykes of the ultramafics (Soibam and Khuman, 2011). The dyke rocks, which have suffered incipient thermal metamorphism, are of alkali basalt lineage.

There are a number of sporadic pockets of massive chromite bodies in the host of the serpentinised ultramafic rocks. The chromites, because of the association with ophiolitic rocks, are considered as podiform type. The massive chromitite is the most abundant while the nodular type is the least in the study area. They are generally found in the form of broken blocks, lenses and pods. The chromites generally occur as floating masses. It is possible that many other hidden blocks are embedded within the host rock beneath the surface.

The chromite is found to occur in a number of localities in Manipur. Mention can be made about the occurrences in Kwatha (**Figs. 2.3.1.13 and 2.3.1.14**), Holenphai and Moreh town areas (**Figs. 2.3.1.15 and 2.3.1.16**) in Tengnoupal District; Phangrei (**Fig. 2.3.1.17**) and Gamnom villages (**Fig. 2.3.1.18**) of Ukhrul and Kamjong Districts. In many of these localities chromites are occurred as floating blocks. The blocks generally range in size from small ones - tens of centimetres in length, breadth and thickness to large ones – with one-two meter long dimensions in space. The chromites of Phangrei village area are extensively quarried and dug out thereby resulting to a rugged topography having a number of ponds (**Fig. 2.3.1.19**). Pod shaped small chromite inclusions are also found in the host of serpentinised peridotitic ultramafics.

2.3.2 The Oceanic Pelagic Sediments

Pelagic sediments are the fine-grained sediments that accumulate as a result of the settling of particle to the floor of the ocean, far from the land. The pelagic sediment of Manipur Ophiolite Melange Zone is a thick sequence comprising of

shale, chert, variegated clay and limestone. Among them shale is the most predominant pelagic sediment and is found either sandwiched with the ultramafics or as a host of tectonically transported exotic rocks generally on both the sides of the Ophiolite Suite. The pelagic shale is different from the Disang flysch sediments. They are found to consist of numbers of alternating comparatively fresh cherty horizon. The pelagic shale including the cherty horizon, when unaltered is dark grey in colour (Khuman, 2009). The colour of the typical soil derived from pelagic shale is generally brownish grey in colour (**Fig. 2.3.2.1**) while that of a typical soil in ophiolite terrain derived from the ultramafics is reddish dark in colour (**Fig. 2.3.2.2**). But when weathered the colour of the pelagic sediments becomes dirty white characterizing this type of shale and differing largely from the light reddish brown earthy coloured weathering product of the Disangs shale. Number of basaltic rocks are also found to intrude within the pelagic shale as concordant thin layers as sills. A number of dykes also cut across this type of pelagic sediment. The host of the pelagic shale with which other exotic rocks are associated intermingle with flysch sediments of the Disang and Barail.



Fig. 2.3.2.1:
Soil developed from pelagic shale.



Fig. 2.3.2.2:
Typical soil and grass derived from the ultramafics.

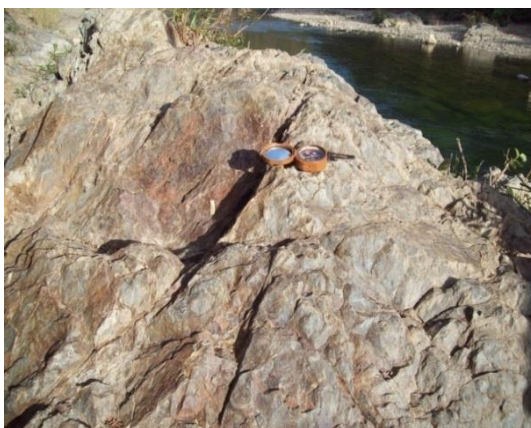


Fig. 2.3.2.3:
Exposure of chert in Lokchao river bank,
Moreh, Tengenupal District.



Fig. 2.3.2.4:
Exposure of Limestone in Ukhrul District.



Fig. 2.3.2.5:
Limestone cavern at Kangkhui Village, Ukhrul District.

The **Chert** is the second most predominant pelagic sediment. In the Manipur Ophiolite Melange Zone, variegated colour of chert viz red, green, brown, white and black are found (**Fig. 2.3.2.3**). The cherts consist of crypto-crystalline to finely crystalline silica and found to have fossil assemblages of radiolarians and coccolithoporids. There is thick igneous intrusion in the form of sill within cherty sediment as observed on the eastern margin of the Mélange Zone. Based on the field evidence of extrusion of the pillow lavas within or over pelagic chert and the observed relationship with other kindred sediments and from the fact of formation of chert at the deepest part of the basin below the CCD, it is inferred that radiolarian chert is lowermost horizon of the pelagic sediments (Khuman, 2009).

The **Limestone** is the least predominant pelagic sediment of the ophiolite belt (**Figs. 2.3.2.4 and 2.3.2.5**). The important localities where limestones occur are Lambui, Hundung, Kangkhui of Ukhrul district and Khudengthabi, Pallel, Nepali basti, Narum of Tengnoupal district. They are found as bedded to massive with varying colours such as white, grey, reddish brown, etc. Fossil assemblages of foraminifera are abundantly preserved in the limestone. The absence of igneous intrusion within the limestone indicates that this pelagic limestone were formed in the upper part of the ocean basin most probably after the formation of a thicker pile of pelagic shale (Khuman, 2009). Oceanic pelagic sediment containing late Mesozoic fossils constrain the age of the Manipur ophiolite rocks units (Tapan pal *et al.*, 2014).

2.3.3 The Exotics Rocks/Bodies

In addition to the Ophiolite Suite, Pelagic sediments, the ophiolite Melange Zone of Manipur comprises a number of blocks/bodies of exotic rocks. They occur within the host of shale or in some cases in the host of ultramafics. Their size and dimension vary from few meters to small hillocks. Khuman, 2009 termed bigger ones-larger than 25 m diameter as exotic bodies while the smaller ones-lesser than 25 m as exotic blocks. The exotic rocks include bodies of gritty sand (**Figs. 2.3.3.1**) of varying hardness and compactness, blocks (< 25 m diameter) mostly of conglomerate (**Fig. 2.3.3.2**), radiolarian chert, pelagic limestone (**Figs. 2.3.2.4 and 2.3.2.5**), fine to medium grained basic volcanic rocks, pillow lavas (**Figs. 2.3.3.3 - 2.3.3.6**).



Fig. 2.3.3.1:
Exposure of exotic sandstone near KondongLairembi,Moreh.



Fig. 2.3.3.2:
Conglomerate exposure in the form of
small hillock near Pushing village,
Ukhrul District.



Fig. 2.3.3.3:
Pillow lava found near
Ukhrul town.



Fig. 2.3.3.4:
Pillow lava at Khudengthabi,
Tengnoupal District.



Fig. 2.3.3.5:
Pillow lava at Kwatha-Lamkhai,
Tengnoupal District.



Fig. 2.3.3.6:
Pillow lava hill near Ukhurul town.



Fig. 2.3.3.7:
Chert boulder in the Lokchao River Bed,
near Moreh, Tengenupal District.



Fig. 2.3.3.8:
Quartz veins in sandstone.



Fig. 2.3.3.9:
Calcite veins in medium grain
exotic rocks.

The floating blocks of gritty sand over the Ultramafics are well observed near Kondong-Lairembi of Moreh area (**Fig. 2.3.3.1**). A numbers of chert blocks are also found floating over the ultramafics in the Lokchao river bed near Indo-Myanmar border bridge (**Fig. 2.3.3.7**). Conglomerate blocks as big as the size of a hillock are found on the western and eastern margins of the Melange Zone but generally beyond the main ophiolitic body (**Fig. 2.3.3.2**). The exotic blocks of conglomerate have variable size of clasts, some of which are very fine grained but generally are of the size of pebbles; but there are exposures, the clasts of which are as big as cobbles. The clasts are principally comprised of chert, sand and limestone. Blocks of pillow lavas of varying sizes are observed mostly on the western margin of the Mélange Zone. (**Figs. 2.3.3.3 - 2.3.3.6**). The gritty sandstone occurring in the eastern margin (near Holenphai village) is found to have primary structures like cross bedding and graded bedding, etc. indicating shallow depositional environment. Multiple quartz veins are developed in sandstones of Holenphai area (**Fig. 2.3.3.8**) which could have been related to thrusting activities. But two kinds of gritty sandstone could be explored in the western margin.

A kind of rock comprising mainly of quartz and calcite (**Fig. 2.3.3.9**), is the one more interesting exotic block found in the Manipur Ophiolite Belt. Formation of such a rock known as spilitic carbonatite could be related to the extrusion of basaltic melt at the vicinity of the spreading centre, which has interacted with percolating hot brine under spilitic metamorphic conditions at depths less than 3km in the oceanic crust (Khuman, 2009). Such type of rock is found mostly in Ukhrul district.

It is observed that when traverses are made across the Ophiolite Mélange Zone either from the east or from the west, in most of the cases the exposures of the mixture of conglomerate, gritty sandstone, dyke rocks in the host of pelagic shale and occasionally in association with some of the other blocks of the Mélange Zone like chert and limestone are encountered and then comes the exposure of the shale sandwiched ultramafic rocks (ophiolite suite), after which the exotic rocks floated exposure is repeated again in the periphery.

Chapter 3

ULTRAMAFIC ROCKS

Ultramafic rocks of the ophiolites have received considerable attention within the geological community in recent years because they provide excellent opportunities to gain insight into the inaccessible realm of the mantle rocks. Most of the ultramafic rocks are formed at the time of differentiation of the earth and occupy in the mantle horizon, part of which could be brought in the sub-surface environment on account of diapiric upflow where there is lithospheric spreading or may be formed because of crystallization of basaltic magma produced by partial melting of the upper mantle rocks in due course of diapirism, and thus study of such kind of ultramafics facilitate in the understanding of the details of fractionation, origin, tectonic history, and other petrological processes (Raymond, 2002). The term ultramafic and ultrabasic relates, respectively, mineralogical and chemical classification of rocks, but both have been used rather loosely.

In Manipur Ophiolite Belt, ultramafic rocks of potential mantle origin occur as emplaced massifs. In the study area of this piece of research work, there are two physically distinct serpentinised ultramafic peridotites (Khuman and Soibam, 2010). One type is almost wholly serpentinised with very intense shearing along closely spaced fractures which sometimes resembles serpentine schist (**Fig. 2.3.1.1**). The other type which is less predominant is comparatively fresh and less serpentinised. They are found occurring as blocks embedded within the earlier type, which are generally found protruding over the exposed surface of peridotitic serpentinites of the Ophiolite Complex (**Figs. 2.3.1.6 and 2.3.1.7**). Highly serpentinised variety generally shows olive green colour while the other type of less serpentinised variety is of dark green to greenish black colour. Phenocrysts of brownish colours are predominantly present in the hand specimen of this type of melanocratic rock. These large crystals show shining appearance in reflected light. These grains are found to be serpentinised pyroxene grains (bastites) when examined in the microscope.

The main concern of this present chapter is to identify, characterize and classify the ultramafic rocks of the Ophiolite Belt of Manipur so as to make a clear picture about their petrogenesis and other aspects related to their evolution through time and space. To achieve the above goal the study of petrography, mineralogy and geochemistry are carried out as follows.

3.1 Petrography and Mineralogy

In Manipur Ophiolite Belt, most of the ultramafic rocks are intensely serpentinised. Not all samples preserve the relics of original protoliths of the different phases. The ultramafic rock (serpentinite) samples of Manipur Ophiolite Belt are essentially comprised of serpentines derived from olivine (**Figs. 3.1.1, 3.1.3 and 3.1.5**), bastites, pseudomorphs of serpentine after pyroxenes showing bronze like metallic luster or schiller, relics of olivine, and primary (**Fig. 3.1.2A**) and secondary (**Fig. 3.1.8**) spinels. These rocks are serpentinised up to 60% to 93% (Khuman and Soibam, 2010). The rocks generally show xenoblastic granular texture and the grain size is quite variable. All the original boundaries of the grains have been corroded, most probably on account of partial melting and hence it is difficult to establish original grain boundaries (**Figs. 3.1.1, 3.1.4 and 3.1.5**) and therefore all the samples of ultramafic rocks whose petrography is carried out are found to have xenoblastic texture. The term xenoblastic is used because the ultramafic rocks are pigeonholed in the field of metamorphic peridotites in most of the geochemical plots (**Figs. 3.1.1.1, 3.2.2.1, 3.3.1.2 and 3.3.1.3**). In most of the samples, the segregation of olivine, orthopyroxene (**Fig. 3.1.3**), clinopyroxene (**Fig. 3.1.4**) and spinels (**Figs. 3.1.2A and 3.1.2B**) is observed. The olivine grains present in many samples are almost completely serpentinised without any indication of orientation (**Fig. 3.1.5**). Whereas the orthopyroxene, clinopyroxene and primary spinels show elongation and alignment (**Figs. 3.1.3, 3.1.4, 3.1.6 and 3.1.2A**). But it is difficult to establish whether these features are related either with primary compositional layering or with metamorphic foliation/diapirism prior to serpentinization or on account of serpentinization because the end product of extreme tectonism and serpentinization is nearly total destruction of the original mineralogy and structures within the parent peridotitic rocks (Khuman, 2009).

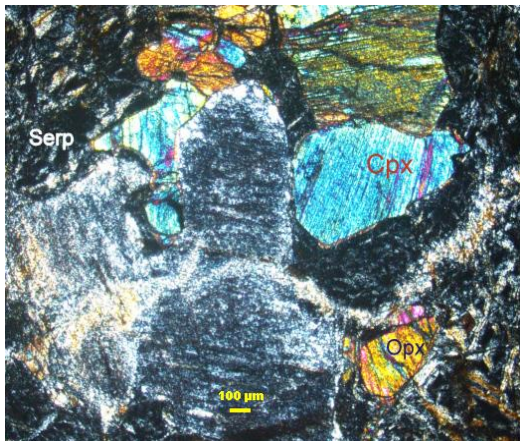


Fig. 3.1.1:
Presence of Opx, Cpx and Serpentine grains in ultramafic (cross polar).

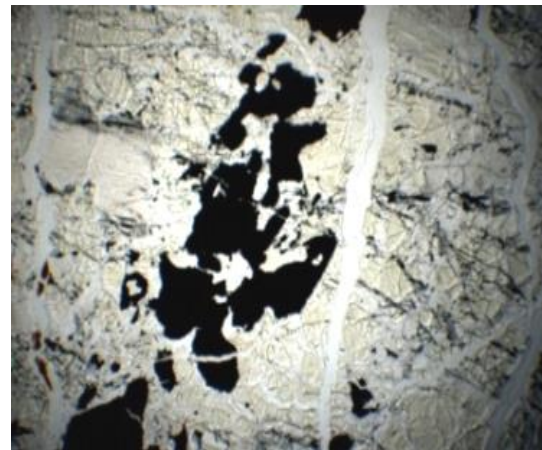


Fig. 3.1.2A:
Primary spinel showing segregation and alignment in ultramafic (width of photo is 4mm) (polarized light).

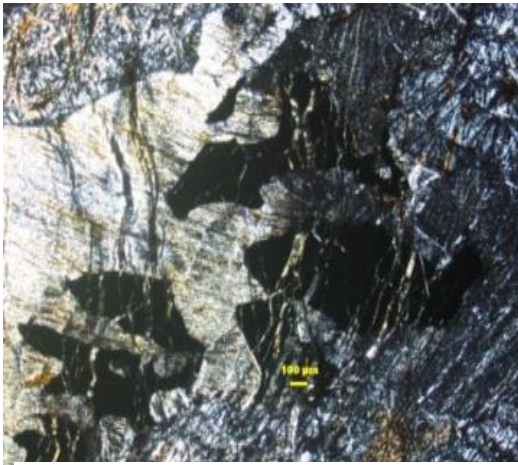


Fig. 3.1.2B:
Fractures developed in primary spinel (cross polar).

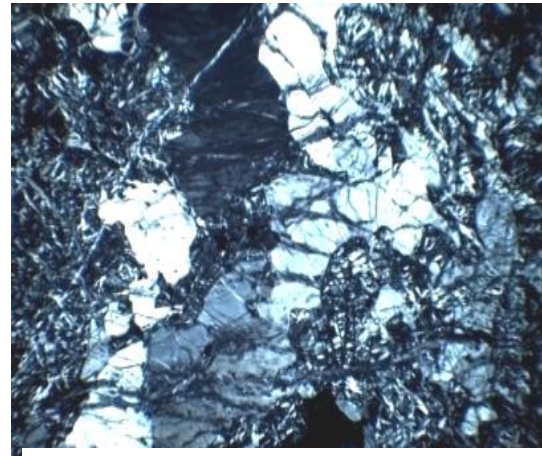


Fig. 3.1.3:
Orthopyroxene grain showing segregation and alignment in ultramafics (width of photo is 4mm) (cross polar).

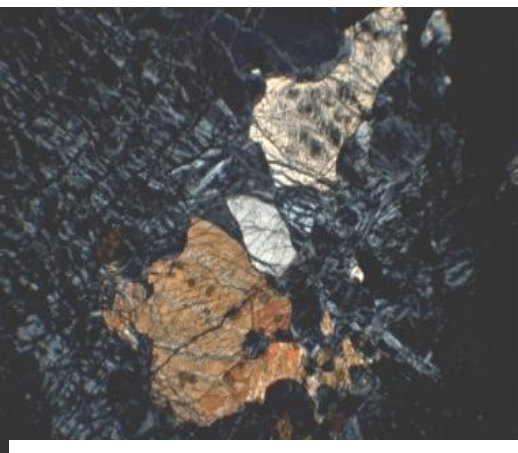


Fig. 3.1.4:
Clinopyroxene grain showing aggregation and alignment in ultramafics (width of photo is 4mm) (cross polar).

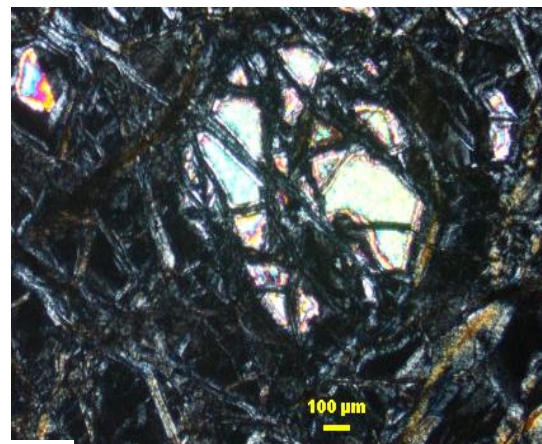


Fig. 3.1.5:
Mesh textured serpentine and relict of olivine (cross polar).

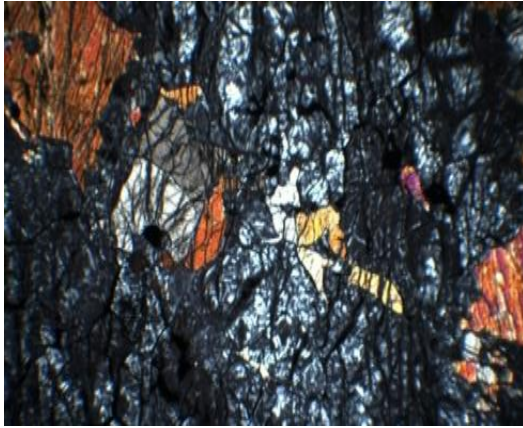


Fig. 3.1.6:
Elongated clinopyroxene grains having tapering ends (width of photo is 4mm) (cross polars)



Fig. 3.1.7:
Olivine relict within serpentinised Orthopyroxene.

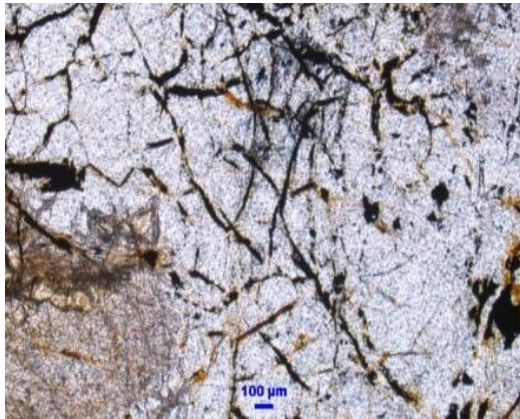


Fig. 3.1.8:
Secondary spinel grains which mimic the shape of the original fracture of olivine (polarized light).



Fig. 3.1.9:
Xenoblastic orthopyroxene showing Corrosive structure at outer margin (width of photo is 4mm, cross polar).

Z

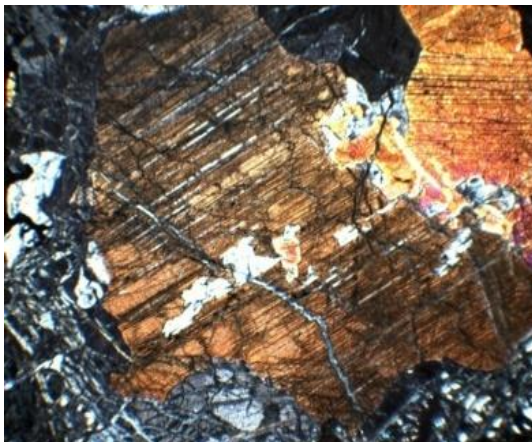


Fig. 3.1.10:
Exsolution lamellae of Orthopyroxene in clinopyroxene host. (width of photo is 4mm) (cross polar).



Fig. 3.1.11:
Growth of serpentine into asbestiform chrysotile (width of photo is 4mm) in extremely serpentinised ultramafic (cross polar).

In ultramafics (serpentinites) of Manipur Ophiolite Belt, **olivine** is the most predominant phase, which also appears to be the coarsest phase with mesh textured serpentine replacement (complete in intensely serpentinitised peridotite) or partial replacement (in less serpentinitised type) with numerous residual angular relic grains broken down from original large olivine grains (**Figs. 3.1.5 and 3.1.11**). The process of serpentinitisation of olivine begins at the periphery and along the internal fractures resulting to anastomosing veinlets of cross fiber serpentine with islets of residual olivine. This process of alteration of olivine to serpentine produces a mesh textured aggregate of fine serpentine with disseminated secondary Fe-oxides (spinel), which mimics the shapes and to a degree, the internal cracks of the original olivine grains (**Fig. 3.1.8**).

Orthopyroxene is the second most predominant phase. The grains are very coarse but their sizes are variable ranging from a fraction of an mm to grains as large as 10 mm in diameter. These tend to be replaced by large plates of serpentine (bastite). In hand specimen the bastite grain show shining appearance in the reflected light. The outer margin of the xenoblastic orthopyroxene grains shows corrosion structure and hence original grain boundaries are obscured (**Figs. 3.1.9 and 3.1.10**). In Manipur Ophiolite Belt, the peridotitic serpentinites show variable amounts (proportions) of orthopyroxene grains. Many of the orthopyroxene grains are having exsolved lamellae of clinopyroxene. The unaltered pyroxene grains have the characteristic pyroxene cleavage (**Fig. 3.1.9**).

The third most abundant phase is **clinopyroxene**. In most of the samples where the degree of serpentinitisation is not very extensive, the clinopyroxene grains show no evidence of alteration to serpentine. The fine grain clinopyroxenes appear to be elongated broken pieces of the crystals, mostly having tapering ends which could have been the result of extensive melting (**Figs. 3.1.4 and 3.1.6**). Exsolution lamellae of clinopyroxene in the orthorhombic host indicate an earlier high temperature solid solution between Mg and Ca-pyroxenes, which have been made failed on account of prolonged subjection to equilibrium conditions of either higher pressure and/or lower temperature environment at situations below the solidus of the corresponding P-T phase diagram.

In intensely serpentinitised samples any of the essential phases including clinopyroxene are not preserved except the primary spinels. The primary spinel grains are elongated and show alignment (**Fig. 3.1.2A**). Composition of spinel varies in the different types (samples) of the peridotitic serpentinites as evident from the changes of colour from black to reddish brown (indicating an increase in the Cr-content).

In extremely serpentinitised peridotite samples, it is difficult to distinguish from which phase the serpentine was derived because all the phases except spinel are altered. In such samples, earlier formed serpentines have started growing into asbestiform chrysotiles (**Fig. 3.1.11**); and almost all the secondary spinels are removed.

As the ultramafics of the ophiolite complex are related to igneous processes, the problem of their petrogenesis must be stated in terms of igneous petrology.

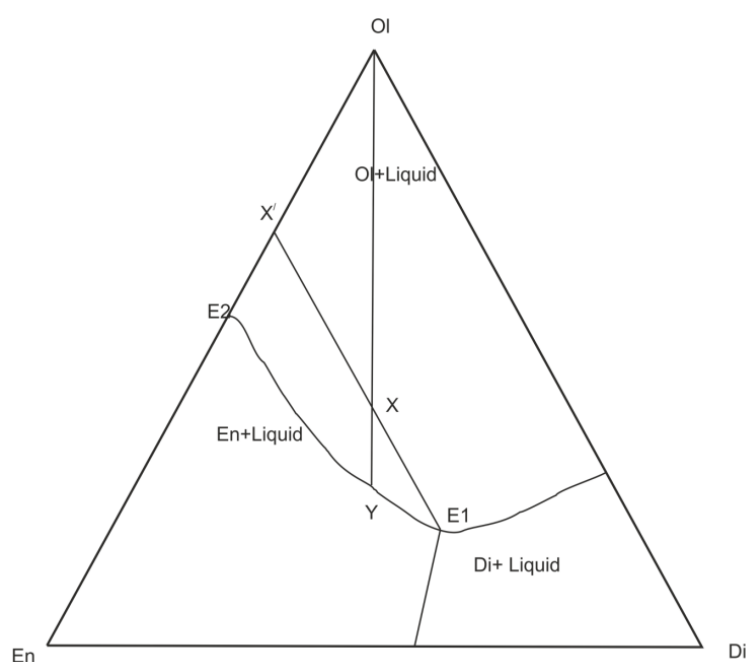


Fig. 3.1.12:
Ternary diagram of Ol-En-Di (modified after barker, 1983)

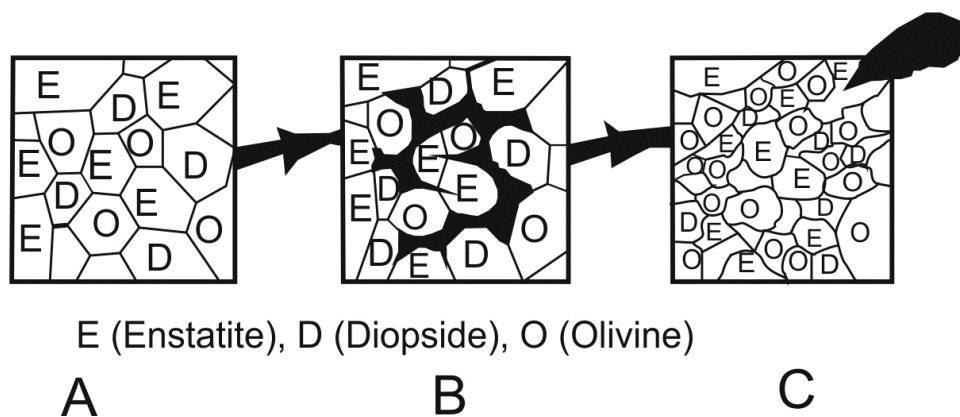


Fig. 3.1.13 (A, B, C):
Different Stages of partial melting and development of residue.

The different phases and their relationships of the ultramafic rocks of the ophiolite belt in Manipur can be expressed in terms of eutectic melting of a model ternary system as shown in the **figure 3.1.12**, in which the end members are Olivine-Enstatite-Diopside. The composition X (40% olivine, 30% Enstatite, 30% Diopside) represents the bulk composition of the hypothetical material in whose partial melting behaviors we are interested. One of the interesting features of ternary systems such as this one is that, regardless of the partial melting mechanism, the initial partial melt will always have the same eutectic composition E_1 . In addition, the closer the bulk composition of the system is to E_1 , the greater the volume of partial melt of E_1 will be generated. A further important point is that, regardless of the bulk composition of the system, the initial partial melt will always have the eutectic composition E_1 . **Figure 3.1.13A-C** shows the changing appearance of the system with progressive partial melting starting with a crystalline solid of composition X with a granular texture (A). The initial liquid E_1 forms only at points where the three phases are in direct contact (B). With progressive partial melting the residual crystals effectively become disaggregated, until a point is reached at which the liquid can percolate upwards, rapidly driven by the density difference between it and the residual crystalline phases; following melt extraction the residual solid may become annealed leaving no trace of the partial melting process it has undergone (C). The samples of the ultramafic rocks are showing similar texture which is best represented by the photomicrograph of **figure 3.1.1**.

3.1.1 Modal Analysis

Mode is the relative amount of different minerals/phases actually present in a rock. The procedure adopted for determination of its mode of a given rock is known as modal analysis. Modal analysis gives a valuable tool in the precise determination of the proportion of minerals present in a rock. It also produces an accurate representation of the distribution and volume percent of the minerals within a thin section. It allows counting of each mineral occurrence along a series of traverse line across a thin section. In essence, the ratio of the area occupied by all minerals (i.e., the total measured area) is a consistent estimate of the volume percentage of the mineral in the rock. The modal analysis gives real proportion of the minerals in vol. %. For this work the principle of modal analysis is adopted using point counting technique with Petrolite (Software Version 3.1.5.0 march 2014) at the Department of Geology, Nagaland University. The result of the modal analysis of 41 representative samples of the peridotitic serpentinites is given in the **table 3.1.1.1**

Table 3.1.1.1: Modal proportions of ultramafic rocks from Manipur Ophiolite Belt.

Sl. No.	Sample	Serpentine from Olivine \pm Olivine	Bastite +/- Orthopyroxene	Clinopyroxene	Spinel
1	F3 (2)	79	14	6	1
2	F3 (3A)	85	14	0	1
3	F3 (3B)	77	18	4	1
4	F3 (9B)	63	27	10	0
5	F2 (A3)	85	14	0	1
6	F3 (9A)	82	17	0	1
7	F3 S15(A)	65	25	6	4
8	F3 SU 75	68	23	6	3
9	F3 SU 79	64	26	7	4
10	S2 (UA)	75	17	7	1
11	S2 (UB)	92	7	0	1
12	S5 (A)	90	8	0	2
13	S8 (B)	81	17	0	2
14	S11 (2B)	84	11	3	2
15	S12 (A)	79	12	6	3
16	S17 (A)	76	17	4	3
17	S17(B)	86	11	2	1
18	S18 (2)	75	24	0	1
19	S18 (2A)	73	25	0	2
20	S75	89	9	0	2
21	S1D (F1)	81	17	0	2
22	43 (A)	71	20	0	9
23	S1	70	18	2	10
24	S2 (2)	69	20	1	10
25	S4 (1)	69	22	3	6
26	S3 (2)	64	21	1	14
27	S4 (B)	71	16	0	12
28	S5(A)	72	15	0	13
29	S6	73	19	2	6
30	S7 (2)	75	13	0	12
31	S8 (1)	65	23	7	5
32	S9 (1)	62	22	8	8
33	S10 (A)	60	21	6	13
34	S11 (2)	63	20	7	10
35	S12	65	22	3	10
36	S13 (A)	73	16	0	11
37	S14 (1)	65	23	5	7
38	S17	67	24	6	3
39	S18 (2)	77	20	0	3
40	SU35 (A)	78	20	0	2
41	S11 (KW)	74	20	1	5

Table 3.1.1.2: Recalculated modal proportions of Olivine, Orthopyroxene and Clinopyroxene.

Sl. No.	Sample	Olivine	Orthopyroxene	Clinopyroxene
1	F3 (2)	77	16	7
2	F3 (3A)	86	14	0
3	F3 (3B)	77	19	4
4	F3 (9B)	63	27	10
5	F2 (A3)	86	14	0
6	F3 (9A)	83	17	0
7	F3 S15(A)	67	26	7
8	F3 SU 75	69	25	6
9	F3 SU 79	66	27	7
10	S2 (UA)	76	17	7
11	S2 (UB)	92	8	0
12	S5 (A)	92	8	0
13	S8 (B)	83	17	0
14	S11 (2B)	86	11	3
15	S12	81	13	6
16	S17 (A)	79	18	3
17	S17	87	11	2
18	S18 (2)	76	24	0
19	S18 (2A)	75	25	0
20	S75	90	10	0
21	S1D (F1)	82	18	0
22	43 (A)	78	22	0
23	S1	78	20	2
24	S2 (2)	77	22	1
25	S4 (1)	74	23	3
26	S3 (2)	75	24	1
27	S4 (B)	81	19	0
28	S5(A)	83	17	0
29	S6	78	20	2
30	S7 (2)	85	15	0
31	S8 (1)	68	25	7
32	S9 (1)	68	24	8
33	S10 (A)	69	24	7
34	S11 (2)	70	23	7
35	S12	72	25	3
36	S13 (A)	82	18	0
37	S14 (1)	70	25	5
38	S17	69	25	6
39	S18 (2)	79	21	0
40	SU35 (A)	79	21	0
41	S11 (KW)	78	21	1

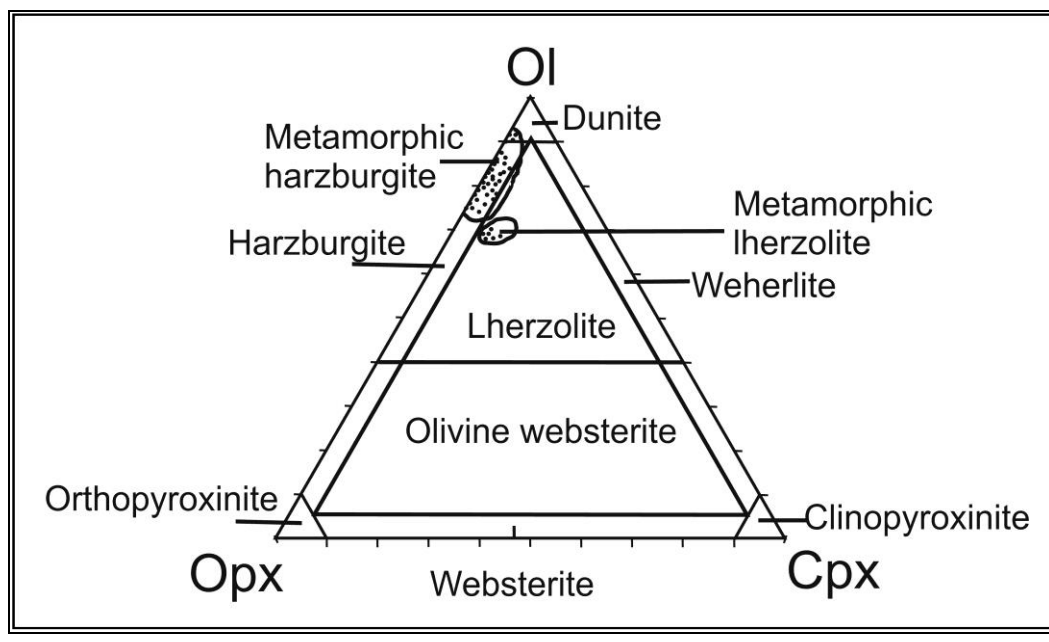


Fig. 3.1.1.1:

Triangular plot of the ultramafic rocks of Manipur Ophiolite on the basis of Modal minerals of olivine (Ol)-orthopyroxene (Opx)- clinopyroxene (Cpx) (after Coleman 1977).

The values of four different phases' modal proportions are again recalculated in terms of three major phases of Olivine, Orthopyroxene and Clinopyroxene and their final values are represented as shown in the **table 3.1.1.2**. Using the data of **table 3.1.1.2**, a triangular diagram is plotted (**Fig. 3.1.1.1**) with end members of Olivine-Orthopyroxene-Clinopyroxene for modal classification of the ultramafic rocks (cf. Harte, 1983). According to this classification, all the ultramafic rocks of Manipur Ophiolite Belt are found to be of metamorphic lherzolite and metamorphic harzburgite with negligible amount of dunite.

In addition to the above information and ideas gathered from the petrographic studies, it is further required to study the mineral chemistry of the individual mineral phases of the rocks to know about the chemistry of dominant phases, ionic interaction and many other aspects related to tectonic setting, equilibrium conditions, etc.

3.2 Mineral Chemistry

For determination of composition of dominant mineral phases of ultramafic rocks from different parts of Manipur Ophiolite Belt, EPMA analysis of the representative samples have been carried out at DST-SERB National Facility, Department of Geology (Center of Advanced Study), Institute of Science, Banaras Hindu University using Electron Probe Micro Analyzer CAMECA SXFive instrument. For this analysis polished thin sections were coated with 20 nm thin layer of carbon using LEICA-EM ACE200 instrument. The CAMECA SXFive instrument was operated by SXFive Software at a voltage of 15 kV and current of 10 nA with a LaB6 source in the electron gun for generation of electron beam. Natural silicate mineral andradite as internal standard was used to verify positions of crystals (SP1-TAP, SP2-LiF, SP3-LPET, SP4-LTAP and SP5-PET) with respect to corresponding wavelength dispersive (WD) spectrometers (SP#) in CAMECA SXFive instrument. The data acquired are recalculated for use in various purposes with respect to the chemistry and other aspects of the various mineral phases.

3.2.1 Olivine

The **table 3.2.1.1** represents the average composition of olivine in one type of ultramafic rock (Sample F3-2) of the Ophiolite complex. After examination and recalculation of the average composition of olivine found in the ultramafic rock of Manipur Ophiolite Belt of the same data (**Table 3.2.1.2**), it is found that the olivine of the Manipur Ophiolite Belt of Manipur is having composition of $\text{Fo}_{90.33}\text{-Fa}_{9.67}$. The value of $\text{Mg}/(\text{Mg} + \text{Fe})$ is found to be about 0.84. And the value of $\text{Mg}/(\text{Mg} + \text{Fe} + \text{Mn})$ of olivine of this Ophiolite complex is about 0.83 and is not consistent with the olivine from Ophiolite metamorphic peridotites (**Fig. 3.2.1.1A**). From the recalculated data, it is found that the value of magnesium number is less, inferring the ultramafic of the study area is less depleted in nature.

Table 3.2.1.1: Olivine composition of representative ultramafic rock (Sample F3-2)
from MOB in percent (EPMA data).

Major Oxide %	(1)	(2)	(3)	(4)	(5)	(6)	(7)	(8)	(9)	(10)	(11)	(12)	Mean
Na ₂ O	0.008	0.051	0.015	0.018	0.022	0.020	0.008	0.010	0.014	0.020	0.014	0.004	0.017
K ₂ O	0.000	0.000	0.000	0.000	0.000	0.000	0.000	0.002	0.000	0.000	0.000	0.000	0.000
MgO	48.700	46.910	48.742	49.337	48.619	48.875	48.230	48.732	48.984	48.956	47.768	48.805	48.555
CaO	0.000	1.792	0.068	0.035	0.068	0.099	0.035	0.059	0.097	0.045	0.012	0.052	0.197
MnO	0.093	0.035	0.197	0.093	0.151	0.012	0.163	0.128	0.128	0.070	0.000	0.012	0.090
FeO	9.433	8.709	9.998	9.286	8.938	8.862	9.294	10.340	9.609	9.042	8.826	9.140	9.290
NiO	0.503	0.236	0.393	0.566	0.630	0.472	0.629	0.267	0.315	0.378	0.409	0.378	0.431
Al ₂ O ₃	0.000	1.038	0.044	0.045	0.021	0.015	0.020	0.013	0.012	0.019	0.001	0.015	0.103
V ₂ O ₃	0.003	0.000	0.000	0.000	0.000	0.000	0.000	0.000	0.000	0.000	0.000	0.000	0.000
Cr ₂ O ₃	0.000	0.193	0.045	0.007	0.017	0.015	0.027	0.003	0.017	0.018	0.000	0.029	0.031
SiO ₂	39.480	41.548	41.540	41.344	41.505	41.935	41.887	41.448	41.909	41.257	41.960	41.405	41.435
TiO ₂	0.006	0.000	0.028	0.005	0.000	0.004	0.000	0.000	0.005	0.006	0.007	0.008	0.006
P ₂ O ₅	0.000	0.000	0.019	0.038	0.000	0.067	0.038	0.000	0.010	0.019	0.000	0.010	0.007
Total	98.226	100.511	101.089	100.773	99.971	100.374	100.330	101.002	101.099	99.828	98.996	99.855	100.171

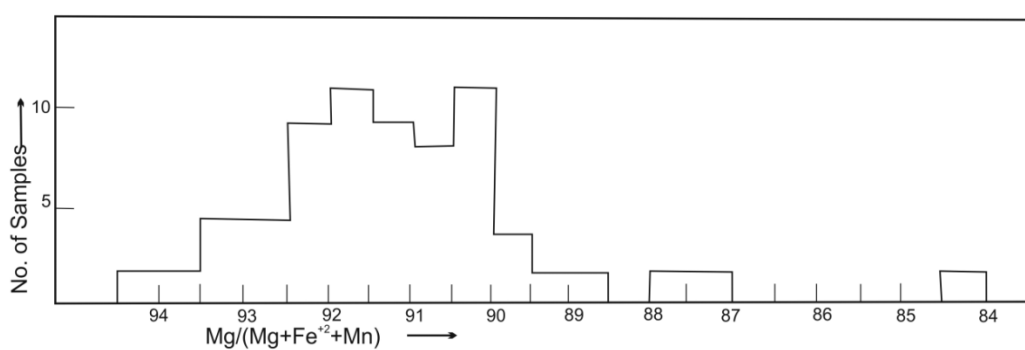


Fig. 3.2.1.1A.

Histogram showing ranges in Composition of Olivine from Ophiolite Metamorphic Peridotite (After Coleman, 1977).

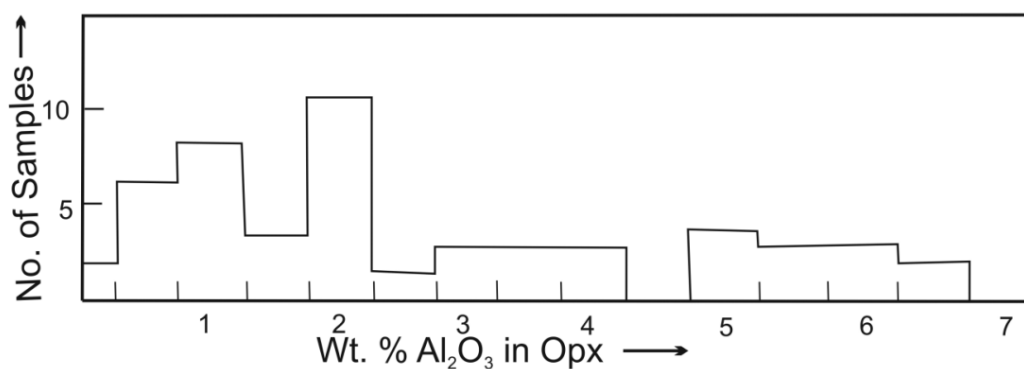


Fig. 3.2.1.1B.

Histogram showing ranges in Al₂O₃ contents of Orthopyroxene from Ophiolite Metamorphic Peridotite (After Coleman, 1977).

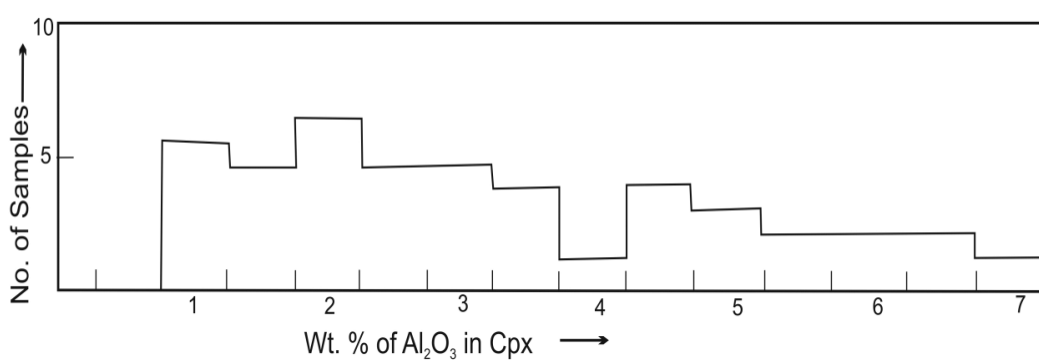


Fig. 3.2.1.1C.

Histogram showing ranges in Al₂O₃ contents of Clinopyroxene from Ophiolite Metamorphic Peridotite (After Coleman, 1977).

3.2.2 Orthopyroxene

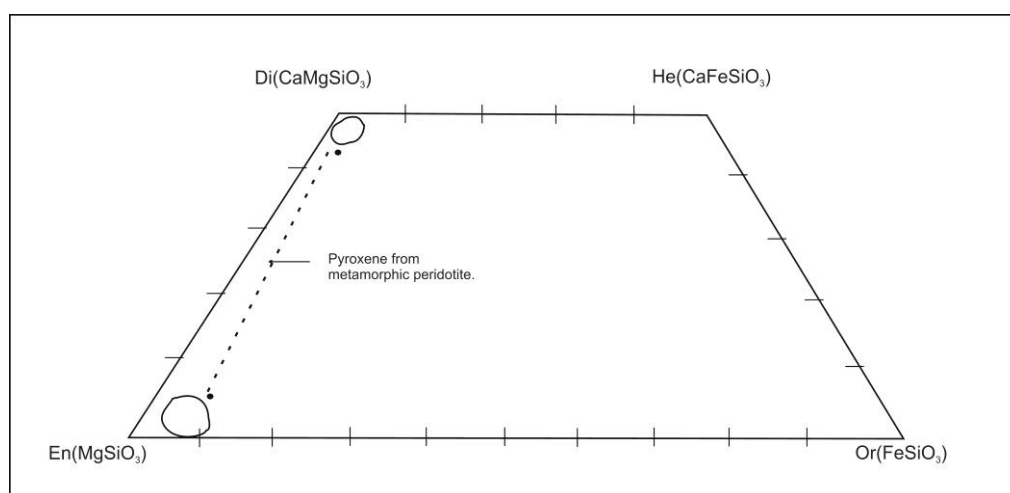
The compositional (EPMA) data of orthopyroxene of Manipur Ophiolite Belt represented by Sample no F3-2 is shown in **table 3.2.2.1**. The mean compositional EPMA data is further recalculated the result of which is shown in **table 3.2.2.2**. From the examination of this recalculated data of orthopyroxene, it is found that the compositional value of orthopyroxene from Manipur Ophiolite Belt is about $\text{En}_{87.266}\text{-Fs}_{9.36}\text{-Wo}_{3.374}$. And the value of magnesium number ($\text{Mg}/(\text{Mg}+\text{Fe})$) of orthopyroxene has nearly identical value of 0.84 which is almost equal to that of 0.84 of the coexisting olivine.

Table 3.2.2.1:Orthopyroxene composition of ultramafic rocks from Manipur ophiolite Belt in percent (EPMA data).

Major oxide %	(1)	(2)	(3)	(4)	(5)	(6)	(7)	(8)	(9)	(10)	(11)	(12)	(13)	Mean
Na ₂ O	0.022	0.023	0.027	0.024	0.033	0.051	0.041	0.042	0.023	0.041	0.028	0.020	0.053	0.033
K ₂ O	0.000	0.000	0.000	0.000	0.000	0.000	0.000	0.000	0.000	0.000	0.000	0.000	0.000	0.000
MgO	31.531	30.985	30.904	31.571	31.416	30.734	31.050	30.653	31.425	31.251	31.855	31.886	31.213	31.267
CaO	1.272	1.448	2.371	1.456	1.674	2.471	1.862	1.831	1.505	1.622	1.675	1.171	1.617	1.690
MnO	0.070	0.047	0.105	0.000	0.059	0.094	0.047	0.105	0.094	0.082	0.105	0.023	0.129	0.074
FeO	5.797	6.278	5.331	5.880	5.747	5.248	5.983	5.847	6.013	6.076	6.523	6.489	6.762	5.998
NiO	0.111	0.110	0.142	0.000	0.079	0.095	0.252	0.315	0.063	0.079	0.016	0.032	0.110	0.108
Al ₂ O ₃	4.668	4.479	4.650	4.634	4.615	4.730	4.711	4.864	4.543	4.453	4.698	4.617	4.459	4.625
V ₂ O ₃	0.000	0.000	0.000	0.000	0.000	0.000	0.000	0.000	0.000	0.000	0.000	0.000	0.000	0.000
Cr ₂ O ₃	0.759	0.717	0.840	0.769	0.801	0.839	0.794	0.802	0.839	0.865	0.812	0.753	0.697	0.791
SiO ₂	55.629	55.617	55.467	55.225	55.530	55.349	54.961	55.420	53.512	54.324	55.101	55.233	55.094	55.112
TiO ₂	0.074	0.021	0.090	0.043	0.057	0.063	0.064	0.082	0.068	0.061	0.057	0.077	0.041	0.061
P ₂ O ₅	0.000	0.000	0.000	0.010	0.029	0.000	0.048	0.000	0.029	0.010	0.000	0.000	0.000	0.010
	99.933	99.724	99.926	99.611	100.039	99.673	99.813	99.962	98.112	98.863	100.870	100.300	100.174	99.769

Table 3.2.2.2: Recalculation of Orthopyroxene Analysis (EPMA) data.

Name of Oxide	(1) wt% Oxide	(2) Mol. Propn Of Oxide	(3) Atomic Propn of cation /Cation Propn	(4) No. of oxygen	(5) Cation on basis of 4 Oxygen	(6) Cation Assignment	(7) End Members recalculation
SiO ₂	55.1124	0.9172	0.9172	1.8344	1.9002	<div><div><div>Si 1.9002</div><div>Al 0.0998</div><div>Al. 0.0883</div><div>Ni .0029</div><div>Ti .0017</div><div>Fe .1730</div><div>Mn .0021</div><div>Cr .0215</div><div>P .0002</div><div>Mg 1.6072</div><div>Ca .0624</div><div>Na .0021</div></div><div><div>=2</div><div>=</div><div>1.963</div><div>~2</div></div></div>	MgO as MgSiO ₃ (En) FeO As FeSiO ₃ (Fs) CaO as CaSiO ₃ (Wo) Using Molecular Proportion MgO= 0.7785 FeO= 0.0835 CaO=0.0301
Al ₂ O ₃	4.6247	0.0454	0.0908	0.1362	0.1881		Total=0.8921
NiO	0.1079	0.0014	0.0014	0.0014	0.0029		Triangular $\left\{ \begin{array}{l} \% \text{ En}=87.2660 \\ \% \text{ Fs}=9.360 \\ \% \text{ Wo}=3.3740 \end{array} \right.$
TiO ₂	0.0613	0.0008	0.0008	0.0016	0.0017		
FeO	5.9980	0.0835	0.0835	0.0835	0.1730		
MnO	0.0738	0.0010	0.0010	0.0010	0.0021		
Cr ₂ O ₃	0.7912	0.0052	0.0104	0.0312	0.0215		
P ₂ O ₅	0.0095	0.0001	0.0001	0.0005	0.0002		
MgO	31.2672	0.7758	0.7758	0.7758	1.6072		
CaO	1.6903	0.0301	0.0301	0.0301	0.0624		
Na ₂ O	0.0329	0.0005	0.0010	0.0005	0.0021		
V ₂ O ₃	-	-	-	-	-		
K ₂ O	-	-	-	-	-		
Total	99.7692			2.8962	3.9613		
Oxygen Factor=6/2.8962 = 2.0717 Mg/(Mg+Fe)=0.84							Binary $\left\{ \begin{array}{l} \% \text{ En}=96.2775 \\ \% \text{ Wo}=3.7225 \end{array} \right.$ Composition ((Mg, Fe,Ca, Cr,Ni, Mn,Na,Ti,P) (Si, Al) ₂ O ₆

**Fig. 3.2.2.1:**

Pyroxene quadrilateral showing compositions of coexisting ortho- and Clinopyroxenes of ultramafics of Manipur Ophiolite.

In the analysis of orthopyroxene of Manipur ophiolite belt, the Al_2O_3 content is 4.625 wt%, which is very uncommon in the metamorphic peridotites as evident from the figure (**Fig. 3.2.1.1B**). When the composition of orthopyroxene is plotted on the pyroxene quadrilateral (**Fig. 3.2.2.1**), it is found that the orthopyroxene of the ultramafics of the Manipur Ophiolite Belt falls very close to the field of metamorphic peridotites.

3.2.3 Clinopyroxene

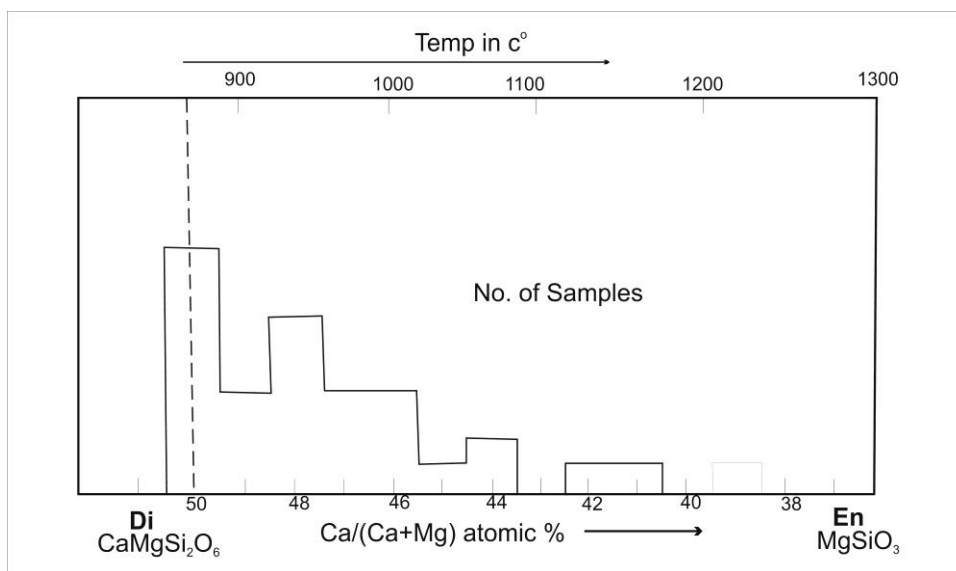
Clinopyroxenes are the least abundant silicate mineral in the ultramafic rocks of the ophiolite belt in Manipur. The EPMA generated data of clinopyroxene (**Table 3.2.3.1**) of the ultramafic rocks of the Manipur Ophiolite Belt (Sample no F3-2) is again recalculated the result of which is shown in **table 3.2.3.2**, for extraction of the information stored in them in the form of chemical codes and for derivation of exact chemical composition (formula) and hence we can perceive the idea of igneous ionic substitution. From this recalculated data, it is found that the composition of clinopyroxene of ultramafic rocks of Manipur Ophiolite Belt, in terms of three end members of Enstatite-Ferrosilite-Wollastonite, is found to be $\text{En}_{51.824}\text{-Fs}_{5.245}\text{-Wo}_{42.931}$. Having an average value of 1.143 wt. % of the Cr_2O_3 in clinopyroxene is an indication of qualifying this clinopyroxene to class as chromium diopside. The Al_2O_3 content is 5.484 wt. % which is fairly compatible with the clinopyroxene from ophiolitic metamorphic peridotites (**Fig. 3.2.1.1C**). Exsolution lamellae of clinopyroxene in the orthorhombic host indicate an earlier solid solution between Mg- and Ca-pyroxenes, which have been made failed on account of prolonged subjection to equilibrium conditions of lower temperature environment in such a way that situations are well below the solidus of the corresponding P-T phase diagram. Plotting the composition of the clinopyroxene on the pyroxene quadrilateral demonstrates that the clinopyroxene of the Ophiolite complex in Manipur is very close to the field of those of metamorphic peridotite (**Fig. 3.2.2.1**).

Table 3.2.3.1: Clinopyroxene composition of ultramafic rocks from Manipur ophiolite Belt in percent (EPMA data).

me of Oxide	(1)	(2)	(3)	(4)	(5)	(6)	(7)	(8)	(9)	(10)	(11)	(12)	(13)	Mean
Na ₂ O	0.285	0.294	0.347	0.310	0.325	0.323	0.286	0.315	0.359	0.569	0.279	0.282	0.383	0.335
K ₂ O	0.000	0.000	0.000	0.000	0.005	0.000	0.000	0.027	0.002	0.002	0.000	0.000	0.000	0.003
MgO	18.069	18.473	17.357	15.916	18.636	17.004	17.712	16.131	15.491	16.993	22.537	16.055	15.868	17.403
CaO	20.612	18.201	20.030	19.744	20.984	22.115	21.231	21.138	21.064	18.950	15.440	20.022	21.227	20.058
MnO	0.094	0.000	0.059	0.164	0.000	0.035	0.000	0.047	0.070	0.000	0.000	0.094	0.000	0.043
FeO	2.569	3.384	3.298	2.814	3.187	3.126	3.116	3.613	2.884	3.105	3.497	2.961	3.226	3.137
NiO	0.219	0.157	0.172	0.125	0.141	0.219	0.094	0.094	0.188	0.016	0.000	0.063	0.141	0.125
Al ₂ O ₃	5.862	5.467	5.567	5.292	5.683	5.262	5.387	5.504	5.542	6.481	5.026	5.016	5.212	5.485
V ₂ O ₃	0.001	0.029	0.030	0.034	0.037	0.028	0.029	0.026	0.025	0.036	0.038	0.013	0.037	0.028
Cr ₂ O ₃	1.223	1.120	1.157	1.071	1.178	1.137	1.126	1.143	1.148	1.448	1.010	0.992	1.110	1.143
SiO ₂	51.473	51.660	52.563	52.243	52.010	50.882	50.428	50.364	51.192	50.408	52.552	52.710	52.694	51.629
TiO ₂	0.164	0.142	0.196	0.209	0.169	0.172	0.175	0.159	0.190	0.197	0.220	0.192	0.173	0.181
P ₂ O ₅	0.000	0.000	0.073	0.000	0.009	0.054	0.009	0.000	0.009	0.000	0.018	0.082	0.027	0.022
Total	100.571	98.926	100.848	97.921	102.363	100.358	99.592	98.560	98.165	98.205	100.618	98.481	100.097	99.593

Table 3.2.3.2: Recalculation of Clinopyroxene Analysis (EPMA) data

Name of Oxide	(1) wt% Oxide	(2) Mol. Propn Of Oxide	(3) Atomic Propn of cation /Cation Propn	(4) No. of oxygen	(5) Cation on basis of 4 Oxygen	(6) Cation Assignment	(7) End Members recalculation
SiO ₂	51.6291	0.8593	0.8782	1.7564	1.8720	Si 1.872	MgO as MgSiO ₃ (En) FeO As FeSiO ₃ (Fs) CaO as CaSiO ₃ (Wo) Using Molecular Proportion. MgO= 0.4318 FeO= 0.0437 CaO=0.3577 <hr/> Total= 0.8332 Triangular { % En=51.824 % Fs=5.245 % Wo=42.931 Binary { % En=54.693 % Wo=45.307 Composition: (Ca, Mg, Na)(Mg, Al, Fe, Cr, Mn,Ti, Ni) (Si, Al) ₂ O ₆
Al ₂ O ₃	5.4846	0.0538	0.1076	0.1614	0.2290	Al 0.229	
TiO ₂	0.1814	0.0023	0.0015	0.003	0.0032	Ti 0.0032	
FeO	3.1369	0.0437	0.0637	0.0637	0.1356	Fe 0.1357	
MnO	0.0433	0.0006	0.0007	0.0007	0.0016	Mn 0.0015	
MgO	17.4033	0.4318	0.6096	0.6096	1.2993	Mg 0.8595	
Na ₂ O	0.3351	0.0054	0.006	0.0030	0.0128	Mg 0.4398	
CaO	20.0583	0.3577	0.1961	0.1961	0.4180	Na 0.0128	
Cr ₂ O ₃	1.1432	0.0075	0.0124	0.0186	0.0265	Ca 0.4180	
NiO	0.1251	0.0017	0.0016	0.0016	0.0040	Cr 0.0265	
Total	99.598			2.8148	4.002	Ni 0.0040	
Oxygen Factor = $6/2.8148 = 2.1316$ Mg/(Mg+Fe)=0.84							

**Fig. 3.2.3.1:**

Ca/(Ca+Mg) ratio of clinopyroxene from ophiolite metamorphic peridotite. Temperature points taken from diopside-enstatite solvus at 30 kbar from Boyd (1970). The ratio in case of MOB is 0.535 and hence in % it comes out to be 53.5.

Plotting the Ca/Ca+Mg (0.535) atomic ratio against the temperature derived by Boyd (1970) for the diopside-enstatite solvus at 30kb suggest that most of the diopside equilibrated at temperature below 1100°C and perhaps even as below as 850°C as shown in **figure 3.2.3.1**.

3.2.4 Spinel

The mean compositional data of three different spinels from ultramafics of Manipur ophiolite belt and their recalculated values are shown in **tables 3.2.4.1 (A,B,C)** and **tables 3.2.4.2(A,B,C)** respectively. From this recalculated data, chemical composition (formula) of three different spinels are derived so that an idea about the ionic substitution could be ascertained. The result of recalculated data of these three representative samples of spinel gives the values of (A) spinel series = 27%, magnetite series = 52%, and chromite series = 21%; (B) spinel series = 79%, magnetite series = 7%, and chromite series = 14%; (C) spinel series = 46%, magnetite series = 12%, and chromite series = 42%; respectively. And the mean recalculated value of the representative of three different types of spinels give the values of spinel series = 51%, magnetite series = 23% and chromite series = 26%.

It is an established fact that spinels from different tectonic settings have different compositions (Dick and Bullen, 1984; Arai, 1994). $Cr\# = Cr/(Cr + Al)$ and $Mg\# = Mg/(Mg+Fe^{+2})$ are important tools used to trace the tectonic settings. The $Cr\#$ values of the three different samples are found to be 0.536, 0.212, 0.577 respectively and $Mg\#$ values to be 0.265, 0.608, and 0.361 respectively. When 100 $Cr/(Cr+Al)$ is plotted against Al_2O_3 weight percent of co-existing orthopyroxene of the three types of spinels (**Fig. 3.2.4.1**), the ultramafic rock is found to be Al-spinel lherzolite (sample-F1M1) and Cr- spinel/lherzolite (Samples -F3-3B and - F1S2B).

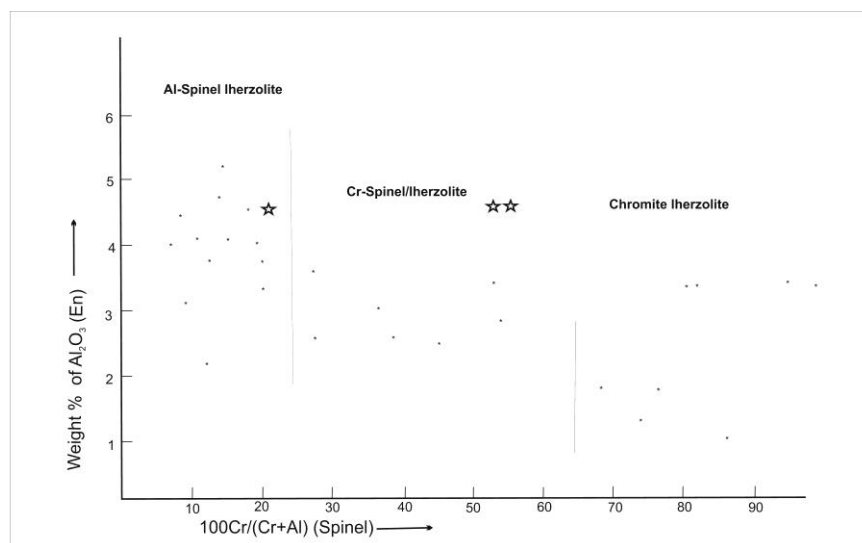


Fig. 3.2.4.1:

Plot of $100\text{Cr}/(\text{Cr} + \text{Al})$ ratio in primary spinels against wt.% Al_2O_3 coexisting orthopyroxene from spinel Iherzolite xenoliths (after Carswell, 1980). Stars are the plot of Manipur Ophiolite ultramafics.

Table 3.2.4.1A Composition of one type of spinel from host ultramafic rocks (Sample F3-3B) from Manipur Ophiolite Belt in percent (EPMA data).

Name of Oxide	(1) Wt%	(2) Wt%	Mean
Na_2O	0.0284	0.0086	0.0185
K_2O	0.0000	0.0000	0.0000
MgO	12.2226	13.8499	13.0363
CaO	0.1542	0.0000	0.0771
MnO	0.9365	0.0000	0.4683
FeO	45.0209	26.8814	35.9512
NiO	0.8383	0.1196	0.4790
Al_2O_3	7.4035	29.5621	18.4828
V_2O_3	0.1031	0.0636	0.0834
Cr_2O_3	17.8152	24.8841	21.3497
SiO_2	7.1428	0.5249	3.8339
TiO_2	0.0058	0.0344	0.0201
P_2O_5	0.0000	0.0000	0.0000
Total	91.6711	95.9286	93.7999

Table 3.2.4.1B: Composition of one type of spinel from host ultramafic rocks
(Sample F1M1) of Manipur Ophiolite Belt in percent (EPMA data).

Major Oxide	(1)	(2)	(3)	(4)	(5)	(6)	Mean
MgO	20.2220	20.0690	20.0050	20.2460	20.0790	20.1950	20.1360
MnO	0.1550	0.1320	0.1250	0.0820	0.1140	0.0800	0.1147
FeO	13.0770	12.8750	12.9440	12.8930	12.9870	12.8430	12.9365
Al ₂ O ₃	53.7920	53.7990	53.4920	53.4320	53.7000	53.8300	53.6742
V ₂ O ₃	0.0010	0.0020	0.0000	0.0010	0.0010	0.0010	0.0010
Cr ₂ O ₃	14.6560	14.9480	13.8900	14.4780	14.5840	14.1370	14.4488
SiO ₂	0.0000	0.0000	0.0000	0.0000	0.0000	0.0000	0.0000
TiO ₂	0.0590	0.0540	0.0830	0.0180	0.0490	0.0600	0.0538
P ₂ O ₅	0.0000	0.0000	0.0000	0.0000	0.0000	0.0000	0.0000
ZnO	0.1430	0.1420	0.1290	0.0780	0.1750	0.1470	0.1357
Total	102.1050	102.0210	100.6680	101.2280	101.6890	101.2930	101.5007

Table 3.2.4.1C: Composition of one type of spinel from host ultramafic rocks
(Sample F1-S2B) from Manipur Ophiolite Belt in percent (EPMA data).

Wt% Oxide	(1)	(2)	(3)	(4)	(5)	(6)	(7)	(8)	(9)	(10)	Mean
Na ₂ O	0.0000	0.0126	0.0095	0.0198	0.0084	0.0000	0.0115	0.0032	0.0000	0.0000	0.0065
MgO	12.5317	12.3760	12.2233	12.1502	12.1473	11.6306	12.5087	12.0942	12.4869	11.8240	12.1973
CaO	0.0000	0.0000	0.0000	0.0000	0.0000	0.0000	0.0024	0.0000	0.0047	0.0738	0.0081
MnO	0.0000	0.0000	0.0000	0.0000	0.0000	0.0000	0.0000	0.0000	0.0000	0.0000	0.0000
FeO	19.2024	21.0589	20.6469	19.1722	19.8840	20.9187	19.7853	21.1125	19.7299	33.4824	21.4993
NiO	0.0005	0.1132	0.0327	0.0971	0.0000	0.0000	0.2264	0.0971	-0.0322	0.0321	0.0567
Al ₂ O ₃	28.9336	27.9644	27.4039	27.3933	26.4347	26.1038	27.3570	27.7195	27.4784	24.4222	27.1211
V ₂ O ₃	0.2876	0.2623	0.2832	0.2320	0.2740	0.2610	0.2688	0.2916	0.2750	0.1817	0.2617
Cr ₂ O ₃	36.3244	36.9436	37.5491	37.9988	39.1507	38.3375	38.5692	37.9325	38.1317	29.5017	37.0439
SiO ₂	0.0000	0.0000	0.0000	0.0000	0.0000	0.0308	0.0408	0.0000	0.0000	0.1503	0.0222
TiO ₂	0.2463	0.1879	0.2202	0.2379	0.2411	0.2706	0.2111	0.2199	0.2387	0.1929	0.2267
P ₂ O ₅	0.0276	0.0732	0.0000	0.0366	0.0091	0.0364	0.0275	0.0548	0.0548	0.0091	0.0329
Total	97.5541	98.9920	98.3687	97.3377	98.1493	97.5896	99.0086	99.5253	98.4002	99.8704	98.4796

Table 3.2.4.2A: Recalculation of Spinel Analysis based on Table 3.2.4.1A.

Name of Oxide	(1) wt% Oxide	(2) Mol. Propn Of Oxide	(3) Atomic Propn of cation /Cation Propn	(4) No. of oxygen	(5) Cation on basis of 4 Oxygen	(6) Cation Assignment	(7) End Members recalculation
Na ₂ O	0.0185	0.0003	0.0006	0.0003	0.0012	Na 0.0012	Al ₂ O ₃ as Spinel series Cr ₂ O ₃ as Chromite series Fe ₂ O ₃ as magnetite series Here mole. Proportion of Fe ₂ O ₃ needs to be derived from Fe ⁺³ value assigned from the total Fe. Fe ⁺³ = 0.7352 Therefore mol prop of Fe ₂ O ₃ = 0.355 Using the Mol. Prop. Al ₂ O ₃ = 0.1813 Cr ₂ O ₃ = 0.1405 Fe ₂ O ₃ = 0.355 <hr/> Total = 0.6768 Triangular { % Sp=27 % Chr=21 % Mgt=52 Composition = (Mg, Fe ⁺² , Ni, Ca, Na) (Al, Fe ⁺³ , Cr, Si, Ti, V) ₂ O ₄
K ₂ O	0.0000	0.0000	0	0.0000	0.0000	Mg 0.6691	
MgO	13.0363	0.3234	0.3234	0.3234	0.6691	Ca 0.0028	
CaO	0.0771	0.0014	0.0014	0.0014	0.0028	Ni 0.0133	
MnO	0.4683	0.0066	0.0066	0.0066	0.0137	Fe ⁺² 0.2999	
NiO	0.4790	0.0064	0.0064	0.0064	0.0133	Fe ⁺³ 0.7352	
FeO	35.951	0.5004	0.5004	0.5004	1.0351	Al 0.7501	
Al ₂ O ₃	18.4828	0.1813	0.3626	0.5439	0.7501	V 0.0025	
V ₂ O ₃	0.0834	0.0006	0.0012	0.0018	0.0025	Cr 0.5813	
Cr ₂ O ₃	21.3497	0.1405	0.281	0.4215	0.5813	Si 0.1320	
SiO ₂	3.8339	0.0638	0.0638	0.1276	0.1320	Ti 0.006	
TiO ₂	0.0201	0.0003	0.0003	0.0006	0.0006		
P ₂ O ₅	0.0000	0.0000	0	0	0.0000		
Total	93.7999			1.9339	3.2016		
Oxygen factor = 4/1.9339 = 2.0686 Mg/(Mg+Fe) i.e Mg# = 0.265; Cr/(Cr+Al) i.e Cr# = 0.536							

Table 3.2.4.2B: Recalculation of Spinel Analysis based on Table 3.2.4.1B.

Name of Oxide	(1) wt% Oxide	(2) Mol. Propn Of Oxide	(3) Atomic Propn of cation /Cation Propn	(4) No. of oxygen	(5) Cation on basis of 4 Oxygen	(6) Cation Assignment	(7) End Members recalculation
MgO	20.1360	0.4996	0.4996	0.4996	0.7840	Mg 0.784	Al ₂ O ₃ as Spinel series Cr ₂ O ₃ as Chromite series Fe ₂ O ₃ as Magnetite series Here mole. Proportion of Fe ₂ O ₃ needs to be derived from Fe ⁺³ value assigned from the total Fe. Fe ⁺³ = 0.0717 Therefore mol prop of Fe ₂ O ₃ = 0.045 Using the Mol. Prop. Al ₂ O ₃ = 0.5264 Cr ₂ O ₃ = 0.0951 Fe ₂ O ₃ = 0.045 Total = 0.6665 Triangular { % Sp = 79 % Chr = 14 % Mgt = 7 Composition = (Mg, Fe ⁺² , Mn, Zn) (Al, Cr, Fe ⁺³ , Ti) ₂ O ₄
MnO	0.1147	0.0016	0.0016	0.0016	0.0025	Mn 0.0025	
ZnO	0.1357	0.0017	0.0017	0.0017	0.0026	Zn 0.0026	
FeO	12.9365	0.1801	0.1801	0.1801	0.2826	Fe ⁺² 0.2109	
Al ₂ O ₃	53.6742	0.5264	1.0528	1.5792	1.6522	Fe ⁺³ 0.0717	
V ₂ O ₃	0.0010	0.0000	0.0000	00.0000	0.0000	Al 1.6522	
Cr ₂ O ₃	14.4488	0.0951	0.1902	0.2853	0.2985	Cr 0.2985	
SiO ₂	0.0000	0.0000	0.0000	0.0000	0.0000	Ti 0.0011	
TiO ₂	0.0538	0.0007	0.0007	0.0014	0.0011		
P ₂ O ₅	0.0000	0.0000	0.0000	0.0000	0.0000		
Total	101.5007			2.5489	3.0234		
Oxygen factor = $4/2.5489 = 1.5693$ Mg/(Mg+Fe) i.e Mg# = 0.608, Cr/(Cr+Al) i.e Cr# = 0.212							

Table 3.2.4.2C: Recalculation of Spinel Analysis based on Table 3.2.4.1C.

Name of Oxide	(1) wt% Oxide	(2) Mol. Propn Of Oxide	(3) Atomic Propn of cation /Cation Propn	(4) No. of oxygen	(5) Cation on basis of 4 Oxygen	(6) Cation Assignment	(7) End Members recalculation
Na ₂ O	0.0065	0.0001	0.0002	0.0001	0.0004	<div><div><div>Na=0.0004</div><div>Mg=0.5644</div><div>Ca=0.003</div><div>Ni=0.0014</div><div>Fe²=0.4336</div><div>Fe³=0.1245</div><div>Al=.9922</div><div>V=.0063=2.038</div><div>Cr=.9090</div><div>Si=.0007</div><div>Ti=.0053</div><div>P=.007</div></div><div>= 1</div></div>	Al ₂ O ₃ as Spinel series Cr ₂ O ₃ as Chromite series Fe ₂ O ₃ as Magnetite series Here mole. Proportion of Fe ₂ O ₃ needs to be derived from Fe ⁺³ value assigned from the total Fe Fe ⁺³ =0.1245 Therefore mol prop of Fe ₂ O ₃ =0.0667 Using the Mol. Prop. Al ₂ O ₃ =0.2660 Cr ₂ O ₃ =0.2437 <u>Fe₂O₃=0.0667</u> Total =0.5764 Triangular <div><div>% Sp=46</div><div>% Chr=42</div><div>% Mgt=12</div></div> Composition=(Mg,Fe ² ,Ca,Ni,Na) (Al,Cr,Fe ³ ,V,P,Ti, Si) ₂ O ₄
K ₂ O	0.0000	0.0000	0.0000	0.0000	0.0000		
MgO	12.1973	0.3026	0.3026	0.3026	0.5644		
CaO	0.0081	0.0001	0.0001	0.0001	0.0003		
MnO	0.0000	0.0000	0.0000	0.0000	0.0000		
NiO	0.0567	0.0008	0.0008	0.0008	0.0014		
FeO	21.4993	0.2992	0.2992	0.2992	0.5581		
Al ₂ O ₃	27.1211	0.2660	0.5320	0.798	0.9922		
V ₂ O ₃	0.2617	0.0017	0.0034	0.0051	0.0063		
Cr ₂ O ₃	37.0439	0.2437	0.4874	0.7311	0.9090		
SiO ₂	0.0222	0.0004	0.0004	0.0008	0.0007		
TiO ₂	0.2267	0.0028	0.0028	0.0056	0.0053		
P ₂ O ₅	0.0329	0.0002	0.0004	0.001	0.0007		
Total	98.4796			2.1444	3.0388		
Oxygen factor=4/2.1445 =1.865 Mg/(Mg+Fe) i.eMg# = 0.361, Cr/(Cr+Al) i.eCr# = 0.577							

In general, peridotites are of two sub-types. The first subtype is the harzburgite (metamorphic peridotite) which is associated with the common ophiolites and represents depleted sub-oceanic mantle rock that underlies fast spreading center. The second subtype is lherzolite which is less depleted and less common in ophiolites that characterizes sub-continental mantle diapirs and slow spreading center (Boudier and Nicolas, 1985). The spinels have different range in composition in terms of Cr# and Mg# variations of less depleted lherzolites compared to those of other rock types of ophiolite suites, as shown in the (**Fig. 3.2.4.2**). The fractional crystallization or partial melting process results in an increase in spinel Cr# and amount of increase in Cr# appears to be directly related to the degree of melting (Dick and Bullen, 1984; Talkington and Malpas, 1984). From the **figure 3.2.4.2**, it is noted that the position of spinels of Manipur Ophiolite Belt fall in the lherzolite field, one at lower

margin and other two at upper margin, reflecting different levels of partial melting of the host rocks.

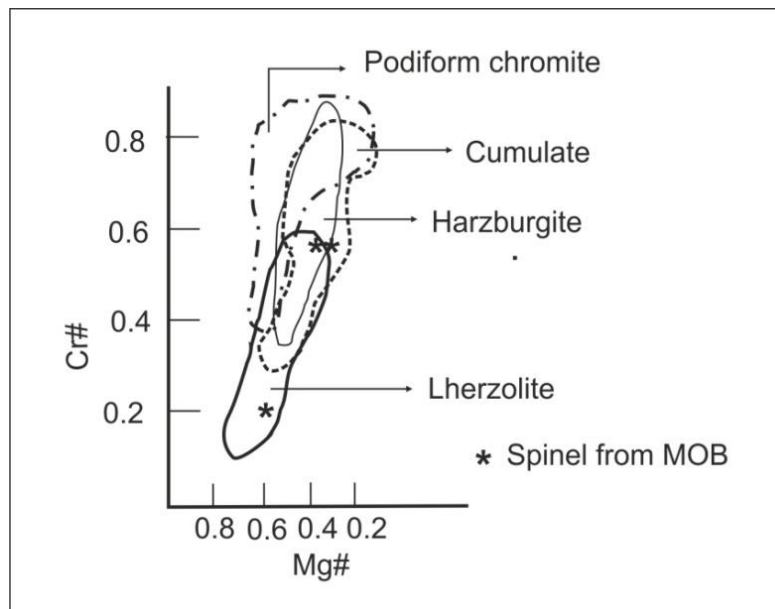


Fig. 3.2.4.2:
Compositional fields of Spinel of host rocks constituting the ophiolite suite (after Pober and Fauph, 1980). The star marks indicate the plot of spinels from Manipur Ophiolite.

The fertile lherzolite with $Cr\# < 0.2$ are most abundant than other kind of peridotites in the sub-continental upper mantle (Nixon, 1987). $Cr\#$ value of Manipur Ophiolite peridotite holds good to the range found in common sub-continental upper mantle rocks.

3.3 Bulk Rock Geochemistry

From Different locations of Manipur Ophiolite Belt, eight (8) representative samples were analyzed using X-ray fluorescence (XRF) spectrometer with recommended matrix corrections at the Department of Instrumentation and USIC, Lab no 201302(3067-3074), Gauhati University, Guwahati for major and minor element oxides, and also trace elements. The major and minor element oxides data

are reproduced in **table 3.3.1**, whereas the data of trace elements are shown in **table 3.3.2.1**

In addition to the eight trace elements of XRF analysis as given in **table 3.3.2.1**, five (5) REE's were also analyzed by the ICP (MS), at Wadia Institute of Himalayan Geology(WIHG), Dehradun, the result of which is enumerated in the **table 3.3.2.2A**.

Table 3.3.1: Chemical analysis (XRF) data of ultramafic rocks from Manipur Ophiolite Belt (Major and Minor elements in wt %)

Oxides	(1) F1S1- D	(2) F1S2- B	(3) F1S3- A	(4) F1S4- A	(5) F1S5- A	(6) F1S9- A	(7) F3-2	(8) F39A	Mean
SiO ₂	34.28	39	37.23	38.51	38.66	40.91	34.97	35.54	37.385
Al ₂ O ₃	6.48	8.38	7.01	7.47	6.49	6.56	9.17	8.44	7.5
Fe ₂ O ₃ (T)	6.42	6.09	7.4	6.93	6.74	5.23	6.18	4.06	6.131
MnO	0.005	0.09	0.072	0.067	0.054	0.057	0.088	0.018	0.056
MgO	33.56	30.48	36.73	35.89	36.22	38.22	39.57	40.47	36.392
CaO	2.24	4.15	6.38	3.2	3.16	2.46	5.95	4.68	4.027
Na ₂ O	1.15	0.045	0.32	1.04	0.98	1.16	1.15	2.25	1.011
K ₂ O	0.17	0.17	0.02	0.16	0.14	0.17	0.17	0.17	0.146
TiO ₂	0.09	0.17	0.01	0.01	0.21	0.08	0.28	0.08	0.116
P ₂ O ₅	0.06	0.08	0.04	0.02	0.05	0.03	0.006	0.002	0.036
LOI	15.545	11.345	4.788	6.703	7.296	5.123	2.466	4.29	7.194

3.3.1 Geochemistry of Major and Minor Element Oxides

For geochemical studies of ultramafics of Manipur Ophiolite Belt exposed in the different locations of the study area, eight (8) representative samples were analyzed (**Table 3.3.1**). During the process of serpentinisation, oxidation of iron thereby formation of secondary magnetite as by product (alteration of olivine except primary spinel to serpentine) is the major chemical change. So, Fe_2O_3 is converted to FeO while calculating the ratio of $\text{MgO}/(\text{MgO}+\text{FeO})$ so as to give the ratio of the unserpentinised parent rocks. Orthopyroxene and olivine have virtually the same ratio of $\text{MgO}/(\text{MgO}+\text{FeO})$, the values in case of Manipur Ophiolite ultramafics being 0.83 and 0.84. Hence, variation in the proportion of orthopyroxene and olivine in the ultramafic rocks does not significantly affect this ratio for the total rock (Coleman, 1977, Khuman and Soibam, 2010). The most of the values of the Manipur ultramafics are found clustering around 0.83-0.88, some having about 0.8. It also can be recalled what was mentioned above that when the degree of serpentinization has been very extensive, all the secondary spinels have been perished. Therefore, the more the value $\text{MgO}/(\text{MgO}+\text{FeO})$, shows the less the degree of serpentinisation and the less the value of $\text{MgO}/(\text{MgO}+\text{FeO})$, the more the degree of serpentinisation. So, in the ultramafic rocks of less $\text{MgO}/(\text{MgO}+\text{FeO})$ value, all the secondary spinels have been perished. Therefore, the lesser value of the ratio could be attributed to the loss of materials from the system on account of certain processes related with serpentinisation. Consequently, it is assumed that the ultramafic rocks of Manipur ophiolite have an extreme restricted range of $\text{MgO}/(\text{MgO}+\text{FeO})$ value. The change in $\text{MgO}/(\text{MgO}+\text{FeO})$ value reflects change in the composition of the co-existing orthopyroxene and olivine. Hence, it appears that even though the different ultramafic rocks of the ophiolite belt in Manipur had different proportion of olivine and orthopyroxene, their compositions were almost the same. Because of variation of degree of serpentinisation, there is a variation in value of lost in ignition (LOI) in ultramafic rocks of Manipur Ophiolite belt. The LOI value ranges from 15.5 (sample no F1S1-D) to 2.5 (sample no F3-2) indicating important addition of volatile components during alteration resulting various degree of serpentinisation.

In Manipur Ophiolite Belt, orthopyroxene, clinopyroxene and spinel are minerals in which Al_2O_3 have been accommodated. Metamorphic peridotitic harzburgite and dunite have mean 0.89% and 0.35% Al_2O_3 content respectively (Coleman, 1977). The most of the ultramafics of Manipur Ophiolite Belt have Al_2O_3 content higher than 5%, the highest being 9.1 % (Sample F3-2); and the average is 7.5 %. The higher value Al_2O_3 content indicates higher proportion of clinopyroxene phase than that of normal ophiolitic harzburgite and dunite; and more fertility (less depleted) of source. And, the chromium content ranges from minimum of 411 to maximum of 1126 ppm and the average of 604.5 ppm, i. e. 0.06045 %. Therefore, the average 100 Cr/ (Cr + Al) value is about 8%. This value is nearer to that of average Al – spinel lherzolite (Carswell, 1980, Table 6), which has been computed to be 13.5 (Value of chrome-spinel lherzolite is 16.2 and that of chrome lherzolite is 28.1). Lower the value of 100 Cr/ (Cr + Al) also indicates fertile mantle source and lesser degree of depletion on account of partial melting.

Loney *et al.*, (1971) reported 0.005% Na_2O and 0.0002% K_2O for dunite; and 0.012% Na_2O and 0.001% K_2O for harzburgite indicating that metamorphic Ophiolite peridotites were truly depleted and that trace amounts of alkalis are present within the pyroxenes. But the Manipur Ophiolite ultramafics are found to have an average of 1.01% Na_2O and 0.15 % K_2O ; which is exponentially higher than those values for dunite and harzburgite given by Loney *et al.*, (1971). Moreover, the clinopyroxene and orthopyroxene of Manipur Ophiolite ultramafics contain average Na_2O values of 0.34% and 0.03% respectively. It indicates that the ultramafics of the studied area are extremely enriched in alkalis indicating fertile source and/or crustal contamination.

When plotting the value of $(\text{Al}_2\text{O}_3 + \text{CaO} + \text{Na}_2\text{O} + \text{K}_2\text{O} + \text{TiO}_2)/\text{SiO}_2$ versus MgO/SiO_2 (**Fig. 3.3.1.1**) it is found that the ultramafic rocks of Manipur Ophiolite Belt fall in the field of ultrabasic rocks dredged from oceanic floors. From the AFM ($\text{Na}_2\text{O} + \text{K}_2\text{O} - \text{FeO} - \text{MgO}$) diagram (**Fig. 3.3.1.2**) and ACM ($\text{Al}_2\text{O}_3 - \text{CaO} - \text{MgO}$) diagram (**Fig. 3.3.1.3**), it is found that most of the analyzed ultramafic rocks are pigeonholed within the fields of metamorphic peridotite.

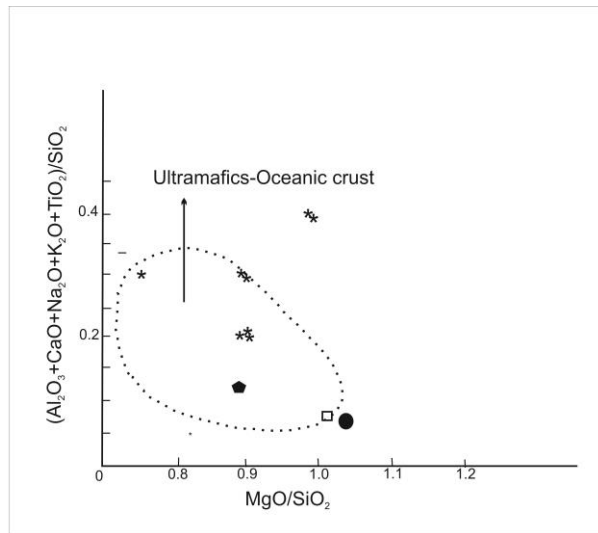


Fig. 3.3.1.1:
The plot of $(\text{Al}_2\text{O}_3 + \text{CaO} + \text{Na}_2\text{O} + \text{K}_2\text{O} + \text{TiO}_2)/\text{SiO}_2$ versus MgO/SiO_2 of the ultramafics of Manipur Ophiolite (stars). Open square represents average of 32 rocks of Ophiolite Suites (Hyndmen, 1985); closed pentagon represents average of Oceanic crust ultramafics (Sheman and Lutts, 1975); and Closed circle represents Alpine type ultramafics (Sheman and Lutts, 1975).

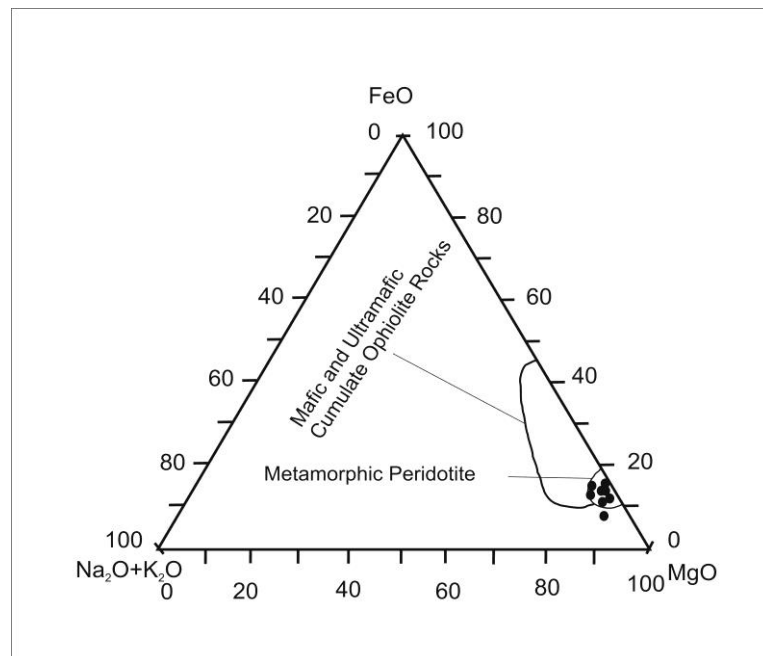


Fig. 3.3.1.2:
AFM plot of Manipur Ophiolite ultramafics. $(\text{Na}_2\text{O} + \text{K}_2\text{O})$ -FeO-MgO plot shows that the ultramafics are pigeonholed within the field of metamorphic peridotite (modified after Coleman, 1977 and Nelson 2007).

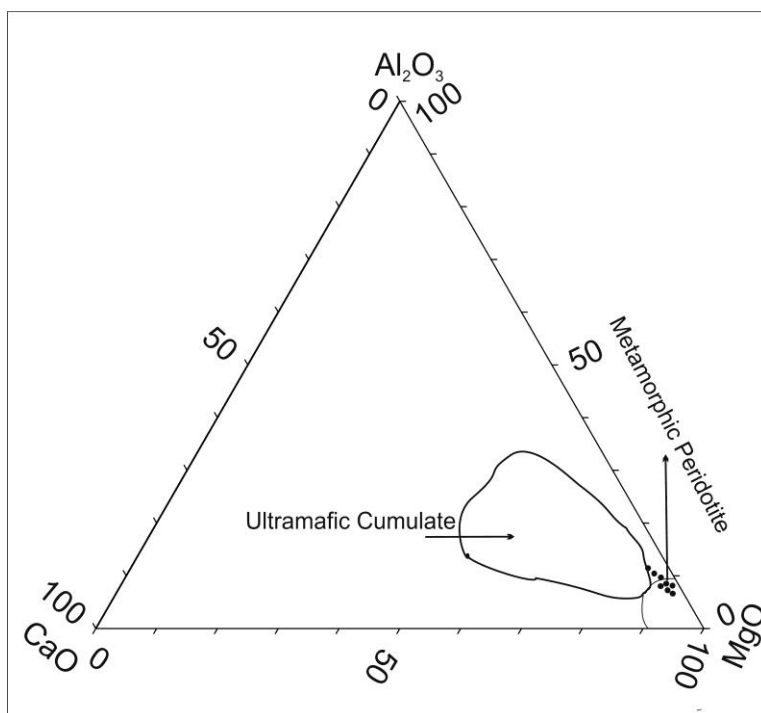


Fig. 3.3.1.3:

ACM (Al_2O_3 -CaO-MgO) plot of Manipur Ophiolite ultramafics shows that the ultramafics are pigeonholed within the field of metamorphic peridotites.

3.3.2 Trace and Rare Earth Elements Geochemistry

Study of characters of the trace and rare earth elements is used as an important tool for better understanding and characterization of ultramafics of Manipur Ophiolite Belt. But to establish an average value of trace elements for the ophiolite assemblage is not a simple task. The average amounts of trace elements and rare earth elements of the study area are given in **table 3.3.2.1** and **table 3.3.2.2A** and their comparison with those in metamorphic ophiolitic peridotites, ultramafics/mafic cumulates and ophiolitic gabbros are also given in **table 3.3.2.3**.

Table 3.3.2.1: Chemical analysis (XRF) data of ultramafic rocks from Manipur Ophiolite Belt (Trace elements in ppm).

Element	(1) F1S1-D	(2) F1S2-B	(3) F1S3-A	(4) F1S4-A	(5) F1S5-A	(6) F1S9-A	(7) F3-2	(8) F3-9A
Ba	14	30	75	120	51	22	78	35
Ce	70	34	38	76	55	43	25	40
Co	79	62	111	90	51	49	42	106
Cr	411	558	774	1126	443	550	461	511
Cu	9220	8550	1005	7693	5001	4891	5552	7693
Nb	12	4	4	8	7	5	1	7
Nd	1	19	12	11	21	20	18	20
Sr	67	50	48	200	33	189	46	86
Y	7	24	19	9	10	30	9	15
Zn	61	70	64	45	105	99	65	90
Zr	41	170	75	85	130	100	58	140

Table 3.3.2.2A: Data of selected REE in ppm (ICPMS) of ultramafic from Manipur Ophiolite Belt.

Element	(1) F1S2B	(2) F1S3A	(3) F1S4A	(4) F1S5A	(5) F3-2	(6) Mean
La	0.12	0.14	0.16	0.1	0.21	0.146
Ce	0.2	0.34	0.33	0.24	0.39	0.3
Pr	0.03	0.04	0.05	0.04	0.05	0.042
Nd	0.22	0.34	0.00	0.25	0.23	0.268
Sm	0.07	0.05	0.07	0.12	0.05	0.072
Eu	0.02	0.02	0.03	0.03	0.02	0.024
Gd	0.12	0.06	0.12	0.19	0.09	0.116
Tb	0.03	0.01	0.03	0.04	0.02	0.026
Dy	0.22	0.09	0.19	0.28	0.14	0.184
Ho	0.06	0.02	0.05	0.07	0.04	0.048
Er	0.17	0.07	0.13	0.02	0.11	0.1
Tm	0.03	0.01	0.02	0.03	0.02	0.022
Yb	0.19	0.08	0.15	0.23	0.13	0.156
Lu	0.03	0.01	0.03	0.04	0.02	0.026

Table. 3.3.2.2B: Normalised (ICPMS) analysis data of selected REE in ppm of ultramafics from Manipur Ophiolite Belt. (Normalised after Sun and McDonough, 1989).

Elements	F1S2B	F1S3A	F1S4A	F1S5A	F3-2	Mean
La	0.506	0.591	0.675	0.422	0.886	0.616
Ce	0.327	0.556	0.539	0.392	0.637	0.490
Pr	0.316	0.421	0.526	0.421	0.526	0.442
Nd	0.471	0.728	0.642	0.535	0.493	0.574
Sm	0.458	0.327	0.458	0.784	0.327	0.471
Eu	0.345	0.345	0.517	0.517	0.345	0.414
Gd	0.584	0.292	0.584	0.925	0.438	0.564
Tb	0.802	0.267	0.802	1.070	0.535	0.695
Dy	0.866	0.354	0.748	1.102	0.551	0.724
Ho	1.060	0.353	0.883	1.237	0.707	0.848
Er	1.027	0.423	0.785	0.121	0.665	0.604
Tm	1.176	0.392	0.784	1.176	0.784	0.863
Yb	1.118	0.471	0.882	1.353	0.765	0.918
Lu	1.181	0.394	1.181	1.575	0.787	1.024

The higher values of the trace elements concentration in Manipur Ophiolite Belt than the normal peridotites and ultramafics (**Table 3.3.2.3**) except Co and Cr indicate that the ultramafics of the study area is from fertile mantle source and therefore inferred to be of sub continental mantle source.

Table 3.3.2.3: Average amount of trace elements in ophiolitic metamorphic peridotite, ultramafic rocks and gabbros compared with that of Manipur Ophiolite ultramafics in ppm (Coleman 1977).

Elements	(1) Ophiolitic metamorphic Peridotite	(2) Ultramafic rocks	(3) Gabbros	(4) Ultramafics of Manipur Ophiolite
K	23	200	797	-
Rb	0.058	~1	1	-
Sr	0.38	~20	116	89.8
Ba	2	~0.4	~2	53
U	0.008	~0.02	-	-
Th	0.01	~0.06	-	-
Zr	5	30-45	~15	99.8
Co	114	110	86	73.75
Cu	14	~30	35	6200.6
Ni	2280	~1500	640	-
Ti	48	300	1355	-
V	25	40	226	-
Pb	0.02	0.05	-	-
Cr	5000	2400	625	604.2
Ce	-	-	-	47.6
Nb	-	-	-	6
Y	-	-	-	15.3
Zn	-	-	-	74.8

Table 3.3.2.4: Normalised values of amount of rare earth elements in ophiolitic metamorphic peridotite, mafic-cumulate, ultramafics and gabbros compared with that of Manipur Ophiolite ultramafics in ppm (Coleman 1977).

Elements	(1) Ophiolitic metamorphic peridotite		(2) Mafic cumulates		(3) Upperlevel gabbro		(4) Manipur ophiolite	
	Average	Normalised	Average	Normalised	Average	Normalised	Average	Normalised
La	0.068	0.23	0.065	0.22	0.443	1.48	0.146	0.616
Ce	0.072	0.09	0.316	0.38	1.68	2	0.3	0.49
Pr	0.006	0.05	-	-	-	-	0.042	0.442
Nd	0.026	0.04	0.384	0.66	1.60	2.76	0.268	0.573
Sm	0.008	0.04	0.173	0.82	0.644	3.07	0.072	0.47
Eu	0.0043	0.06	0.119	1.61	0.323	4.36	0.024	0.413
Gd	0.0125	0.04	0.297	0.93	1.38	4.31	0.116	0.564
Tb	0.0007	0.0014	-	-	-	-	0.026	0.695
Dy	0.0175	0.06	0.424	1.40	1.41	4.65	0.184	0.724
Ho	0.003	0.04	-	-	-	-	0.048	0.848
Er	0.0215	0.10	0.275	1.31	0.763	3.63	0.1	0.604
Tm	0.001	0.03	-	-	-	-	0.022	0.862
Yb	0.016	0.094	0.306	1.8	0.74	4.35	0.156	0.917
Lu	0.004	0.129	0.053	1.7	0.126	4.1	0.026	1.023

Rare Earth Elements (REE) are more resistant to weathering and hydrothermal alteration than other elements and therefore their abundance patterns may provide clues to decipher petrogenesis of igneous rocks. For the present work, five representative samples were analyzed for selected REE's by the ICP (MS), at WIHG, Dehradun, the result of which is enumerated in the **table 3.3.2.2A**. The normalized concentration (based on chondritic meteorites) of the REE of ultramafics of the study area based on their mean values and comparison of this value with that of metamorphic peridotite, mafic- cumulate and upper level gabbro is shown in **table 3.3.2.4**. From this table we come to know that most of the elements in the ultramafics of the study area, there are two or three orders of magnitude more than common ophiolitic metamorphic peridotites and even one order of magnitude more than the common ophiolitic gabbros.

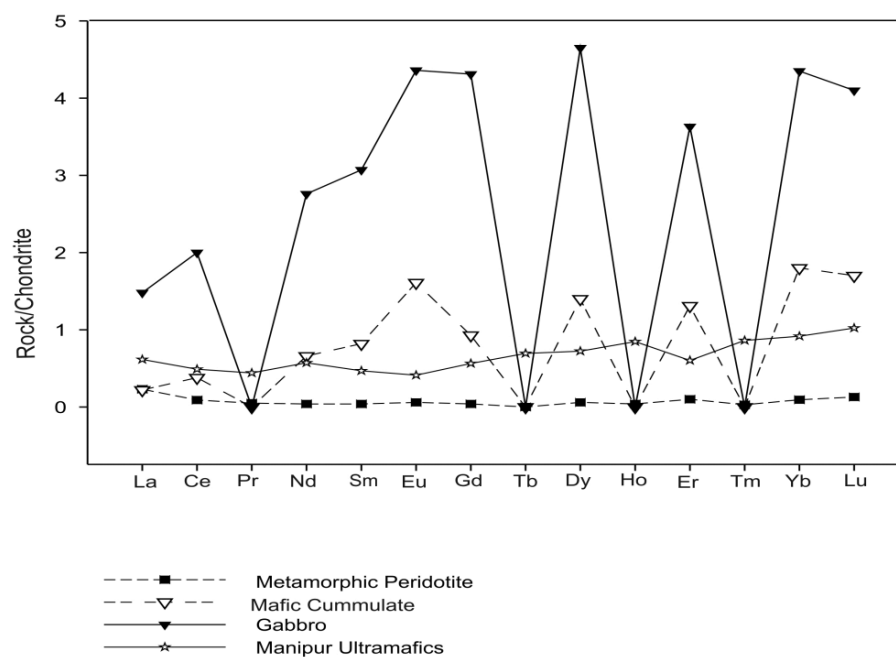


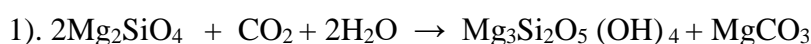
Fig. 3.3.2.5:
Comparison of REE pattern of ultramafics of Manipur Ophiolite Belt with that of normal ophiolite sequences.

Average REE pattern for separate members of the normal ophiolite sequences and that of Manipur ophiolite are plotted (**Fig. 3.3.2.5**) as the function of increasing atomic number. The high value of REE in the Manipur ophiolitic ultramafics (except very few) than the normal metamorphic peridotites is another reason to infer a fertile source possibly of sub- continental upper mantle and therefore is of lherzolite sub-type (Jackson and Thayer, 1972).

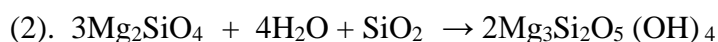
Chapter 4

SERPENTINISATION

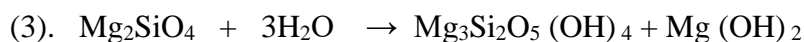
The term serpentine is the name given to a mineral group that consists of three main polymorphs- lizardite, chrysotile and antigorite. Serpentinisation is the process as a result of which the mafic minerals of rocks usually ultramafics that are formed in an anhydrous high temperature system are changed into serpentine group of minerals owing to retrograde metamorphism on account of subjection of the rock into the equilibrium condition of lower temperature and water rich environment. Modifications of ultramafics of ophiolite assemblage by such retrograde metamorphic processes are very common. Possible serpentinisation reactions involving chiefly olivine are as follows (Hess, 1955; Best, 2001):



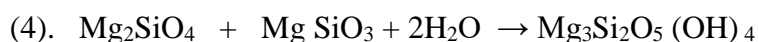
Olivine (Forsterite) introduced Serpentine Magnesite



Olivine (Forsterite) introduced Serpentine



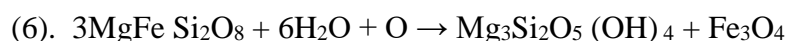
Olivine (Forsterite) introduced Serpentine Brucite



Olivine (Forsterite) Enstatite Serpentine



Olivine (Forsterite) introduced Serpentine removed in solution



Fe-bearing Forsterite introduced Serpentine Magnetite

In the above reactions, the first four reactions required large volume expansion in denser mineral assemblages, whereas the fifth and sixth reaction maintain almost constant volume; but with considerable MgO and SiO₂ lost in the fifth reaction.

The serpentine minerals may have overlapping fields of stability that are controlled by composition, oxygen fugacity and activity of water. Lizardite and chrysotile can be formed at temperatures less than 350°C down to ambient temperatures (Barnes and O'Neil, 1969), whereas antigorite is apparently stable upto temperatures slightly above 500°C, occurring mostly in high grade metamorphic terrains (Chidester, 1962). Thus, serpentine can be formed at temperature as high as 500°C, either by action of pure water on olivine-enstatite mixture, or from olivine alone if the aqueous solution is rich in CO₂ and so is capable of removing magnesia from the system. Above 500°C, olivine cannot be converted to serpentine by any means. In the presence of aqueous solution capable of adding SiO₂ or removal of MgO, olivines are liable to other types of alteration at higher temperature.

1. Between 500⁰ and 625⁰C., olivine → Talc.
2. Between 625⁰ and 800⁰C., olivine → enstatite → Talc.
3. Above 800⁰. Olivine → enstatite.

To decipher the actual mode of serpentinisation in ultramafic rocks is of paramount importance in solving certain variety of petrologic problems. Ascertaining the kind of serpentinisation with the possible reactions involved in relation, either with constant volume or with volume increase, and any other related process, can also be of good value in establishing P-T conditions. Consequently, recognition of serpentine species, their chemistry with respect to that of their respective parent rocks (ultramafics) and ascertaining the kind of the possible reactions are very helpful in deciphering the tectonic conditions prevailed in due course of serpentinisation.

In Manipur Ophiolite Belt, extremely serpentinised ultramafic massifs are found to have very occasional lenses of leucocratic vein rocks filling in very small veinlets which are generally few centimeters wide that pinches out after few meters. Besides these vein rocks, limited cobbles as well as fragments of some leucocratic rocks are also found in some river beds particularly in the Namjet Lok near the Kwatha village and Lokchao river of Tengnoupal district of the state. These leucocratic rocks are inferred as rodingite (**Fig. 2.3.1.4**), which is identified to be

hydrogrossular major. Rodingites are metasomatic rocks composed mostly of grossular-andradite garnet and calcic pyroxene. They are commonly associated in the ophiolite belt in Manipur with mafic rocks which are in the host of serpentinised ultramafic rocks. The mafic rocks are altered by high pH - Ca^{+2} and OH^- -rich fluid, which are byproduct of the serpentinisation giving rise to rodingites. As rodingites are formed on account of metasomatism of varied rock types associated with serpentinites and the metasomatism is due to the processes of serpentinisation on account of tectonic emplacement of the ophiolite but not with high-temperature contact metasomatism (Coleman, 1977), rodingites and rodingitisation are also discussed along with the phenomena related to the processes of serpentinisation. Rodingites are small-scale localized metasomatic occurrences and are not related to a regional metasomatism (Coleman, 1997).

4.1 Petrography and Mineralogy

Serpentine is typically colourless to pale yellow or pale green in plane polarized light and it is commonly intergrown with opaque Cr-spinel and magnetite. In thin section, it is difficult to distinguish the different polymorphs. But generally, lizardites have platy habit, chrysotiles are fibrous and antigorites may either be fibrous or lath shaped crystals (Ehler and Blatt, 1987).

When olivine grains are serpentinised, the anastomosing veinlets of cross fiber serpentine resulting to a mesh textured aggregate appear to fill in the open spaces in between the numerous residual angular grains that could have been the broken pieces from original olivine crystals (**Fig. 3.1.5**), possibly due to expansion in volume. The bastites on the other hand, even though are pseudomorphs after the pyroxenes, which have a number of cleavage planes, emerged as compact grains obliterating the original pyroxene cleavages. The open spaces of cleavages of pyroxene have been occupied by increased volume of serpentine i.e., bastite. These features appear to indicate that the serpentinisation took place along with an increase in volume, consequently having relationship with spreading tectonics. The concentration of fine grained secondary spinels mostly along the continuous lines of

original fractures of olivine crystals indicates isotropic expansion of volume by virtue of which the original shapes are maintained (**Fig. 3.1.8**).

Considering just the minerals forsterite, enstatite and serpentine, a simple calculation (cf. O'Hanley, 1996) shows that if the volume is conserved, approximately 35% of the original MgO and SiO₂ must be removed, with little evidence to indicate where these components went. The system would be open with respect to all components. On the other hand, if it is assumed that MgO and SiO₂ are immobile, a similar calculation shows that the hydration of forsterite and enstatite would lead to an increase in volume by as much as 53%, which appears to be disproportionately large with respect to the field relations in terms of their respective emplacement. The system would be closed with respect to MgO and SiO₂, but open with respect to H₂O. While the extreme positions are equally untenable for different reasons, it is concluded that an increase in volume generally accompanies serpentinisation (O'Hanley, 1992, 1996).

The accumulation of secondary spinel (mostly magnetite) grains along the open fractures of olivine indicates migration of Mg⁺², Fe⁺² (oxidized as Fe⁺³) and SiO₂ outward from the crystalline olivine into open channels (cf. Abbott *et al.*, 1999). The pyroxenes in the ultramafics of the Manipur Ophiolite Belt contain considerable amounts of iron (maximum of 6.7 wt. %). As when serpentinised, no magnetite grain is formed within the bastite grains; it is assumed that there is limited volume expansion at the later stage of serpentinisation. Because of the unavailability of sufficient space for concentration of secondary spinels, ions in the form of Fe⁺³, Mg²⁺ and SiO⁺² must have been either migrated from the grains of pyroxene to those of olivine where open channels are available or are locked up in the structure of serpentine. But the system as a whole appears to be almost closed with these components with respect to serpentinisation during the spreading regime because of the volume expansion. The MgO/(MgO+FeO) values of the majority of the samples of the ultramafics fall around 0.83-0.87 as against the original value of about 0.845 of olivine (Chapter 3, section 3.3.1). At the later stage of emplacement (obduction during the collision regime) of the ophiolite complex, certain portions of the massifs appear to have been suffered limited serpentinisation at constant volume. It is

proved by the limited occurrence of rodingite lensoids in the form of small veins in the extensively serpentinised ultramafic massifs, since rodingites are recognized as by-products of the serpentinisation processes (Coleman, 1977). Metasomatism to form rodingite is possible only when ionic constituents produced during serpentinisation are flown out of the system; and hence the system could have been opened and therefore the volume during this phase of serpentinisation must have been conserved. Consequently, there must have been processes of serpentinisation during the compressive tectonic regime. The ultramafics of the study area must have experienced less degree of serpentinisation during the compressive tectonic regime as revealed by the limited and localized occurrence of rodingite. During the process of serpentinisation, Mg, Ca and Si must have been withdrawn from the system indicating constant volume replacement (Khuman, 2009).

During the processes of serpentinisation of ultramafic rocks, some typical minerals are produced which can be shown on a compositional triangle (**Fig. 4.1.1**) whose corners are MgO, SiO₂, and H₂O+CO₂ (cf. Ehlers & Blatt, 1987). In the figure, the line drawn through the serpentine composition point from the H₂O apex of the triangle; the lower end of the line intersects the MgO-SiO₂ edge at X between the composition points of forsterite and enstatite.

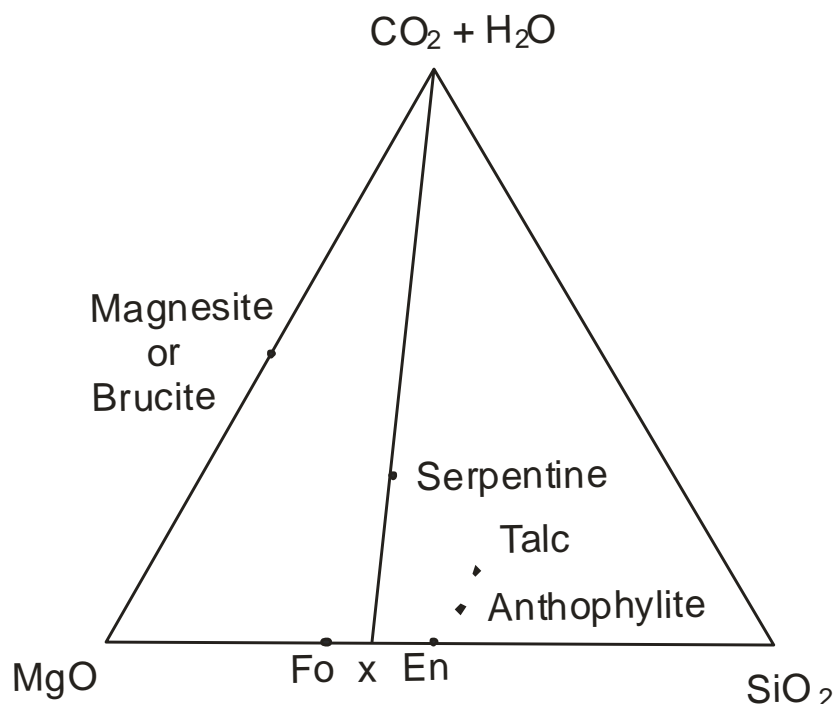


Fig. 4.1.1:
Minerals present in the system $\text{MgO-SiO}_2\text{-H}_2\text{O+CO}_2$

This intersection point indicates the ratio of MgO and SiO_2 that is contained in serpentine. If an ultramafic rock contains the same ratio of MgO and SiO_2 (in the form of forsterite and enstatite), metamorphism in the presence of water could produce a rock consisting entirely of serpentine. On the other hand, if the ultramafic rock was a dunite that contained only forsterite, serpentinisation would leave an excess of MgO . In this case, serpentinisation would produce mainly serpentine and minor amounts of a more MgO rich phase such as brucite or periclase (or perhaps magnesite if some CO_2 were also present). Serpentinisation of an ultramafic rock composed of enstatite (or a mixture of enstatite and forsterite that fall between the enstatite composition point, and point X) would produce serpentine and more silica rich mineral such as talc. Although both types of serpentine assemblages may be present in the same ultramafic body if it is compositionally layered, the average ultramafic rocks fall in composition between forsterite and the point X.

The absence of magnesite or brucite but the presence of talc in the serpentinites of the ophiolite complex (Khuman, 2009) indicates that the parent rocks from which the serpentinites were derived may be peridotites richer in silica

than dunite. And, therefore, these could be harzburgite and/or lherzolite rather than dunite. This supports the modal analysis data and related aspects of the ultramafic rocks of the Ophiolite complex of Manipur as discussed in Chapter 3. Again, as brucite and/or magnesite are absent and since the ultramafic rocks are silica under saturated, the first three reactions of the six possible equations given above are ruled out in the case of serpentinisation of the ultramafic rocks of Manipur Ophiolite Belt.

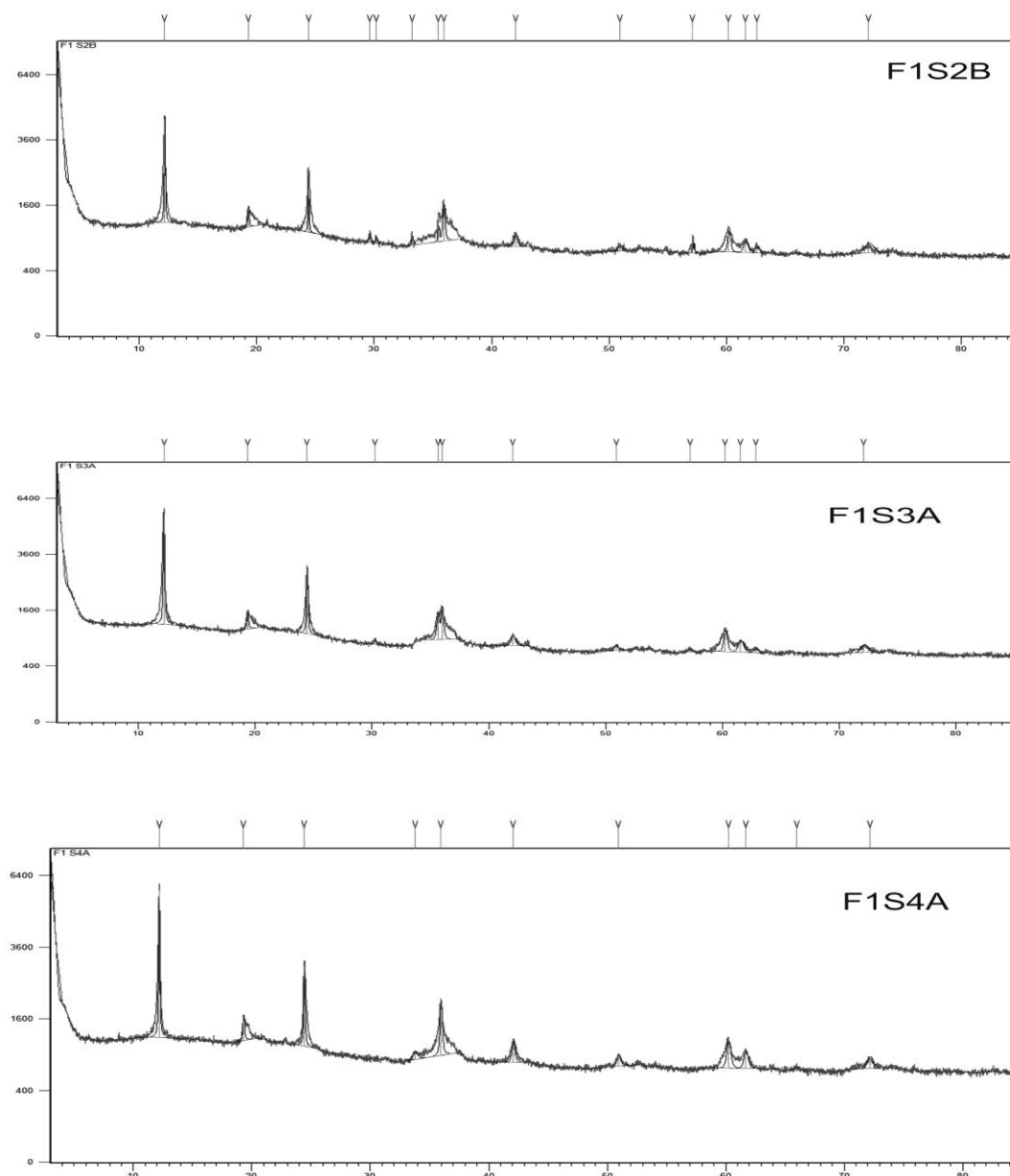


Fig. 4.1.2 A:
X-ray diffraction (XRD) patterns of 3 (three) representative serpentinite samples from Manipur Ophiolite Belt.

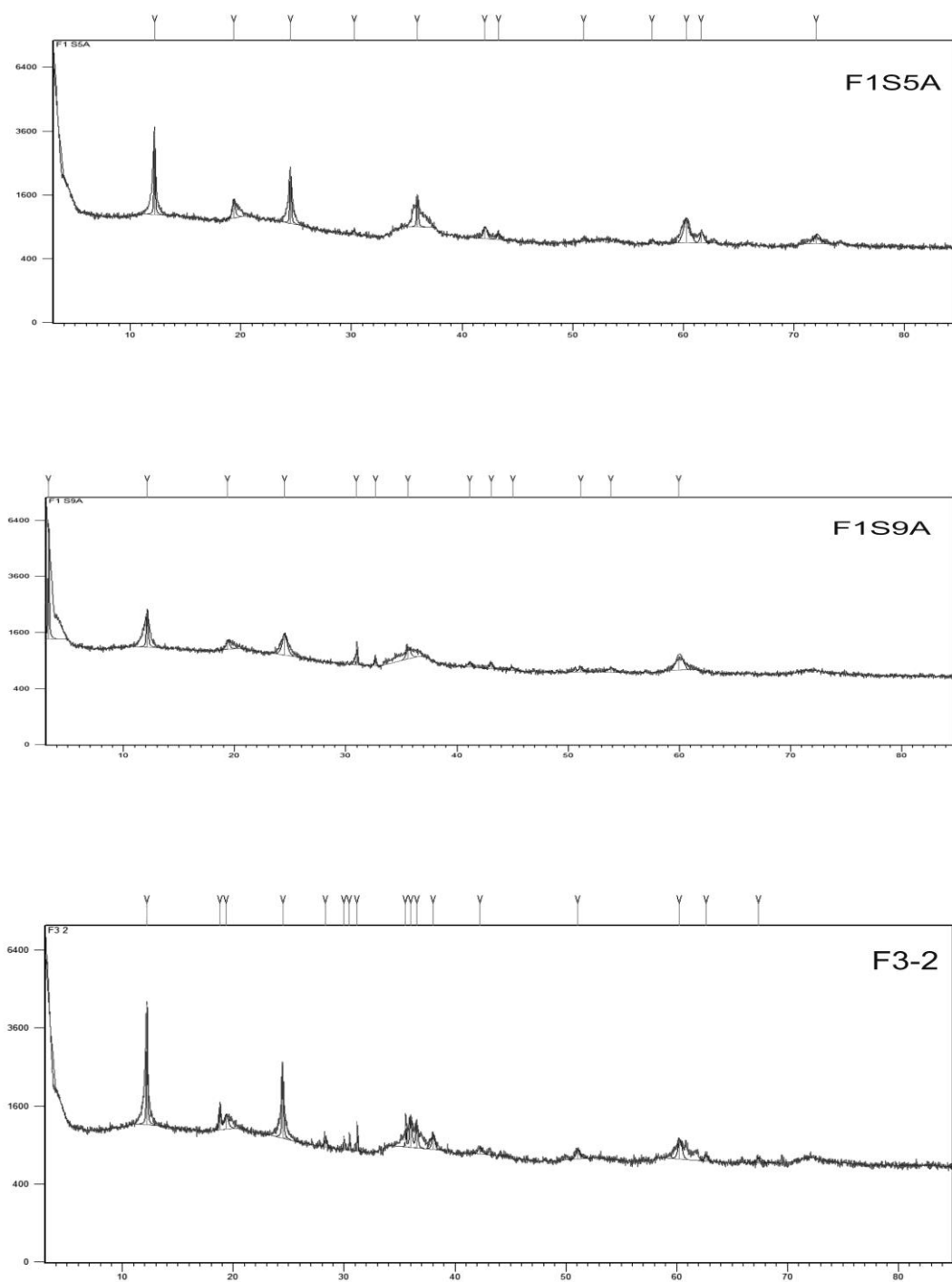


Fig. 4.1.2 B:
X-ray diffraction (XRD) patterns of 3 (three) representative serpentinite samples from Manipur Ophiolite Belt.

For detail studies of the different mineral phases and their chemical compositions of serpentine minerals of ultramafic rocks of the ophiolite belt in Manipur, the X-Ray diffraction (XRD) analysis is carried out at Wadia Institute of Himalayan Geology, Dehradun. Altogether 6 (Six) representative samples of peridotitic serpentinites from different parts of the Manipur Ophiolite Belt are analysed (**Fig. 4.1.2A and 4.1.2B**). From the result of the analysis, it is found that the types of serpentine of the ultramafic rocks are mainly of ortho- and clino-chrysotile, nickel serpentine (nepouite), lizardite, etc. (**Table 4.2.4**). The rareness of antigorite variety indicates that serpentinisation of Manipur Ophiolite Belt mostly took place below 350⁰C (cf. Barnes and O'Neil, 1969). This result is also consistent with MgO vs SiO₂ plot (**Fig. 4.1.3**). It also further suggests that the Manipur Ophiolite belt have not undergone extensive progressive metamorphism (cf. Chidester, 1962).

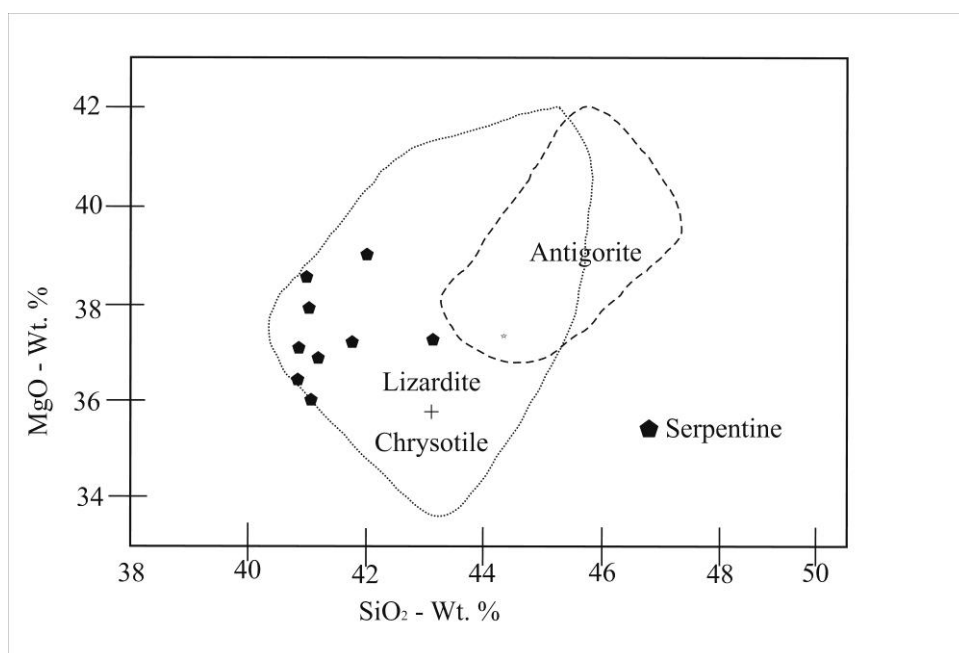


Fig. 4.1.3:
SiO₂ vs. MgO plot for the analysed serpentine minerals in serpentinites from Manipur Ophiolite Belt.

4.2 Mineral and Bulk Rock Geochemistry

This section will try to bring out the chemical aspects of serpentinisation so that all the discussions made in the previous section of this chapter and the related sections of chapter-3 are more strengthened and/or some new ideas/thoughts are put forth. Therefore, EPMA data of the different phases of serpentinites from different localities and XRF data of serpentinites will be critically examined with respect to serpentinisation and tectonic evolution of ultramafic rocks of Manipur Ophiolite Belt. The EPMA analysis has been carried out at DST-SERB National Facility, Department of Geology (Centre of Advanced Study), Institute of Science, Banaras Hindu University using Electron Probe Micro Analyzer CAMECA SXFive instrument.

The mean of the analytical data (EMPA) of 9 representative samples of the compositions of serpentine are given in **table 4.2.1**(EPMA data) and their recalculated values are shown in **table 4.2.2** (Recalculation table) for derivation of the exact composition of serpentine. The composition is found to be $(\text{Mg,Ca,Na,Ni,Al,Fe,Cr})_3\text{SiO}_2\text{O}_5(\text{OH})_4$. The MgO/SiO_2 ratio of serpentine is 0.88 (\approx 0.90) and the $\text{MgO}/(\text{Mg}+\text{FeO})$ ratio is found to be 0.89.

Table 4.2.1: Serpentine Composition of ultramafic rocks from parts of MOB in percent.

Wt% Oxide	(1) F1-S2B	(2) F1-S1D	(3) F2-B1	(4) F2-B2	(5) F3-2	(6) F3-3B	(7) F3-9A	(8) F3-5A1	(9) F3-5A2	Mean
Na ₂ O	0.029	0.049	0.015	0.099	0.016	0.015	0.059	0.175	0.113	0.063
MgO	37.759	36.242	38.681	35.370	38.844	36.316	34.120	35.605	35.174	36.457
CaO	0.022	0.008	0.001	0.156	0.221	0.287	0.082	0.079	0.073	0.103
MnO	0.012	0.000	0.000	0.000	0.026	0.000	0.042	0.000	0.000	0.009
FeO	2.911	4.748	1.435	2.474	6.255	5.634	6.881	3.883	5.380	4.400
NiO	0.044	0.038	0.085	0.322	0.256	0.022	0.178	1.478	1.833	0.473
Al ₂ O ₃	1.277	2.990	1.916	1.367	0.099	1.666	2.260	0.776	0.327	1.409
V ₂ O ₃	0.003	0.000	0.000	0.000	0.000	0.000	0.000	0.000	0.000	0.000
Cr ₂ O ₃	0.030	0.041	1.141	0.002	0.000	0.022	0.509	0.059	0.012	0.202
SiO ₂	41.418	41.162	40.587	40.742	42.002	39.361	40.563	43.474	41.136	41.161
P ₂ O ₅	0.019	0.021	0.002	0.000	0.002	0.000	0.005	0.004	0.000	0.006
Total	83.686	85.299	83.863	85.247	87.721	83.362	84.717	85.547	84.050	84.833

Table 4.2.2: Recalculation of Serpentine Analysis.

Name of Oxide	(1) Wt%	(2) Mol Wt	(3) Mol. Propn of Oxide	(4) Atomic Prop of cation or Cation Prop	(5) No. of oxygen	(6) Cation on basis of 9 Oxygen	(7) Cation Assignment	(8) Chemical Composition
SiO2	41.161	60.085	0.685	0.685	1.370	1.878	Si-1.159 1.954	Average Composition = (Mg,Ca,Na,Ni,Al,Fe,Cr) ₃ Si ₂ O ₅ (OH) ₄
Al ₂ O ₃	1.409	101.961	0.014	0.028	0.042	0.076	Al-0.076 = 2	
FeO	4.400	71.846	0.061	0.061	0.061	0.167	Fe-0.159	
NiO	0.473	74.709	0.006	0.006	0.006	0.017	Ni-0.017	
MgO	36.457	40.304	0.905	0.905	0.905	2.480	Mg-2.479	
MnO	0.009	70.937	0.000	0.000	0.000	0.000		
CaO	0.103	56.079	0.002	0.002	0.002	0.005	Ca-0.05 =2.679	
K ₂ O	0.000					0.000		
Na ₂ O	0.063	61.979	0.001	0.002	0.001	0.005	Na- 0.05	
TiO ₂	0.000					0.000		
Cr ₂ O ₃	0.202	151.990	0.001	0.002	0.003	0.005	Cr-0.007	
							OH- 4.793]=	
H ₂ O	15.723	18.000	0.874	1.748	0.892	4.793	4.793	
	100.000				3.282	9.428		
Oxygen Factor=9/3.276=2.742, MgO/SiO ₂ = 0.88, MgO/ (MgO + FeO) = 0.89								

Table 4.2.3: Recalculated values of XRF data of some ultramafics from Manipur Ophiolite Belt.

Oxides	(1) F1S1-D	(2) F1S2-B	(3) F1S3-A	(4) F1S4-A	(5) F1S5-A	(6) F1S9-A	(7) F3-2	(8) F39A
SiO ₂	34.28	39	37.23	38.51	38.66	40.91	34.97	35.54
MgO	33.56	30.48	36.73	35.89	36.22	38.22	39.57	40.47
FeO(T)= Fe ₂ O ₃ (T)x0.9	5.78	5.48	6.66	6.24	6.07	4.71	5.56	3.68
MgO/SiO ₂	0.98	0.78	0.99	0.93	0.94	0.93	1.13	1.14
MgO/(MgO+Fe)	0.85	0.85	0.84	0.85	0.86	0.89	0.88	0.92

Table 4.2.4: X- ray diffraction data of serpentinised ultramafic rocks from MOB (showing different types of serpentines)

Sample	Score	Remark/compound name
F3-2	41	Clinochrysotile
	34	Nepouite
F1S9A	49	Clinochrysotile
F1S5A	46	Clinochrysotile
	64	Beryllium Carbide
	43	Cesium Manganese Oxide Hydrate
F1S4A	69	Lizardite
	33	Pecoraite
F1S3A	55	Nepouite
F1S2B	43	Clinochrysotile
	48	Beryllium Carbide
	28	Iron Oxide

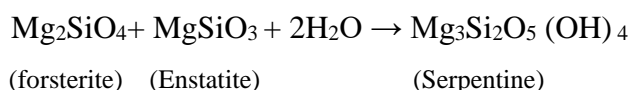
The average $\text{MgO}/(\text{MgO}+\text{FeO})$ value of about 0.867 of serpentine of the ophiolite complex of Manipur (as against the original value of about 0.845 in the parent ultramafic), indicates that the serpentinisation is an isochemical process except the introduction of water (cf. Coleman, 1977); and, therefore, confirms an increase in volume and hence imperative of serpentinisation during spreading regime. The average MgO/SiO_2 ratio for dunite is about 1.23 and if serpentinisation of dunite is accomplished only by addition of water, this ratio should remain constant (Coleman and Keith, 1971). For ophiolite harzburgites the average MgO/SiO_2 ratio is about 1.02; and for lherzolites the ratio is considerably lower and brucite is uncommon (Coleman, 1977). **Table 4.2.3** indicates that the MgO/SiO_2 ratios of the ultramafics mostly range from 0.93 to 0.99, the lowest being 0.78 and the highest being 1.14. The range of values of MgO/SiO_2 indicates that host ultramafics from which serpentinization took place range from lherzolite to harzburgite and the MgO/SiO_2 ratio of the serpentines is also falling within the range of lherzolite and harzburgite. As there was no considerable loss of the components it is observed that serpentinisation involved was associated with increase in volume.

This supports the discussions in Chapter 3 that the ultramafic rocks of Manipur Ophiolite Belt are mostly of lherzolite and harzburgite, which are the residues of spinel lherzolite source after differential partial melting. The value of MgO/SiO₂ ratio of the serpentine mineral in the analyzed samples in **table 4.2.2** conforms well to that of the ultramafics and indicates that the sample could have been derived from lherzolite parent rock.

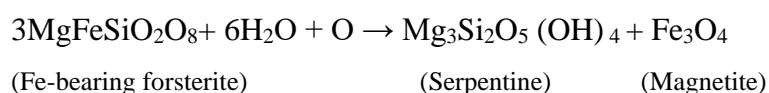
In the **table 3.1.1.1** (Modal data), it is seen that in a very few extensively serpentinised samples particularly in the sample no. F39B, F2A3, and S2 UA, almost all of the secondary spinels are perished. This appears to be related with localized later stage serpentinisation during the post spreading compressive tectonic history of ophiolite emplacement in which limited and localized rodingitisation also took place. The serpentinisation must have taken place without any change in volume as a result of which some components like Mg, Fe, Ca, etc. were lost from the system. From the above observations and discussions, logically we conclude that in Manipur Ophiolite Belt, one of the possible reactions attributed to the later stage of compressive regime is-



Such type of reaction must have taken place at a limited extent and in localized manner. During the spreading regime, the other possible reactions which must have taken place for the serpentinisation of parent ultramafics of the Manipur Ophiolite Belt are-



And



During the process of volume conserved serpentinisation, calcium oxide (CaO) component is removed from the peridotite with $\text{Ca}^{+2}\text{-OH}^{-1}$ type water (Barnes and O'Neil, 1969). Later on, this potentially active calcium hydroxide water reacts with the rocks of higher in silica than the peridotites. In the reaction the calc-silicate minerals will replace and invade the host rock whereby veins of rodingites were formed in the open fractures of the ultramafics of Manipur Ophiolite Belt. Therefore, it is inferred that rodingites are the by-product of serpentinisation processes and not the result of high temperature contact phenomenon on account of ophiolitic igneous activity.

Chapter 5

CHROMITE AND CHROMITE MINERALISATION

Chromite is an oxide mineral belonging to the spinel group. It is a complex mineral containing magnesium, iron, aluminium, and chromium in varying proportions depending on the type and environment of mineralisation, the composition of which can be represented as FeCr_2O_4 or $(\text{Fe}^{+2}, \text{Mg})(\text{Cr}, \text{Al}, \text{Fe}^{+3})_2\text{O}_4$. It is iron-black or brown black in colour with brown streak, faint sub-metallic lustre, and uneven brittle fracture and is having hardness of 5.5 and specific gravity of 4.5 to 4.8. It is the only source of chromium metal.

In the ophiolite belt in Manipur chromites are generally found in the serpentinised peridotitic ultramafics, which are mostly of metamorphic harzburgite and metamorphic lherzolite, the remnants of upper mantle rocks, that have suffered limited partial melting (Khuman and Soibam, 2010; Soibam *et al.*, 2015). They occur as a number of sporadic pockets of massive chromite bodies in the host of the serpentinised ultramafic rocks. They are generally found in the form of broken blocks, lenses, nodules and pods either floating over or encaged in the host rocks. There is possibility of having many other hidden blocks that are still embedded within the host rock beneath the surface. In the study area, massive chromites are extensively more abundant than the nodular type (Singh *et al.*, 2013). The nodular type is almost negligible. According to the form and texture, chromite deposits have been broadly classified as “stratiform” and “Podiform” types (Thayer, 1973). The chromite deposits of Manipur Ophiolite Belt fall under podiform types. The chromite bodies occurred in the MOB contains more than 95 volume percent of chromite mineral. The other minerals associated with chromite are mostly those filled secondarily in the later developed fractures and cracks. Hence, they are not considered as chromitites.

In Manipur Ophiolite Belt, chromites occur in various forms in different localities. Mention can be made about the occurrences in Kwatha (**Figs. 2.3.1.13 and 2.3.1.14**) which is located at about 7 km away to the east of the Imphal-Moreh

Highway from Khudengthabi check-post junction, Tegnoupal and Holenphai villages of Moreh town area (**Figs. 2.3.1.15 and 2.3.1.16**) of Tegnoupal District. Limited blocks of chromite having pods found in Holenphai village occur within the soil horizon developed over the ultramafic peridotite. Massive chromites are found in Phangrei (**Fig. 2.3.1.17**), Gammon (**Fig. 2.3.1.18**) and Sirui villages of Ukhrul District and Kamjong area of the new Kamjong District. The chromite bodies of Sirui and Gamnom areas occurring in variable sizes are highly brecciated (as observed in the microscope). In almost all the localities chromites are occurred as broken blocks. The blocks generally range in size from small ones - tens of centimeters in length, breadth and thickness to large ones – with one to two-meter-long dimensions in space. The chromite deposits of Phangrei village area are extensively quarried and dug out thereby resulting to a rugged topography having a number of ponds. Some pod shaped small chromites are also found in the host of serpentinised peridotitic ultramafics.

Any two consecutive members of the sequence of the ophiolite belt either amongst the igneous members or in between chromite and host rocks, are found to have been seldom preserved intact. All are dismembered, discontinuous and thoroughly jumbled and therefore any relationship of chromite and host rock generated prior to obduction of the litho-units of the ophiolite is not available in the field. Hence, evidences from the host rocks and the chromite bodies are very carefully examined in interpreting and revealing the geologic and tectonic conditions of the origin of chromite of this ophiolite belt.

In this Chapter, observations are made mostly on the petrography and mineral chemistry of the samples of chromites with an aim to decipher information about their origin in due course of the generation of the ocean floor stratum during the spreading regime and subsequent obduction as an ophiolite belt owing to the orogenesis of the IMR as a consequence of tectonic reversal and concomitant evolution that led to the occurrence of the chromite bodies in the present-day field setting.

5.1 Petrography and Mineralogy

It is a well-established fact that the composition of chromites and the nature of the included minerals of the chromites can be used as an indicator of tectonic setting of formation and evolution of host mafic and ultramafic rocks (Kamenetsky *et al.*, 2001; Mondal *et al.*, 2006; Rollinson, 2008,). Thus, the study of petrography and geochemistry of chromites generally give an important clue about the tectonic implications of the host rocks emplaced in different geotectonic environments such as the mafic-ultramafic intrusions in the deep crust (Barnes and Roeder, 2001) and continental suture zones (Dick and Bullen, 1984; Zhou *et al.* 1996; Rollinson, 2008), as well as detrital spinels in sediments (Barnes and Roeder, 2001; Kamenetsky *et al.*, 2001; Arai *et al.*, 2006). Thus, an attempt is made to use petrography and geochemistry of the chromites of the MOB as a tool to decrypt the tectonic environment of their genesis and host rock as well.

In Manipur Ophiolite Belt, chromite bodies are found principally in metamorphic lherzolite and harzburgite host rocks, which are the residues of upper mantle rocks, that have suffered limited partial melting (Khuman and Soibam, 2010; Romendro *et al.*, 2017; Romendro and Khuman, 2021). Thus, metamorphic lherzolite and harzburgite are the two principal host rocks of Chromites in MOB. The host ultramafic rock (serpentinite) samples are principally composed of serpentines derived from olivine, bastites (pseudomorphs of serpentine after pyroxenes showing bronze like metallic luster or schiller), relics of olivine, orthopyroxene, clinopyroxene (in samples with protoliths) and primary and secondary spinels (Chapter 3). The primary spinel is the one originally formed along with other main phases of the rock, while the secondary one is developed during serpentinisation of principally of olivine and are generally very fine grained and mostly found clustered around the original fractures and cracks (Khuman, 2009) of olivine (**Fig. 3.1.8**). The host harzburgitic and lherzolititic tectonites are highly to moderately serpentinised with interpenetrating texture of serpentine containing rare relics of olivine pseudomorph (**Figs. 5.1.8A and 5.1.8B**). The rocks generally show xenoblastic granular texture and the grain size is quite variable and it is difficult to establish original grain boundaries (**Fig. 3.1.1**). All the faces of the essential primary

phases are corroded. These features indicate that the host rocks of the chromites under investigation are residues of upper mantle rocks, which have suffered partial melting. No lherzolite and harzburgite samples with euhedral grains of the constituent phases are found in the ophiolite belt in Manipur (where sporadic chromite bodies are occurred) indicating that the chromites have not been formed because of cumulate crystallisation of the later generated melt from the partial melting of the diapiric upper mantle rocks.

Most of the chromite samples are heavily fractured with lobate grain boundaries and traversed by anastomosing cataclastic zone of varying thickness ranging between 50–800 μm (Ghosh *et al.*, 2014). The chromite samples are intensely fractured and the broken pieces are separated apart and filled by secondary silicate phases, which are predominantly of serpentine (**Fig. 3.1.2B**). Small crystals of chromite also occur in inter-granular spaces of other phases of the host rock. Some of the chromite grains show extensive brecciation (**Fig. 5.1.2**). Along the boundaries of cracks kin minerals like ferritchromite or magnesioferrite or magnetites are observed. Some chromite samples exhibit a zonation in which a euhedral Cr-spinel core is mantled by ferritchromite/magnesioferrite. Many of the chromite samples present small amount of inclusions of phases like pyroxene (**Figs. 5.1.5, 5.1.6 and 5.1.9**), chrome diopside (**Fig. 5.1.6**) and magnetite (**Figs. 5.1.3 and 5.1.4**). There are some chromite samples which have inclusions of nepouite (Ni-bearing serpentine) crystals (**Fig. 5.1.7B**) also.

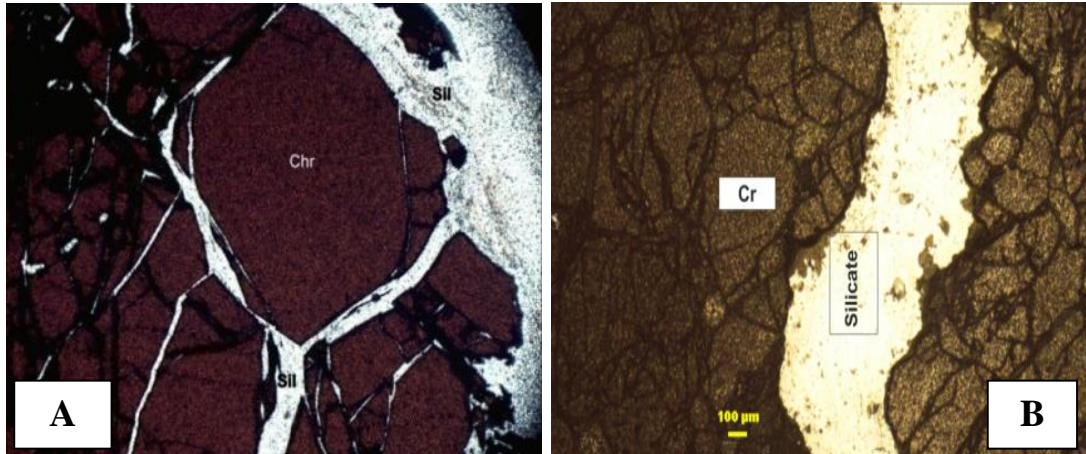


Fig. 5.1.1 (A, B):

Photomicrograph showing chromite with secondarily filled silicates in the fracture spaces (polarised light). Photo width is 4 mm.

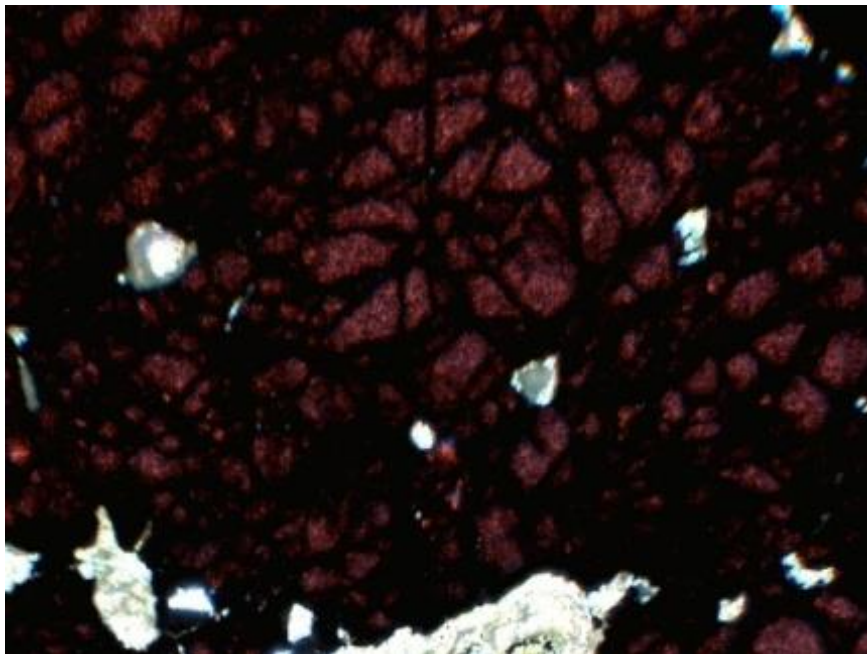
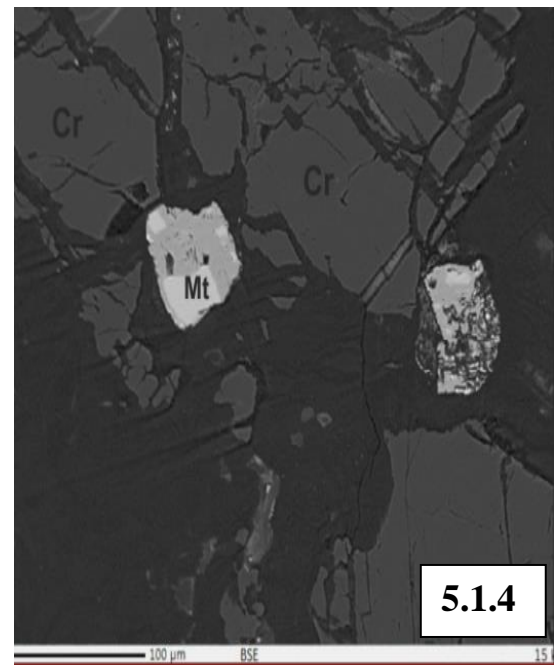
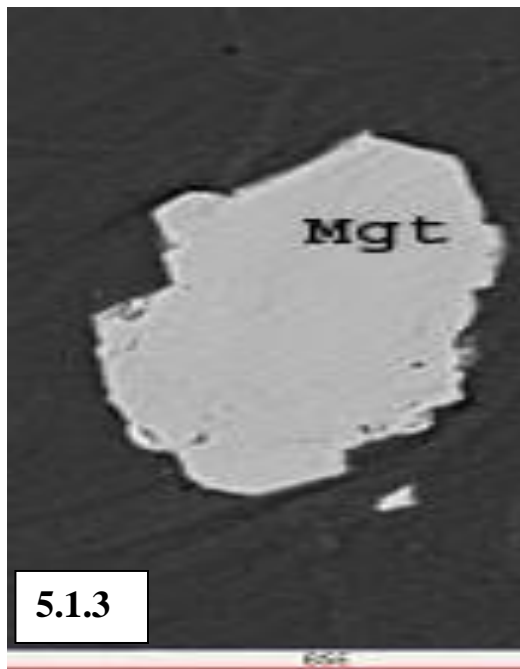


Fig. 5.1.2:

Photomicrograph showing highly brecciated chromite (polarised light). Photo width is 4 mm.



Figs. 5.1.3 and 5.1.4:
BSE images showing inclusion of magnetite in chromites.

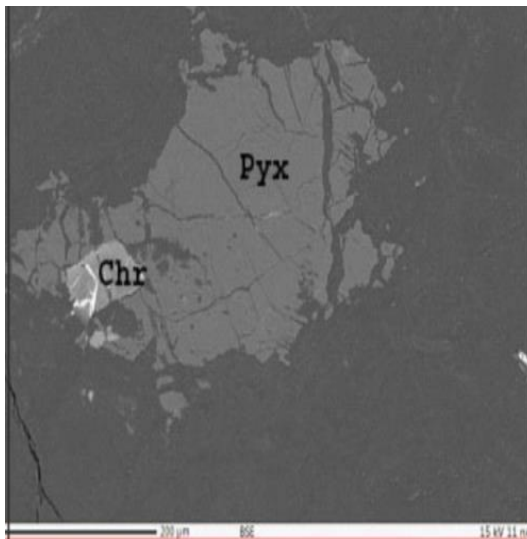


Fig. 5.1.5:
BSE image showing chromite grain in pyroxene
in the body of massive chromite.

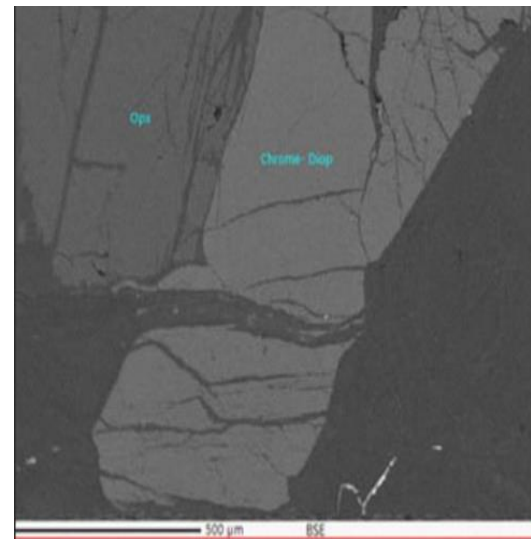


Fig. 5.1.6:
BSE image showing orthopyroxene and
chrome-diopside in chromite.

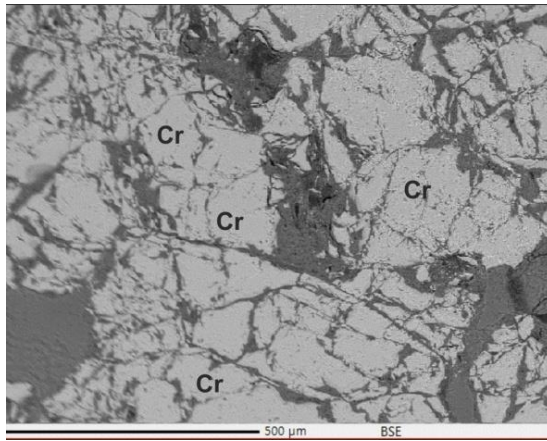


Fig. 5.1.7A:
BSE image showing fractured
chromite with serpentine.

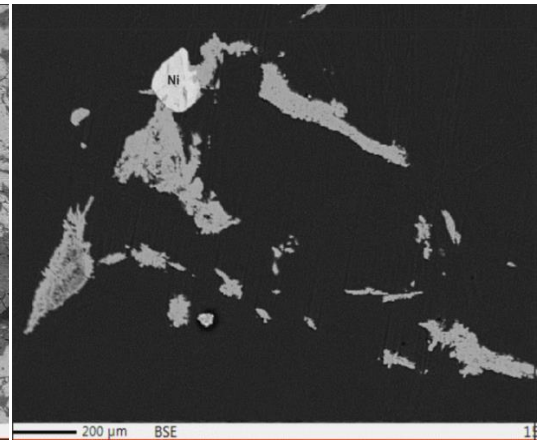
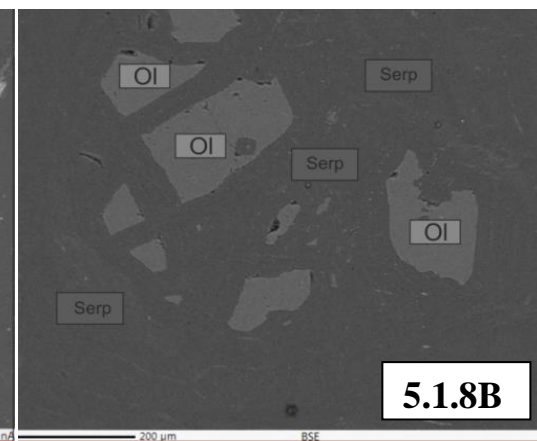
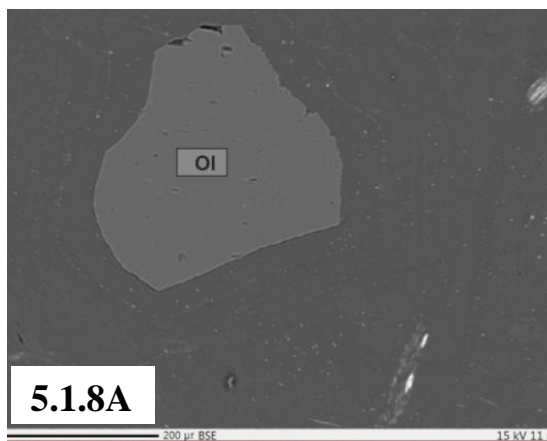


Fig. 5.1.7B:
BSE image showing presence
of nickel mineral, nepouite.



Figs. 5.1.8A and 5.1.8B:
BSE images showing relicts of olivine surrounded by serpentine.

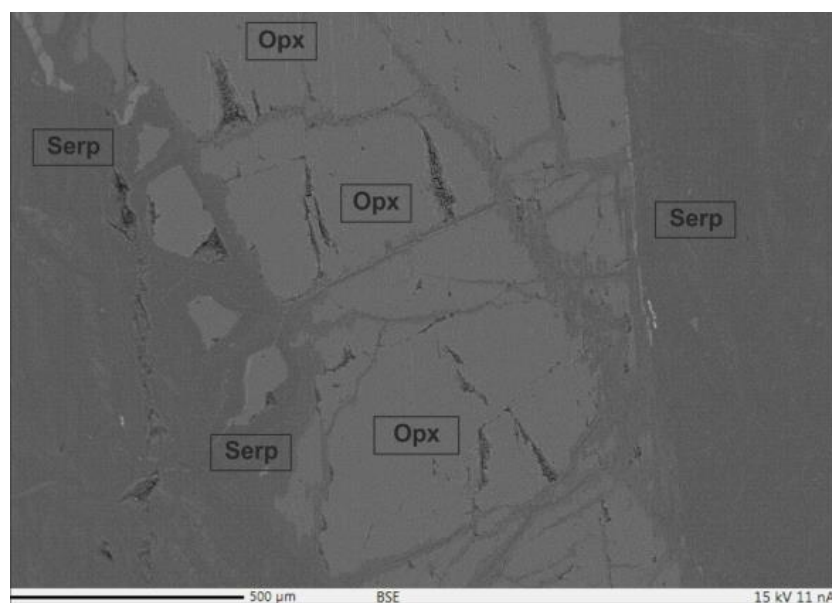


Fig. 5.1.9:
BSE image showing orthopyroxene and serpentine.

The serpentine mass shows a mesh to interpenetrating texture. The brecciation of chromite suggests that either post magmatic deformation or further evolutionary changes like serpentinization, diapirism, etc. of the host rocks was pronounced and was of volume expansion type. The brecciation is more pronounced in chromites of Ukhrol area than those of Tegnoupal area.

5.2 Mineral Chemistry

The EPMA analysis of representative samples of chromite has been carried out at the Electron Probe Micro Analyzer CAMECA SXFive instrument at DST-SERB National Facility, Department of Geology (Centre of Advanced Study), Institute of Science, Banaras Hindu University. Polished thin sections were coated with 20 nm thin layer of carbon for electron probe micro analyses using LEICA-EM ACE200 instrument. The CAMECA SXFive instrument was operated by SXFive Software at a voltage of 15 kV and current 10 nA with a LaB6 source in the electron gun for generation of electron beam. Natural silicate mineral andradite is used as internal standard to verify positions of crystals (SP1-TAP, SP2-LiF, SP3-LPET, SP4-LTAP and SP5-PET) with respect to corresponding wavelength dispersive (WD) spectrometers (SP#) in CAMECA SX-Five instrument.

The host rocks of the chromite bodies generally throw some light about the origin of the associated host rocks. It is also an established fact that spinels from different tectonic settings have different compositions (Dick and Bullen, 1984; Arai, 1994; Barnes and Roeder, 2001). $Cr\# = Cr / (Cr + Al)$ and $Mg\# = Mg / (Mg + Fe^{+2})$ of the spinels are important tools used to trace the tectonic settings of the host rocks. Hence, EPMA data of the composition of various grains of spinels (primary) from different samples of the host rocks are examined (Chapter 3).

Table 5.2.1A: Microprobe data of representative chromite sample (No. F₁-S₂A)

Wt% Oxide	1	2	3	4	5	6	7	8	9	10	11	12	13	14	Mean
Na ₂ O	0.0235	0.0000	0.0168	0.0000	0.0000	0.0000	0.0020	0.0000	0.0109	0.0149	0.0417	0.0000	0.0229	0.0000	0.0095
K ₂ O	0.0000	0.0000	0.0000	0.0000	0.0000	0.0021	0.0000	0.0000	0.0000	0.0000	0.0000	0.0000	0.0000	0.0000	0.0002
MgO	16.7864	15.0714	15.2347	15.1957	15.1870	15.2323	14.8690	15.3896	15.3233	14.0236	14.8303	14.9037	14.9622	14.8923	15.1358
CaO	0.0021	0.0000	0.0105	0.0000	0.0000	0.0000	0.0000	0.0000	0.0000	0.0000	0.0000	0.0000	0.0000	0.0000	0.0009
MnO	0.0000	0.0000	0.0000	0.0000	0.0000	0.0000	0.0000	0.0000	0.0000	0.0000	0.0000	0.0000	0.0000	0.0000	0.0000
FeO	12.9928	13.3197	12.8515	13.4452	13.0819	13.1798	13.4572	13.4281	13.3750	13.6687	13.3996	13.4344	13.9737	13.5346	13.3673
NiO	0.0299	0.2974	0.0446	0.2081	0.0595	0.1783	0.2081	0.1190	0.0746	0.0000	0.0892	0.1784	0.0746	0.1187	0.1200
Al ₂ O ₃	17.0192	16.2455	16.0560	16.0561	16.0256	16.1592	15.9858	16.0930	16.1803	15.6194	15.7920	16.1559	16.1251	15.9448	16.1041
V ₂ O ₃	0.1365	0.1292	0.1187	0.1273	0.1355	0.1238	0.1261	0.1031	0.1316	0.1189	0.1319	0.1499	0.1338	0.1491	0.1297
Cr ₂ O ₃	53.6271	53.4236	53.5671	53.8136	53.7340	54.0052	53.0196	53.3486	53.5244	53.8693	53.7835	53.4244	53.1568	53.5061	53.5574
SiO ₂	0.0000	0.0354	0.0051	0.0000	0.0202	-0.0076	0.0013	0.0051	0.0001	0.3057	0.0177	0.0000	0.0241	0.0126	0.0003
TiO ₂	0.2563	0.2325	0.2322	0.2754	0.2693	0.2358	0.2372	0.2733	0.2326	0.2246	0.2251	0.2619	0.2084	0.2381	0.2431
P ₂ O ₅	0.0000	0.0000	0.0000	0.0000	0.0000	0.0083	0.0000	0.0000	0.0000	0.0000	0.0000	0.0000	0.0000	0.0000	0.0006
Total	100.873	98.7546	98.1371	99.1215	98.5129	99.1247	97.9063	98.7597	98.8528	97.8452	98.3110	98.5086	98.6816	98.3964	98.6990

Table 5.2.1B: Recalculation of chromite analysis data (Sample No F₁-S₂A)

Name of Oxide	(1) wt% Oxide	(2) Mol. Propn Of Oxide	(3) At. Propn of cation or Cation Propn	(4) No. of oxygen	(5) Cation on basis of 4 Oxygen	(6) Cat. Assignment	(7) End members
MgO	15.1358	0.3755	0.3755	0.3755	0.7139	<div><div>Mg 0.3755 Ni 0.0031 Fe⁺² 0.283</div><div>=1</div><div><div>Fe⁺³ 0.0707 Al 0.6003 V 0.0034 Cr 1.3398 Ti 0.0058</div><div>=2.02</div></div></div>	Chemical Composition: (Mg,Fe ⁺² ,Ni,Mn) (Cr,Al,Fe ⁺³ ,Ti,V) ₂ O ₄
NiO	0.1200	0.0016	0.0016	0.0016	0.0031		
FeO	13.3673	0.1861	0.1861	0.1861	0.3537		
Al ₂ O ₃	16.1041	0.3158	0.4737	0.4737	0.6003		
V ₂ O ₃	0.1297	0.0018	0.0027	0.0027	0.0034		
Cr ₂ O ₃	53.5574	0.7048	1.0572	1.0572	1.3398		
TiO ₂	0.2431	0.0030	0.006	0.006	0.0058		
Na ₂ O	0.0095	0.0004	0.0000	0.0000	0.0000		
K ₂ O	0.0002	0.0000	0.0000	0.0000	0.0000		
CaO	0.0009	0.0000	0.0000	0.0000	0.0000		
MnO	0.0000	0.0000	0.0000	0.0000	0.0000		
SiO ₂	0.0003	0.0005	0.0000	0.0000	0.0000		
P ₂ O ₅	0.0006	0.0000	0.0000	0.0000	0.0000		
	98.6990		2.1040		3.02		
Oxygen Factor=4/2.1040=1.901 Mg# {Mg/(Mg+Fe ²)}=0.531, Cr# {Cr/(Cr+Al)}=0.768							

Table 5.2.2 A: Microprobe data of representative chromite sample (No. F₂-B₁)

Wt% Oxide	1	2	3	4	5	6	7	8	Mean
Na ₂ O	0.0000	0.0000	0.0241	0.0368	0.0001	0.0000	0.0000	0.0130	0.0003
K ₂ O	0.0070	0.0047	0.0048	0.0000	0.0000	0.0000	0.0000	0.0279	0.0006
MgO	14.8078	15.4770	14.3814	14.7608	15.1537	15.0310	15.0278	15.1796	14.9774
CaO	0.0254	0.0000	0.0002	0.0000	0.0394	0.0047	0.0162	0.0070	0.0006
MnO	0.0000	0.0000	0.0000	0.0000	0.0000	0.0000	0.0000	0.0000	0.0000
FeO	13.6701	14.2657	14.3478	13.7945	13.8210	13.9107	14.3347	13.8334	13.9972
NiO	0.2283	0.4086	0.3262	0.1467	0.0818	0.2937	0.4240	0.3099	0.2774
Al ₂ O ₃	17.5205	19.3112	16.3993	17.3259	18.0051	17.7423	17.9811	17.7429	17.7535
V ₂ O ₃	0.0864	0.0754	0.0916	0.1048	0.0893	0.1234	0.0846	0.0922	0.0935
Cr ₂ O ₃	50.7906	49.8704	51.3821	51.6598	51.6025	51.6323	51.4022	51.6876	51.2534
SiO ₂	0.0000	0.0000	0.0044	0.0000	0.0000	0.0000	0.0613	0.0195	0.0007
TiO ₂	0.3022	0.2419	0.2798	0.2609	0.2481	0.2533	0.2541	0.2744	0.2643
P ₂ O ₅	0.0000	0.0000	0.0000	0.0182	0.0000	0.0000	0.0000	0.0182	0.0006
Total	97.4384	99.6549	97.2416	98.1084	99.0411	98.9913	99.5861	99.2058	98.6585

Table 5.2.3 A: Microprobe data of representative chromite sample (No. F₃-5A₁)

Wt% Oxide	1	2	3	4	5	6	7	8	9	10	Mean
Na ₂ O	0.0031	0.0000	0.0000	0.0020	0.0000	0.0000	0.0000	0.0092	0.0061	0.0041	0.0025
K ₂ O	0.0000	0.0000	0.0000	0.0000	0.0042	0.0000	0.0000	0.0000	0.0000	0.0000	0.0004
MgO	14.1894	14.0980	13.9242	14.3063	14.1216	14.1284	14.2196	14.4928	13.8581	14.1071	14.1446
CaO	0.0104	0.0000	0.0000	0.0000	0.0000	0.0000	0.0000	0.0292	0.0000	0.0000	0.0040
MnO	0.0000	0.0000	0.0000	0.0000	0.0000	0.0000	0.0000	0.0000	0.0000	0.0000	0.0000
FeO	13.4939	14.4390	13.2379	13.5370	13.2936	13.3732	13.9741	14.4702	13.0749	13.6098	13.6504
NiO	0.1627	0.1036	0.1330	0.0885	0.1922	0.0002	0.2218	0.1038	0.1181	0.0296	0.1154
Al ₂ O ₃	11.7070	11.8677	11.4671	11.8149	11.5124	11.4530	11.7396	12.6425	11.1563	11.3976	11.6758
V ₂ O ₃	0.1595	0.1274	0.1468	0.1123	0.1743	0.1401	0.1141	0.1345	0.1547	0.1451	0.1409
Cr ₂ O ₃	58.4549	57.8297	59.2765	58.8141	59.5363	59.8846	58.3707	58.2283	58.8566	59.3815	58.8633
SiO ₂	0.0087	0.0324	0.0771	0.0784	0.0000	0.0511	0.0000	0.1225	0.0410	0.0000	0.0411
TiO ₂	0.2089	0.2439	0.1813	0.2495	0.2097	0.1663	0.2297	0.2128	0.2235	0.1946	0.2120
P ₂ O ₅	0.0000	0.0082	0.0000	0.0244	0.0000	0.0000	0.0000	0.0164	0.0000	0.0000	0.0049
Total	98.3985	98.7498	98.4439	99.0273	99.0443	99.1969	98.8696	100.4621	97.4893	98.8694	98.8551

Table 5.2.3B: Recalculation of chromite analysis data (Sample No. F₃-5A₁)

Name of Oxide	(1) wt% Oxide	(2) Mol. Propn Of Oxide	(3) At. Propn of cation or Cation Propn	(4) No. of oxygen	(5) Cation on basis of 4 Oxygen	(6) Cat. Assignment	(7) End Members
MgO	14.1446	0.3509	0.3509	0.3509	0.6823	<div><div><div>Mg 0.6823</div><div>Ni .0030</div><div>Fe⁺² 0.3146</div></div><div>=1</div></div> <div><div><div>Fe⁺³ 0.0548</div><div>Al .4452</div><div>V .0035</div><div>Cr 1.5059</div><div>Si .0013</div><div>Ti .0052</div></div><div>= 2.01</div></div>	Chemical Composition: (Mg,Fe ⁺² ,Ni,Mn) (Cr,Al,Fe ⁺³ ,Ti, V,Si) ₂ O ₄
NiO	0.1154	0.0015	0.0015	0.0015	0.0030		
FeO	13.6504	0.1900	0.1900	0.1900	0.3694		
Al ₂ O ₃	11.6758	0.1145	0.2290	0.3435	0.4452		
V ₂ O ₃	0.1409	0.0009	0.0018	0.0027	0.0035		
Cr ₂ O ₃	58.8633	0.3873	0.7746	1.1619	1.5059		
SiO ₂	0.0411	0.0007	0.0007	0.0014	0.0013		
TiO ₂	0.2120	0.0027	0.0027	0.0054	0.0052		
P ₂ O ₅	0.0049	0.0000	0.0000	0.0000	0.0000		
Na ₂ O	0.0025	0.0000	0.0000	0.0000	0.0000		
K ₂ O	0.0004	0.0000	0.0000	0.0000	0.0000		
MnO	0.0000	0.0000	0.0000	0.0000	0.0000		
CaO	0.0040	0.0001	0.0001	0.0001	0.0001		
	98.8553			2.0574	3.0159		
Oxygen Factor=4/2.0575=1.9441 Mg# {Mg/(Mg+Fe ⁺²)}=0.508, Cr# {Cr/(Cr+Al)}=0.834							

Table 5.2.4A: Microprobe data of representative chromite sample (No. F₃-5A₂)

Wt% Oxide	1	2	3	4	5	6	7	Mean
Na ₂ O	0.0022	0.0000	0.0000	0.0463	0.0271	0.0235	0.0292	0.0183
K ₂ O	0.0389	0.0000	0.0137	0.0320	0.0092	0.0115	0.0000	0.0150
MgO	14.2824	14.0994	14.2782	12.3737	13.1942	14.2826	13.7390	13.7499
CaO	0.0000	0.0182	0.0000	0.0318	0.0274	0.0593	0.0137	0.0215
MnO	0.3408	0.2588	0.0000	0.0000	0.0000	0.0000	0.0000	0.0857
FeO	13.7908	13.3390	13.2391	12.6472	14.0611	13.7161	13.9080	13.5288
NiO	0.5665	0.1943	0.2591	0.4367	0.1783	0.1946	0.1296	0.2799
Al ₂ O ₃	11.2216	11.2346	11.1855	10.1393	11.2616	11.4220	11.0865	11.0787
V ₂ O ₃	0.2133	0.2373	0.0672	0.0000	0.1113	0.0869	0.0741	0.1129
Cr ₂ O ₃	60.5781	59.9982	60.0415	58.5716	59.1504	59.1627	59.3463	59.5498
SiO ₂	0.0000	0.0000	0.0095	0.0978	0.0505	0.0833	0.0273	0.0383
TiO ₂	0.2277	0.2536	0.1652	0.1891	0.1654	0.1678	0.1666	0.1908
P ₂ O ₅	0.0000	0.0000	0.0000	0.0000	0.0000	0.0000	0.0447	0.0064
Total	101.2623	99.6334	99.2591	94.6583	98.2364	99.2104	98.5648	98.6892

Table 5.2.4B: Recalculation of chromite analysis data (Sample F₃ 5A₂, Phangrei)

Name of Oxide	(1) wt% Oxide	(2) Mol. Propn Of Oxide	(3) At. Propn of cation or Cation Propn	(4) No. of oxygen	(5) Cation on basis of 4 Oxygen	(6) Cat. Assignment	(7) End Members
Na ₂ O	0.0183	0.0003	0.0006	0.0003	0.0012	Na .0012	Chemical Composition: (Mg,Fe ⁺² ,Ni,Mn,Na) (Cr,Al,Fe ⁺³ ,Ti,V,Si) ₂ O ₄
MgO	13.7499	0.3412	0.3412	0.3412	0.6670	Mg 0.6670	
MnO	0.0857	0.0012	0.0012	0.0012	0.0024	Mn .0024	
NiO	0.2799	0.0037	0.0037	0.0037	0.0073	Ni .0073	
FeO	13.5288	0.1883	0.1883	0.1883	0.3682	Fe ⁺² .3206	
Al ₂ O ₃	11.0787	0.1087	0.2174	0.3261	0.4250	Fe ⁺³ 0.0475	
V ₂ O ₃	0.1129	0.0008	0.0016	0.0024	0.0031	Al .4250	
Cr ₂ O ₃	59.5498	0.3918	0.7836	1.1754	1.5319	V .0031	
SiO ₂	0.0383	0.0006	0.0006	0.0012	0.0012	Cr 1.5319	
TiO ₂	0.1908	0.0024	0.0024	0.0048	0.0047	Si .0012	
CaO	-	-	-	-	-	Ti .0047	
K ₂ O	-	-	-	-	-		
P ₂ O ₅	-	-	-	-	-		
Total	98.6892			2.0451	3.0134		
Oxygen factor=4/2.0451=1.955 Mg# {Mg/(Mg+Fe ⁺²)}=0.495, Cr# {Cr/(Cr+Al)}=0.843							

Table 5.2.5: Summary of microprobe data of four representative chromite samples from MOB.

Oxide	F3-5A2	F3-5A1	F2-B1	F1-S2A
Na ₂ O	0.0183	0.0025	0.0003	0.0095
K ₂ O	0.0150	0.0004	0.0006	0.0002
MgO	13.7499	14.1446	14.9774	15.1358
CaO	0.0215	0.0040	0.0006	0.0009
MnO	0.0857	0.0000	0.0000	0.0000
NiO	0.2799	0.1154	0.2774	0.1200
FeO	13.5288	13.6504	13.9972	13.3673
Al ₂ O ₃	11.0787	11.6758	17.7535	16.1041
V ₂ O ₃	0.1129	0.1409	0.0935	0.1297
Cr ₂ O ₃	59.5498	58.8633	51.2534	53.5574
SiO ₂	0.0383	0.0411	0.0007	0.0003
TiO ₂	0.1908	0.2120	0.2643	0.2431
P ₂ O ₅	0.0064	0.0049	0.0006	0.0006
Total	98.676	98.855	98.658	98.698
Formula units based on 4 oxygen				
Na	0.0012	0.0000	0.0004	0.0008
K	0.0008	0.0000	0.0004	0.0000
Mg	0.6670	0.6823	0.7035	0.7139
Ca	0.0007	0.0001	0.0004	0.0000
Mn	0.0024	0.0000	0.0000	0.0000
Ni	0.0073	0.0030	0.0070	0.0031
Fe	0.3681	0.3694	0.3680	0.3537
Al	0.4250	0.4452	0.6591	0.6003
V	0.0031	0.0035	0.0023	0.0034
Cr	1.5319	1.5059	1.2766	1.3398
Si	0.0012	0.0013	0.0003	0.0009
Ti	0.0047	0.0052	0.0063	0.0058
P	0.0000	0.0000	0.0000	0.0000
Total	3.0134	3.0159	3.0243	3.0218
Mg#	0.495	0.508	0.817	0.531
Cr#	0.843	0.834	0.742	0.768
Average Mg# 0.606, Cr# 0.806				

Table 5.2.6: Percentage Fe⁺³, Cr, Al in chromites of Manipur Ophiolite Belt

	F3-5A2	F3-5A1	F2-B1	F1-S2A	Mean
Fe ⁺³	0.0475	0.0548	0.0796	0.0714	0.063
Cr	1.5319	1.5059	1.2766	1.3398	1.41
Al	0.4250	0.4452	0.6591	0.6003	0.53
Total	2.004	2.006	2.015	2.012	2.00

Fe ⁺³ %	3	3	4	3	3.25
Cr %	76	75	63	67	70.25
Al %	21	22	33	30	26.50
Total	100	100	100	100	100

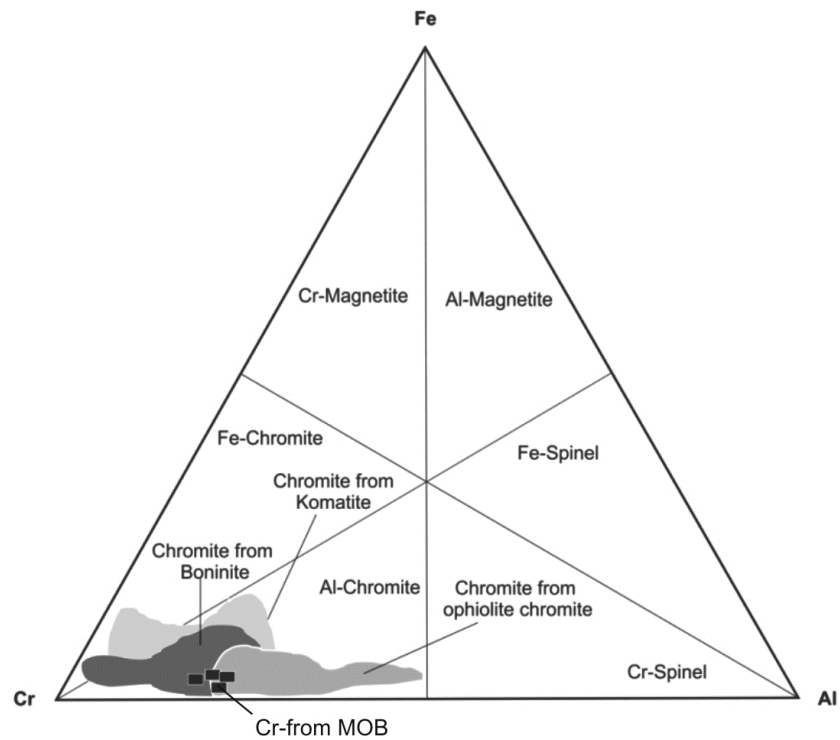


Fig. 5.2.1:

Plot of trivalent cations. The MOB chromites fall in the field of Al-chromite being pigeonholed mostly in ophiolite chromite.
(after Stevens, 1944; Barnes and Roeder, 2001)

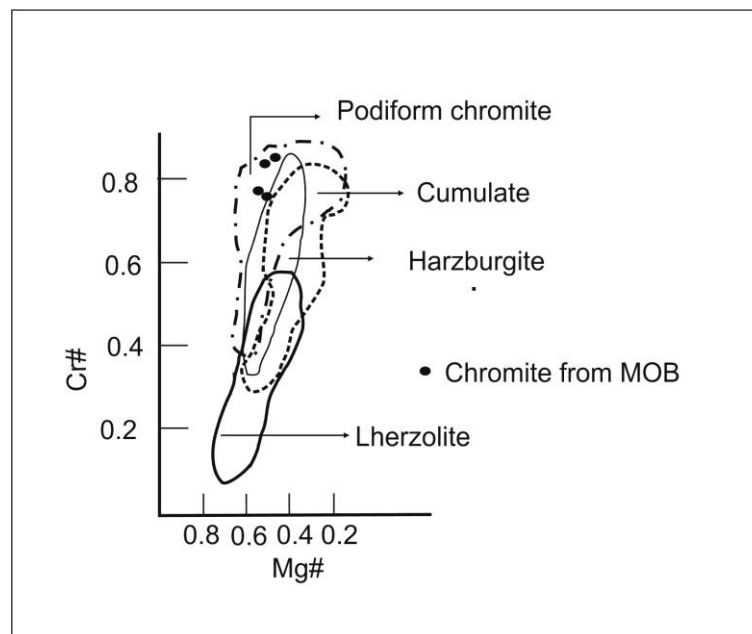


Fig. 5.2.2:

Compositional field of chromites from Manipur Ophiolite Belt
(after Pober and Fauph, 1980)

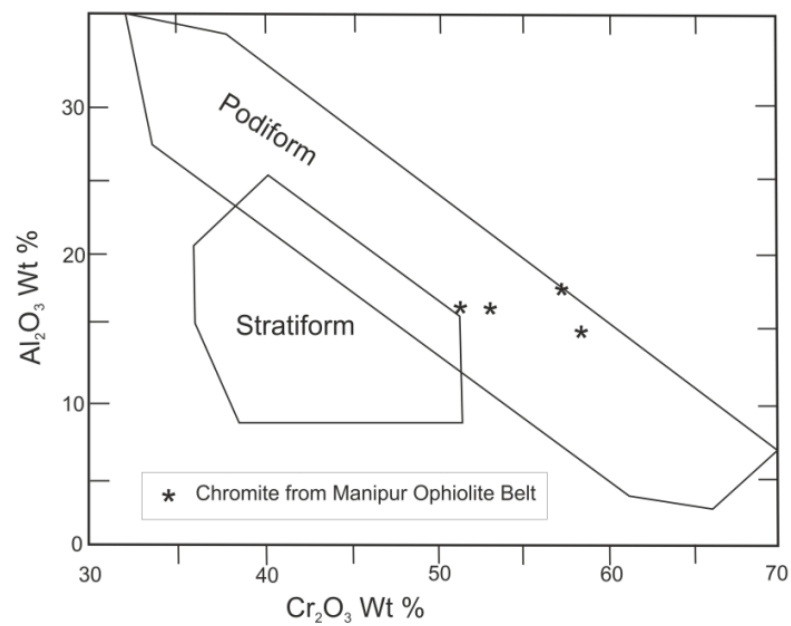


Fig. 5.2.3:

Plot of Cr_2O_3 Wt % versus Al_2O_3 Wt % showing the chemical composition of chromite from Manipur Ophiolite Belt with a comparison of podiform and stratiform chromitites (after Arai *et al.*, 2004).

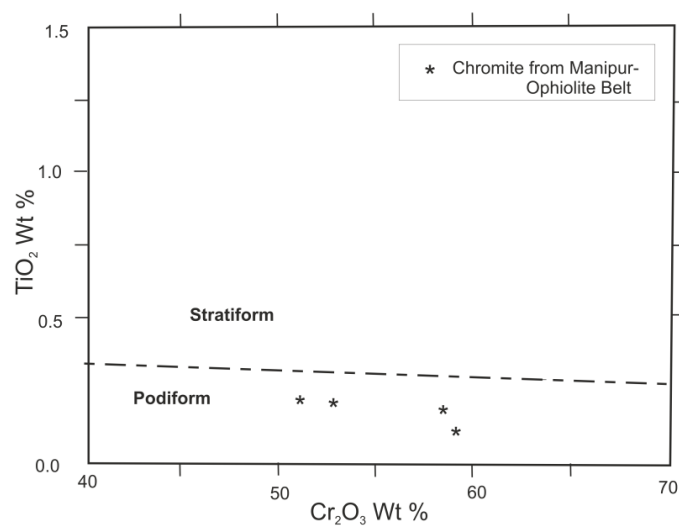


Fig. 5.2.4:

Plot of Cr_2O_3 Wt % versus TiO_2 Wt % showing the chemical composition of chromite from Manipur Ophiolite Belt with comparison of podiform and stratiform chromitites (after Arai *et al.*, 2004).

The compositions of the spinels in a variety of samples of host serpentinised residual ultramafic rocks are found considerably variable as discussed in Chapter 3. Even if the compositions are widely variable, they are found to have been clustered to three limiting ranges (groups) of approximately similar values. Thus, it is claimed that there are three varieties of spinels co-exist together with the other phases of the residual ultramafic rocks. Such spinels from groups of similar compositions are respectively taken together and their means are calculated (**Tables 3.2.4.1-ABC**). The mean compositional data of each group of spinels are then recalculated as shown in the (**Table 3.2.4.2-ABC**) respectively for derivation of exact chemical compositions (formulae) and also for finding out respective Cr# and Mg# values. The triangular compositional proportions of the three groups of spinels are found respectively to be (i) spinel = 27%, chromite = 21%, magnetite = 52%; (ii) spinel = 79%, chromite = 14%, magnetite = 7% and (iii) spinel = 46%, chromite = 42%, magnetite = 12%. The Cr# value range from 0.212 to 0.577 and the Mg# values spread from 0.265 to 0.608 for the three kinds of spinels.

EPMA analysis of representative samples of chromites from different locations is carried out. The data of such chromites and their means are enumerated in **tables 5.2.1A, 5.2.2A, 5.2.3A and 5.2.4A**. Based on the mean compositional data of each group of chromites enumerated in **tables 5.2.1A, 5.2.2A, 5.2.3A and 5.2.4A** are then recalculated as shown in the **tables 5.2.1B, 5.2.2B, 5.2.3B and 5.2.4B** respectively for derivation of the exact chemical compositions (formulae). The respective Cr# and Mg# values of each type of chromites are also found out and are as shown in the respective tables. The data and recalculated values of different chromite samples from different localities are again shown in **table 5.2.5**. The triangular proportion of the mean composition of the representative chromite samples (**Table 5.2.6**) is found to be spinel = 26.50%, chromite = 70.25%, magnetite = 3.25%. The Cr# value range from 0.742 to 0.843 and the Mg# values spread from 0.495 to 0.817 for the analysed chromite samples.

The Fe^{+3} - Cr - Al, triangular compositional proportions of the four groups of chromites are found respectively to be (i). For Sample F3-5A2 - $\text{Fe}^{+3}\%$ = 3, Cr% = 76, Al% = 21; (ii). For Sample F3-5A1 - $\text{Fe}^{+3}\%$ = 3, Cr% = 75, Al% = 22; (iii). For

Sample F2-B1 - Fe^{+3} % = 4, Cr % = 63, Al % = 33; (iv). For Sample F1-S2A - Fe^{+3} % = 3, Cr % = 67, Al % = 30. The $\text{Cr\#} = \text{Cr}/(\text{Cr} + \text{Al})$ value range from 0.742 to 0.843 and the $\text{Mg\#} = \text{Mg}/(\text{Mg} + \text{Fe})$ values spread from 0.495 to 0.817 for the four kinds of chromites. The trivalent cations (Fe^{+3} - Cr – Al) are plotted in triangular diagram (**Fig. 5.2.1**) and it is found that chromites of Manipur Ophiolite Belt fall in the field of Al-chromite type pigeonholed mostly in ophiolite chromite field. The $\text{Cr\#} = \text{Cr}/(\text{Cr} + \text{Al})$ versus $\text{Mg\#} = \text{Mg}/(\text{Mg} + \text{Fe})$ is also plotted and it is established that they cluster in the field of podiform chromite (**Fig. 5.2.2**). The spinels in serpentinised ultramafics are lower in Cr\# (0.212 to 0.577), than in chromites (0.742 to 0.843). The TiO_2 Wt. % in chromites range from 0.19 to 0.26. It is very low in case of Cr-spinel. The analysis of electron microprobe data of Cr_2O_3 Wt. % versus Al_2O_3 Wt.% and Cr_2O_3 Wt.% and TiO_2 Wt% are plotted respectively in the diagrams shown in the **figures 5.2.3** and **5.2.4**, where all the chromites fall in the podiform chromite field (Arai *et al.*, 2004). It is also supported by compositional field diagram of chromites (**Fig. 5.2.2**).

Chapter 6

DISCUSSION AND CONCLUSION

The present work is a geological investigation carried out on some parts of Manipur Ophiolite Belt which is the southern extension of the ophiolite belt in Nagaland. The study encompasses both petrological, mineralogical and geochemical analyses of some units of the ophiolite sequence of the study area. The area is an ideal one as it represents one of the best sections of the dismembered ophiolite complex. The petrological studies can reveal some clues about the tectonic environment. The information gathered from petrography and mineralogy can also tell something about the geologic setting prevailed during the formation of the ultramafics of the rock suite and chromite mineralisation as well. The geochemical information which are embedded within rocks and minerals are extracted in the form of Major and Minor Oxide composition (XRF), and Trace and Rare Earth Elements (ICP-MS) concentrations of ultramafic rocks and associated chromite bodies of the ophiolite sequence, as well as, from the composition of individual minerals (EPMA), which may help in understanding the tectonic setting with respect to their petrogenesis. From studies of all the petrological, mineralogical, geochemical, geological features and related processes, it can reveal about the mechanism of generation of the ultramafics and associated chromites of Manipur ophiolite during the formation of the Indo-Myanmar basin and consequent evolution to give rise to the present field setting of the rock units. The study also aims to provide logical explanation through the analytical interpretations of the various data generated in this piece of research work so as to decipher a picture how the studies of petrology and geochemistry of the ultramafic rocks lead to reveal the processes of mineralization and occurrence of chromites in the ophiolite belt in Manipur. Attempt is also made to examine whether the petro-tectonic conditions of serpentinisation of the ultramafic rocks are playing an important role in chromite mineralization.

6.1 Discussion

To draw some conclusions of the present study, systematic discussions are carried on the basis of results, findings and observations on various aspects of the preceding chapters.

6.1.1 Geological and Tectonic Setting (Field Setting)

Manipur is a small state situated in the north eastern corner of India bordering with the Union Socialist Republic of Myanmar (Burma) extending approximately between 23°50' N-25°41' N latitudes and 93°00'E-94°45'E longitudes having an area of about 22,327 Km². The rock formations of the state are predominantly made up of Tertiary and Cretaceous sediments with minor igneous and metamorphic rocks where flysch sediments of constitute nearly 65% of the state's total area (Khuman and Soibam, 2010). The regional trend of Manipur is NNE-SSW and occur between the NE-SW trending Naga-Patkai Hills in the north and N-S trending Chin-Mizo Hills in the south forming an integral part of the Indo-Myanmar Hill Ranges (IMR). The different litho-units in Manipur are intensely deformed and juxtaposed against each other with imbricate thrust systems having NNE-SSW trend in such a way that the younger ones are on the west while the older ones are on the east (Soibam, 2000; Soibam and Pradipchandra, 2006; Khuman and Soibam, 2010).

This oldest group of rocks is comprised of a metamorphic complex. The Metamorphics exposed on the eastern part of the state is assigned as Naga Metamorphics. This part is comprised of intensely thrust group of metasediments, which is predominantly made up of low to medium grade phyllitic schists, hornblende schists, quartzite, quartz-sericite schist, mylonite, etc. Brunnschweiler (1966) assigned them Pre-Mesozoic or older age but Acharyya *et al.* (1986), however, assigned them Proterozoic age. These rocks occur as klippen thrusting westward over the younger Ophiolite Melange Zone (MOMZ).

The MOMZ is an assembly of tectonic slices of various units of the ocean floor rocks of an ancient basin representing the ultramafic suite, mafic dykes and sills, pillow lavas, pelagic sediments, etc., which occur in a jumbled manner. The ultramafics are mostly harzburgite with small amount of lherzolite, residues of upper mantle rocks, which have suffered partial melting (Khuman and Soibam, 2010; Soibam *et al.*, 2015). No exposure of cumulate ultramafics is so far encountered in the MOMZ. There are also a number of exotic blocks of various rock types mostly in the hosts of pelagic shales and to a lesser extent in the peridotitic ultramafics. The exotic rocks include a number of blocks of variable dimensions of diabasic dyke, pillow lava, conglomerate, radiolarian chert, limestone, gritty sandstone (mélange sandstone) and rocks kindred with lava extrusion (volcanoclastic sediments?). The peridotitic ultramafics having sporadic diabasic dykes cutting across them are found to have been sandwiched with pelagic shale. There are two physically distinct peridotitic ultramafics (serpentinites) in the complex. One type is almost wholly serpentinitised with very intense shearing along closely spaced fractures which sometimes resembles serpentine schist. The other type (comparatively less predominant) is comparatively fresh and less serpentinitised. The second group is found occurring as blocks embedded within the earlier type and are generally found protruding over the exposed surface of peridotitic serpentinites of the Ophiolite Complex. The mafic dykes and pillow lavas are spillitic in character and hence have suffered greenschist facies hydrothermal metamorphism (Khuman and Soibam, 2010, Soibam and Khuman, 2011), which imply that they have been formed in the shallow depth environment which should be less than 3 km. (Coleman, 1977; Soibam and Khuman, 2011).

The chromite is found to occur in a number of localities in Manipur. Mention can be made about the occurrences in Kwatha and Tengenoupal villages as well as Holenphai village of Moreh town area in Tengenoupal District; Phangrei and Gamnom villages of Ukhrul District; and Kamjong area of the new Kamjong District. In many of the localities chromite is occurred as floating blocks. The blocks generally range in size from small ones - tens of centimeters in length, breath and thickness to large ones – with one- to two-meter-long dimensions in space. The chromite of Phangrei village area is extensively quarried and dug out thereby

resulting to a rugged topography having a number of ponds. Limited Pod shaped small chromite inclusions are also found in the host of serpentinised peridotitic ultramafics.

The Manipur Ophiolitic Mélange Zone is found to over thrust the younger flysch sediments known as the Disangs and the Barails (Evans, 1932; Mathur and Evan, 1964; Mallet, 1876). Disang and Barail sediments occupy the major central part of the state. The age of the Disang sediments is assigned to be Eocene to Upper Cretaceous while that of the Barail sediments to be Oligocene to Upper Eocene. Disang sediments are a group of monotonous sequence of dark grey to black splintery shales which has sometimes intercalations of siltstone and fine to medium grained sandstones of light to brownish grey. Barail sediments are predominantly arenaceous characterized by light grey to brown, fine to medium grained sandstones with minor to considerably thick inter-bands of shale. The Barail group is unconformably overlain by the molasse sediments characterized as the Surma (Evans, 1932) and Tipam (Mallet, 1876) Groups, whose age is mainly Miocene but may extend upto Oligocene. The MOMZ in which the present study is carried out, over thrusts the Disang-Barail flysch belt (Soibam 1998; Soibam and Khuman, 2008).

Alluvium deposits overlie the Tipam Group. It may be because of the upliftment of the region above the depositional level after the deposition of Tipam. The major depositions of alluviums take place in the Imphal valley, which is likely to have been formed since Pleistocene times. The alluvium deposits of Manipur can be grouped into two – the Old Alluvium and the New Alluvium. The older Alluvium is found mainly in Barak valley of newly created Jiribam district, whereas the new alluvium occurs in the Imphal valley (central plain). The Manipur valley (Imphal valley) has a column of alluviums of fluvio-lacustrine origin. It may have a thickness of about 150 to 350 m although, variable at places (Soibam, 1998; Soibam and Hemanta Singh, 2007).

Soibam (2006), also computed plate motion in and around Manipur using rotation vectors given by various workers (e.g., De Mets et al, 1990; Minster and Jordan, 1978; Curray *et al.*, 1976). Analysis of plate kinematics in and around

Manipur by Soibam (2006) reveals that the structural and tectonic features of the Indo-Myanmar Hill Ranges and that of Manipur Hills in particular have been evolved as a result of interaction between the Indian and Myanmar plates rather than Indian and Eurasian plates or Myanmar and Eurasian.

From the analysis it is observed that relative motion of Indian plate with respect to Eurasian plate (${}_E V_I$) is almost parallel to NNE, the tectonic strike of the region and, therefore, such a motion cannot produce compression structures which are parallel to the motion. Similarly, ${}_E V_M$ is towards N only slightly different from the regional strike and so, may not be responsible for the evolution of structural and tectonic features of the state and its adjoining region. Thus, ${}_M V_I$, which moves towards NE, induces a dextral shear couple deformation mechanism of the region to produce the tectonic features of the state. Such a deformation mechanism caused the rocks of the region to have been compressed in the WNW-ESE (E-W) and extended in the NNE-SSW (N-S) directions. And such a deformation mechanism is responsible for evolution of the Indo-Myanmar Hill Ranges leading to the present juxtaposition of Ophiolite Mélange Zone and other litho-units of the adjoining area in due course of subduction orogenesis.

6.1.2 Ultramafic Rocks

In Manipur Ophiolite Melange Zone, there are two physically distinct ultramafic peridotites (serpentinites). One is almost wholly serpentinitised with very intense shearing along closely spaced fractures which sometimes resembles serpentine schist. The other type is comparatively fresh and less serpentinitised and less predominant. The latter are found occurring as blocks embedded within the earlier type, which are generally found protruding over the exposed surface of earlier type. These two types of ultramafics occupy more than 90 percent of total igneous ophiolitic rocks. The degree of serpentinitisation of the ultramafic rocks of Manipur Ophiolite ranges approximately between 60-93%.

The ultramafic rocks (serpentinite) samples of Manipur Ophiolite Belt essentially comprise of serpentines derived from olivine, bastites (pseudomorphs of

serpentine after pyroxenes showing bronze like metallic lustre or schiller), relics of olivine, orthopyroxene, clinopyroxene and primary and secondary spinels. The rocks generally show xenoblastic granular texture and the grain size is quite variable and it is difficult to establish original grain boundaries. All the different phases are found as segregated groups. Elongation and alignment are also shown by the grains of orthopyroxene, clinopyroxene and primary spinel. From the modal proportions of olivine, orthopyroxene and clinopyroxene, the ultramafic rocks of Manipur Ophiolite range from lherzolite to harzburgite. The least serpentinised ultramafics are found to be mostly of lherzolite and the extensively serpentinised types are of harzburgite.

The recalculated data of olivine of the ultramafics of Manipur Ophiolite Belt is found to be $\text{Fo}_{90.33}$ - $\text{Fa}_{9.67}$. The value of $\text{MgO}/(\text{MgO} + \text{FeO})$ and $\text{Mg}/(\text{Mg} + \text{Fe} + \text{Mn})$ are found to be the same (about 0.84) which reflect less depleted nature of the ultramafic rocks of Manipur Ophiolite. The recalculated compositional data of orthopyroxene exhibit $\text{En}_{87.266}$ - $\text{Fs}_{9.36}$ - $\text{Wo}_{3.374}$ and that of clinopyroxene as $\text{En}_{51.824}$ - $\text{Fs}_{5.245}$ - $\text{Wo}_{42.931}$. When plotted the composition of orthopyroxene and clinopyroxene on the pyroxene quadrilateral, it is found that the ultramafics of Manipur Ophiolite is very close to the field of metamorphic peridotite (**Fig. 3.2.2.1**). From the result of recalculated mean from three different types of spinels, it is known that it has value of spinel series = 51%, magnetite series = 23% and chromite series = 26%. It is generally agreed that spinels from different tectonic settings have different compositions. $\text{Cr\#} = \text{Cr}/(\text{Cr} + \text{Al})$ and $\text{Mg\#} = \text{Mg}/(\text{Mg} + \text{Fe}^{+2})$ are important tools used to trace the tectonic settings. The Cr# values of the three different samples are found to be 0.536, 0.212, 0.577 and Mg# value to be 0.265, 0.608, 0.361. When 100 $\text{Cr}/(\text{Cr} + \text{Al})$ of three different spinel samples are plotted against Al_2O_3 weight percent of co-existing orthopyroxene, the ultramafic rock (**Fig. 3.2.4.1**) is found to be Aluminium-spinel lherzolite (Sample F1M1) and Cr-spinel/lherzolite (Sample F3-3B & F1S2B). When Mg# is plotted against Cr# of spinels it is found that the spinels pigeonholed in the field of lherzolite host rock (**Fig. 3.2.4.2**).

The values of the $\text{MgO}/(\text{MgO} + \text{FeO})$ of the ultramafic rocks of Manipur Ophiolite cluster around 0.84. Orthopyroxene and olivine have virtually the same

ratio of $\text{MgO}/(\text{MgO}+\text{FeO})$, the values in case of Manipur Ophiolite ultramafics being 0.83 and 0.84. Hence, variation in the proportion of orthopyroxene and olivine in the ultramafic rocks does not significantly affect this ratio for the total rock (Coleman, 1977, Khuman and Soibam, 2010). Consequently, it is observed that the ultramafic rocks of Manipur ophiolite have an extreme restricted range of $\text{MgO}/(\text{MgO}+\text{FeO})$ value. The change in $\text{MgO}/(\text{MgO}+\text{FeO})$ value reflects change in the composition of the co-existing orthopyroxene and olivine. Hence, it appears that even though the different ultramafic rocks of the ophiolite belt in Manipur had different proportion of olivine and orthopyroxene, their compositions were almost the same. The AFM and ACM diagrams (**Figs. 3.3.1.2 and 3.3.1.3**) indicate that the ultramafic rocks of Manipur Ophiolite are of metamorphic peridotites.

Most of the ultramafics of Manipur Ophiolite Belt have Al_2O_3 content higher than 5%. The higher value Al_2O_3 content indicates higher proportion of clinopyroxene phase than that of normal ophiolitic harzburgite and dunite; and the source is more fertile (less depleted). The average values of Na_2O and K_2O of Manipur Ophiolite are 1.01% and 0.15% which are extremely enriched compared with the normal ophiolite ultramafics. This also indicates that the ultramafic rocks of Manipur Ophiolite are from a fertile source.

From the study of the trace elements concentrations in samples from Manipur Ophiolite Belt, it is found that most of the values are higher than the metamorphic peridotites and normal ultramafics indicating their fertile mantle source thereby inferring to be of sub continental mantle source. The normalized concentrations (based on chondritic meteorites) of the REE of the ultramafics of the study area when compared with that of metamorphic peridotite, mafic cumulate and upper-level gabbro, it is observed that these are two or three orders of magnitude more than common ophiolitic metamorphic peridotites and even one order of magnitude more than the common ophiolitic gabbros. The high value of REE in the Manipur ophiolitic ultramafics than the normal metamorphic peridotites (**Fig. 3.3.2.5**) is another reason to infer a fertile source possibly of sub-continental upper mantle. From the aforesaid observations it is finally inferred that the ultramafic rocks of

Manipur Ophiolite Belt are ranging from spinel lherzolite to chrome-spinel-lherzolite of sub-continental upper mantle source origin.

6.1.3 Serpentinisation

Serpentinisation is the process as a result of which the mafic minerals of rocks usually ultramafics that are formed in an anhydrous high temperature system, are changed into serpentine group of minerals owing to retrograde metamorphism on account of subjection of the rock into the equilibrium condition of lower temperature and water rich environment. It is learnt that the ultramafic rocks of Manipur Ophiolite have undergone serpentinisation. In Manipur ophiolite Belt, extremely serpentinised ultramafic massifs are found to have very occasional lenses of leucocratic vein rocks filling in very small veinlets which are generally few centimeters wide that pinches out after few meters (**Fig. 2.3.1.4**). These leucocratic rocks are inferred as rodingites. Studies of serpentinisation and subsequent rodingitisation on account of cold metamorphism of serpentinites, throw lights on the tectonic history of the Ophiolite belt in Manipur.

When olivine grains are serpentinised the anastomosing veinlets of cross fiber serpentine are produced resulting to a mesh textured aggregate. The bastites on the other hand, even though are pseudomorphs after the pyroxenes, which have a number of cleavage planes, emerged as compact grains obliterating the original pyroxene cleavages (**Fig. 3.1.9**). The open spaces of cleavages of pyroxene must have been occupied by increased volume of serpentine i.e., bastite. These features appear to indicate that the serpentinisation took place along with an increase in volume, consequently having relationship with spreading tectonics. The concentration of fine grained secondary spinels mostly along the continuous lines of original fractures of olivine crystals also indicates isotropic expansion of volume by virtue of which the original shapes are maintained (**Fig. 3.1.8**). When the mean of the analytical data (EMPA) of nine (9) representative samples of serpentine are recalculated for derivation of the exact composition of serpentine, the composition is found to be $(\text{Mg,Ca,Na, Ni, Al, Fe, Cr})_3 \text{SiO}_2\text{O}_5 (\text{OH})_4$.

Altogether Six (6) representative samples of peridotitic serpentinites from different parts of the Manipur Ophiolite Belt are analysed (**Figs. 4.1.2A and 4.2.2B**) for the XRD. From the result of the analysis, it is found that the types of serpentine of the ultramafic rocks are mainly of ortho- and clino-chrysotile, nickel serpentine (nepouite), lizardite and very rare antigorite (**Table 4.2.4**). The rareness of antigorite variety indicates that serpentinisation of Manipur Ophiolite Belt mostly took place below 350°C (cf. Barnes and O'Neil, 1969).

Considering just the minerals forsterite, enstatite and serpentine, a simple calculation (cf. O'Hanley, 1996) shows that if the volume is conserved, approximately 35% of the original MgO and SiO₂ must be removed, with little evidence to indicate where these components went. The system would be open with respect to all components. On the other hand, if it is assumed that MgO and SiO₂ are immobile, a similar calculation shows that the hydration of forsterite and enstatite would lead to an increase in volume by as much as 53%, which appears to be disproportionately large with respect to the field relations in terms of their respective emplacement. The system would be closed with respect to MgO and SiO₂, but open with respect to H₂O. While the extreme positions are equally untenable for different reasons, it is concluded that an increase in volume generally accompanies serpentinisation (O'Hanley, 1992; 1996).

The average MgO/(MgO+FeO) value of about 0.85 of serpentine of the ophiolite complex of Manipur (as against the original value of about 0.845 in the parent ultramafic), indicates that the serpentinisation is an isochemical process except the introduction of water (cf. Coleman, 1977); and, therefore, confirms an increase in volume and hence imperative of serpentinisation during spreading regime.

The average MgO/SiO₂ ratio for dunite is about 1.23 and if serpentinisation of dunite is accomplished only by addition of water, this ratio should remain constant (Coleman and Keith, 1971). For ophiolite harzburgites the average MgO/SiO₂ ratio is about 1.02; and for lherzolites the ratio is considerably lower and brucite is uncommon (Coleman, 1977). **Table 4.2.3** indicates that the MgO/SiO₂ ratios of the ultramafics mostly range from 0.93 to 0.99, the lowest being 0.78 and

the highest being 1.14. The range of values of MgO/SiO_2 indicates that host ultramafics from which serpentinization took place range from lherzolite to harzburgite and the MgO/SiO_2 ratio of the serpentines is also falling within the range of lherzolite and harzburgite. As there was no considerable loss of the components it is observed that serpentinization involved was associated with increase in volume.

From the modal data of the ultramafic rocks it is observed that in a very few extensively serpentinised select samples particularly in the sample No. F39B, F2A3, and S2 UA, almost all of the secondary spinels are perished. This appears to be related with localized later stage serpentinisation during the post spreading compressive tectonic history of ophiolite emplacement in which limited and localized rodingitisation also took place. The serpentinisation at this stage must have taken place without any change in volume as a result of which some components like Mg, Fe, Ca, etc. were lost from the system. Such type of reaction must have taken place at a limited extent and in localized manner. During the process of volume conserved serpentinisation, calcium oxide (CaO) component is removed from the peridotite with $\text{Ca}^{+2}\text{-OH}^{-1}$ type water (Barnes and O'Neil, 1969). Later on, these potentially active calcium hydroxide water reacts with the rocks of higher in silica than the peridotites. In the reaction the calc-silicate minerals will replace and invade the host rock whereby veins of rodingites were formed in the open fractures of the ultramafics of Manipur Ophiolite Belt. Therefore, it is inferred that rodingites are the by-product of serpentinisation processes and not the result of high temperature contact phenomena on account of ophiolitic igneous activity.

6.1.4 Chromite and Chromite Mineralisation

In the ophiolite belt in Manipur chromites are generally found in the serpentinised peridotitic ultramafics, which are mostly of metamorphic harzburgite and metamorphic lherzolite, the remnants of upper mantle rocks, that have suffered limited partial melting (Khuman and Soibam, 2010; Soibam *et al.*, 2015). They occur as a number of sporadic pockets of massive chromite bodies in the host of the serpentinised ultramafic rocks and of podiform type. They are generally found in the form of broken blocks, lenses, nodules and pods either floating over or encaged in

the host rocks. The chromite deposits of Manipur Ophiolite Belt fall under podiform types. The chromite bodies occurred in the MOB contains more than 95 volume percent of chromite mineral. Hence, they are not considered as chromitites.

Petrographically, it has been observed that the host ultramafic rock (serpentinite) samples are principally composed of serpentines derived from olivine, bastites (pseudomorphs of serpentine after pyroxenes showing bronze like metallic luster or schiller), relics of olivine, orthopyroxene, clinopyroxene and primary and secondary spinels. The host rocks generally show xenoblastic granular texture and the grain size is quite variable and it is difficult to establish original grain boundaries. All the faces of the essential primary phases are corroded. These features indicate that the host rocks of the chromites under investigation are residues of upper mantle rocks, which have suffered partial melting. No lherzolite and harzburgite samples with euhedral grains of the constituent phases are found in the Ophiolite belt in Manipur (where sporadic chromite bodies are occurred) indicating that the chromites have not been formed because of cumulate crystallisation of the later generated melt from the partial melting of the diapiric upper mantle rocks.

The chromite samples are intensely fractured and the broken pieces are separated apart and filled by secondary silicate phases, which are predominantly of serpentine. Small crystals of chromite also occur in intergranular spaces of other phases of the host rock. Some of the chromite grains show extensive brecciation. Along the boundaries of cracks kin minerals like ferritchromite or magnesioferrite or magnetites are observed. Some chromite samples exhibit a zonation in which a euhedral Cr-spinel core is mantled by ferritchromite/magnesioferrite. Many of the chromite samples present small amount of inclusions of phases like pyroxene, chrome diopside and magnetite. There are some chromite samples which have inclusions of nepouite (Ni-bearing serpentine) crystals also.

The primary spinel is the one originally formed along with other main phases of the rock, while the secondary one is developed during serpentinisation of principally of olivine and are generally very fine grained and mostly found clustered around the original fractures and cracks (Khuman, 2009) of olivine. The chromites are highly fractured and bracciated. The serpentinisation is also of volume expansion

type (Khuman, 2009). The petrographic features of the host rocks indicate that they have evolved from higher pressure regime to lower pressure regime indicating that the chromites along with the host rocks have come up from deeper upper mantle environment to the sub-surface condition on account of diapiric upflow during the spreading regime and suffered volume expansion.

EPMA analysis of representative samples of chromites from different locations is carried out. The chromites have almost similar compositions except some minor variations in certain oxides. But one sample viz. F1-S2A has exceptionally high value of NiO and low value of FeO. The other chromites have high FeO and low NiO values. The triangular proportion of the mean composition of the representative chromite samples is found to be spinel = 26.50%, chromite = 70.25%, magnetite = 3.25%. The Cr# value range from 0.66 to 0.78 and the Mg# values spread from 0.67 to 0.71 for the analysed chromite samples.

When Cr# is plotted against Mg# (after Pober and Fauph, 1980) for the primary spinels from the host rocks are pigeonholed mostly in the field of lherzolite confirming that the host rocks come from the upper mantle and metamorphic in nature. On the other hand, while Cr# versus Mg# plot for the associated chromite bodies established that they cluster in the field of podiform chromites. Thus, the broken chromite bodies occurring in lherzolite and harzburgite host, even if appear massive as in case of stratified chromites of igneous complexes, are podiform in nature. The podiform chromite bodies occurring in the ophiolites were originally segregated bodies within the upper mantle rocks that have come up along with the host rocks or formed because of melt-mantle interaction at greater depths (Arai and Yurimoto, 1994; Stevens, 1994).

When the trivalent cations (Fe^{+3} - Cr - Al) are plotted in triangular diagram it is found that chromite of Manipur Ophiolite Belt fall in the field of Al-chromite type pigeonholed mostly in ophiolite chromitite field. The $\text{Cr\#} = \text{Cr}/(\text{Cr} + \text{Al})$ versus $\text{Mg\#} = \text{Mg}/(\text{Mg} + \text{Fe})$ plot for the studied chromite samples shows that they cluster in the field of podiform chromite (**Fig. 5.2.2**).

At the same time magnetite is also present as inclusion in the chromite bodies. Magnetite as small grain is a by-product of serpentinisation of olivine and is found as secondary spinels. Therefore, these inclusions could have resulted in the later phase of mantle uprising and serpentinisation of the refractory mafic phases in the near surface environment. This also supports that the chromite bodies have come up from greater depths.

6.2 Conclusion

Considering the observations made from the studies of petrography, mineral chemistry of constituent phases, bulk geochemistry (major oxides, trace elements and RRE) of the ultramafic rocks it is quite reasonable to arrive at a conclusion that new oceanic crust was created because of diapiric upwelling of fertile sub-continental upper mantle material of Aluminium-Spinel to Chrome-Spinel Lherzolite composition. The ocean floor rocks of the new basin were mostly made of residual upper mantle rocks of metamorphic lherzolite and harzburgite composition, which had suffered limited partial melting. The ocean floor rocks had limited proportion of other igneous ophiolitic rocks like ultramafic cumulates and other related differentiates. Continued upwelling of the lherzolitic and harzburgitic ultramafics, even after partial melting died out, made them reached almost to the ocean floor during which extensive serpentinisation took place. The serpentinisation took place along with an increase in volume, consequently having relationship with spreading tectonics. The rareness of antigorite variety infers that serpentinisation of Manipur Ophiolite Belt mostly took place below 350°C, i.e., in the sub-surface environment. The serpentinization of the mafic phases like olivine produce secondary spinels of magnetite major, not chromites; hence, serpentinisation processes have no direct link with chromite mineralisation. But the studies of serpentinisation contribute to reveal the fact that the host rocks and chromites itself have evolved from higher pressure regime to lower pressure regime indicating that the chromites along with the host rocks have come up from deeper upper mantle environment to the sub-surface condition on account of diapiric upflow during the spreading regime and suffered volume expansion. After the spreading regime

tectonic inversion took place leading to the orogenesis of the Indo-Myanmar Hill Ranges and in due course of orogenesis obduction of ocean floor rocks have taken place giving rise to the Manipur Ophiolite Belt. Thus, Manipur Ophiolite is a part of the newly created oceanic crust on account of rifting of crustal landmass, fragments of which were emplaced in due course of tectonic inversion during the subduction of Indian plate beneath the Myanmar micro-plate.

Thus, it is also concluded that the chromite bodies occurring as discontinued broken bodies within the host of residual peridotites of lherzolite and harzburgite composition were originally formed in the upper mantle environment and originally associated with metamorphic lherzolitic and harzburgitic source rocks. The chromite blocks in the present-day field setting of the MOMZ could have been originally lenticular or forming segregated layers within the host rocks of metamorphic lherzolite of the then upper mantle environment. In due course of diapiric upflow of the upper mantle rocks during the spreading regime they were broken into pieces and brought up along with the host rocks. The host rocks suffered partial melting. Depending upon the degree of melting lherzolitic source rock gave rise to lherzolite and harzburgite. Rocks with lesser degree of melting didn't lose much clinopyroxene and hence resulted to lherzolite of near surface environment, while those with higher degree of melting lost greater amount of clinopyroxene, thus becoming harzburgite; this is as a consequence of diapiric upflow during the spreading regime and consequent formation of ocean floor rocks of the resultant basin. In due course of time tectonic reversal started leading to convergence and subsequent orogenesis of the IMR owing to the subduction of the oceanic margin of the Indian plate below the Myanmar micro-plate. Thus, the different litho-units of the ocean floor rocks were obducted as tectonic slices in a jumbled manner giving rise to the ophiolite belt of the IMR. The subsequent evolution of the IMR in general and the ophiolite belt in particular led to the generation of the existing topography and geology of the region. The chromite bodies are more resistant than the host serpentinised lherzolite and harzburgite. Consequently, the chromite bodies are found as tectonic fish in the present-day field setting.

BIBLIOGRAPHY

- Abbott, R.N., 1999. The serpentinisation of peridotite from Cedar valley, Jamaica: *International Geology Rev.*, 41, 836-844.
- Acharyya, S.K., 1986. Tectonostratigraphic history of Naga hills ophiolite: *Geol Sur. India, Memoirs*, 119, 94-103.
- Ahmad, T., Tanaka, T., Sachan, H.K., Asahara, Y., Islam, R. and Khanna, P.P., 2008. Geochemical and isotopic constraints on the age and origin of the Nidar Ophiolitic Complex, Ladakh, India: Implications for the Neo-Tethyan subduction along the Indus suture zone. *Tectonophysics*. 451 (1-4), 206-224.
- Ahmed, Z., 1993. Leucocratic rocks from the Bela ophiolite, Khuzadr district, Pakistan. In: Searle MP, Treloar PJ. eds. *Himalayan Tectonics: Geological Society of London Special Publication*. 74, 89-100.
- Aitchison, J.C. and Davis, A.M., 2004. Evidence for the multiphase nature of the India-Asia collision from the Yarlung Tsangpo suture zone, Tibet: *Geological Society, London, Special Publications*. 226(1), 217-233.
- Aitchison, J.C., Davis, A.M., Abrajevitch, A.V., Ali, J.R., Liu, B.J., Luo, H., Mc Dermid, I.R.C., and Ziabrev, S.V., 2003. Stratigraphic and sedimentological constraints on the age and tectonic evolution of the Neotethyan ophiolites along the Yarlung Tsa constraints on the age and tectonic evolution of the Neotethyan ophiolites along the Yarlung Tsangpo suture zone, Tibet: *Geological Society, London, Special Publications*, 218, 147-164.
- Allegre, C.J., Courtillot, V., Tapponnier, P., Hirn, A., Mattauer, M., Coulon, C., Jaeger, J.J., Achache, J., Schärer, U., Marcoux, J., Burg, J.P., Girardeau, J., Armijo, R., Gariépy, C., Göpel, C., Li, T., Xiao, X., Chang, C., Li, G., Lin, B., Teng, J., Wang, N., Chen, G., Han, T., Wang, X., Den, W., Sheng, H., Cao, Y., Zhou, J., Qiu, H., Bao, P., Wang, S., Wang, B., Zhou, Y. And Ronghua, X., 1984. Structure and evolution of the Himalaya-Tibet orogenic belt. *Nature*, 307, 17-22.
- Alleman, F., 1979. Time of emplacement of the Zhob valley ophiolite and Bela ophiolite, Balochistan (preliminary report, *Geological survey of Pakistan*, 215-242.
- Anon, 1974. *Geology and minerals resources of the states of India-Arunachal Pradesh, Assam, Manipur, Meghalaya, Mizoram, Nangaland, and Tripura: Geol. Surv. Ind., Misc. pub., v. 30 (iv)*.
- Anonymous, 1974. *Geology and mineral resources of the states of India: Geol. Sur. India, misc. Publ., 30(4), 124*.

- Arai, S., 1994. Characterization of spinel peridotites by olivine-spinel compositional relationship – Review and interpretation: *Chemical Geology*, 113, 191-204.
- Arai, S., Shimizu, Y., Ismail, S.A., Ahmed, A.H., 2006. Low-T formation of high-Cr spinel with apparently primary chemical characteristics within podiform chromitite from Rayat, northeastern Iraq: *Mineral. Mag.* 70, 499–508.
- Arai, S., Uesugi, J., Ahmed, A. H., 2004. Upper crustal podiform chromitite from the northern Oman ophiolite as the stratigraphically shallowest chromitite in ophiolite and its implication for Cr-concentration. *Contrib. Mineral. Petrol.* 147, 145–154.
- Arai, S., Yurimoto, H., 1994. Podiform chromites of the Tari-Misaka ultramafic complex, southwestern Japan, as mantle-melt interaction products: *Econ. Geol.* 89, 1279–1288.
- Barnes, I. and O’Neil, J.R., 1969. The relationship between fluids in some alpine-type ultramafics and possible model of serpentinisation, Western United states: *Geol. Soc. Am. Bull.*, 80, 1947-1960.
- Barnes, S.J., Roeder, P.L., 2001. The range of spinel compositions in terrestrial mafic and ultramafic rocks: *J. Petrol.* 42(12), 2279–2302.
- Benson, W.N., 1926. The tectonic conditions accompanying the intrusion of basic and ultrabasic igneous rocks: *U.S. Natl. Acad. Sci. Mem.*, 1, 1-90.
- Best, M.G., 2001. *Igneous and metamorphic petrology* (Reprint of 1st Indian Edition), CBS Publishers and Distributors, New Delhi, 630.
- Bhandari, L.L., Fuloria, R.C. and Shastri, V.V., 1973. Stratigraphy of Assam valley: *Am. Assoc. Petro. Geol. Bulletin*, 57, 642-654.
- Boudier, F. And Nicolas, A., 1985. Harzburgite and lherzolite in ophiolite and oceanic environments: *Earth and Plan. Sc. Lett.*, 76, 84-92.
- Boudier, F., and Nicolas, A., 1985. Harzburgite and Lherzolite subtype in ophiolitic and oceanic environment : *Earth and Planetary Science Letter*, v. 84-92.
- Bowen, N.L. and Tuttle, O.F., 1949. The system $\text{MgO-SiO}_2\text{-H}_2\text{O}$: *Geol. Soc. Am. Bull.*, 60, 439-460.
- Bowen, N.L., (1927). The origin of ultrabasic and related rocks: *Am. J. Sci.*, 14, 89-108.
- Boyd, F. R., (1970). Garnet peridotite and the system $\text{CaSiO}_3\text{-MgSiO}_3\text{-Al}_2\text{O}_3$: *Minerlog. Soc. Am. Spec. paper*, 3, 63 - 75.

- Brongniart, A., 1827. Classification et caractères minéralogiques des roches homogènes et hétérogènes, Paris: F.G. Levrault.
- Brunn, J.H., 1960. Mise en place et différentiation Pluto- volcanique du cortègeophiolitique: *Rev. Geogr. Phys. Dyn.*, 3, 115-132.
- Brunn, J.H., 1961. Les sutures ophiolitiques - Contribution à l'étude des relations entre phénomènes magmatique et orogéniques: *Rev. Géogr. Phys. Géol. Dyn.*, 4, 89-96, 181-202.
- Brunnschweiler, R.O., 1966. On the geology of Indo-Burman Ranges: *J. Geol. Soc. Australia*, 13, 137-195.
- B.V. Rao and Ranjit Nayak, 2016. Ultramafic cumulates from Naga Ophiolite Belt, India: Implications for petrogenesis and Tectonic Setting. In S K Srivastava (ed.), *Recent Trends in Earth Science Research with special reference to NE India*. P. 197-212.
- Carswell, D.A., 1980. Mantle derived lherzolite nodules associated with kimberlite, carbonatite and basaltic magmatism-A review: *Lithos*, 13, 121-138.
- Cawood et al., 2009, Accretionary orogen through Earth history: *Geological society of London*, 318, 1-36.
- Chan, GH-N., Crowley, Q., Searle, M., Aitchison, J.C., Horstwood, M., 2007. U–Pb zircon ages of the YarlungZangbo suture zone ophiolites, south Tibet: In 22th Himalaya–Karakoram–Tibet workshop, Hong Kong, China, workshop abstract 12.
- Chattopadhyay, B.M., Venkataraman, P., Roy, D.K., Ghose, S., Bhattacharya, S. 1983. Geology of Naga Hills ophiolites: *Record of Geological Survey of India*. 113, 59–115.
- Chidester, A.H., 1962. Petrology and geochemistry of selected talc-bearing ultramafic rocks and adjacent country rocks in north-central Vermont: *U.S. Geol. Surv. Pro. Paper*, 345, 1-207.
- Chisoi, 2010, Petrology and Geochemistry of mafic and ultramafic cumulate from parts of Phek district, Nagaland with special reference to group mineralization. Unpublished PhD Thesis of Nagaland University, Kohima.
- Chungkham, P., and Jafar, S.A., 1998. Late Cretaceous (Santonian-Maastrichtian) integrated Coccolith- Globotruncanid biostratigraphy of pelagic limestone from the accretionary prism of Manipur, Northeastern India: *Micropaleontology* 44, 68–83.
- Church, W.R., 1972. Ophiolite – its definition, origin as oceanic crust, and mode of emplacement in orogenic belts, with special reference to the Appalachians. *Dept. Energy, Mines Res. Canada Publ.*, 42, 71-85.
- Cloos, M., 1993, Lithospheric buoyancy and collisional orogenesis, subduction of oceanic plateaus, continental margins, island arcs, spreading ridges and seamounts: *Geological Soc. of Amer. Bull.*, 105, 717-737.
- Coleman, R.G. and Keith, T.E., 1971. A chemical study of serpentinisation - Burro Mountain, California: *J. Petrol.*, 12, 311-328.

- Coleman, R.G., 1971a. Plate tectonic emplacement of upper mantle peridotites along continental edges: *J. Geophys. Res.*, 76, 1212-1222.
- Coleman, R.G., (1977). *Ophiolites – ancient oceanic lithosphere?* Springer-Verlag, Berlin–Heidelberg, 229.
- Curry, J. R., Moore, D. G., Lawver, L. A., Emmel, F. J., Raitt, R. W., Henry, M. And Kieckhefer, R. 1978. Tectonics of the Andaman Sea and Burma. In: Watkins, J., Montadert, L. And Dickerson, P. eds. *Geological and Geophysical Investigations of Continental Margins: American Association of Petroleum Geologists, Memoirs*, 29, 189–198.
- Curry, J.R. and Moore, D.G., 1974. The Bengal Geosyncline from rift to orogeny: *Geology*.
- Dalziel, I.W.D., Sharon Mosher; and Lisa, M., 2000. Laurentia-Kalahari collision and the assembly of Rodinia: *Jour. of Geol.*, 198, 499-513.
- Davies, H.L., 1971. Peridotite-Gabbro-Basalt complex in eastern papua, an overthrust plate of oceanic mantle and crust: *Australian Bur. Min. Resur. Bull.*, 128, 48.
- De Mets, C., Gordon, R. G., Argus, D. F. and Stein, S. 1990. Current plate motions: *Geophysical Journal International*, 101, 425–478.
- Desmurs, L., Müntener, O. and Manatschal, G., 2002. Onset of magmatic accretion within a Magma-poor rifted margin: a case history from the Platta ocean-continent transition, eastern Switzerland. *Contribution to Mineralogy Petrology*, 144, 365-382.
- Deva Singh, N., 1993. Spatial distribution of scheduled tribes in Manipur: *The Deccan Geographer*, 31(2), 63-70.
- Dewy, J.F. and Bird, J.M., 1971. Origin and emplacement of the ophiolite suite-Appalachian ophiolites in Newfoundland. *J. Geophys. Res.*, 76, 3179-3206.
- Dick, H.J.B. and Bullen, T., 1984. Chromian spinel as a petrogenetic indicator in abyssal and alpine type peridotites and spatially associated lavas: *Contrib. to Miner. and Petro.*, 86, 54-76.
- Dilek and Flower, 2003, Arc-trench rollback and forearc accretion: 2. A model template for ophiolite in Albania, Cyprus, and Oman: *Geological society of London*, 218, 43-68.
- Dilek, Y., 2003. Ophiolite pulses, mantle plumes and orogeny: *Geological Society, London, Special Publications*. 218(1), 9-19.

- Dilek, Y., and Furnes, H., 2011. Ophiolite genesis and global tectonics: geochemical and tectonic fingerprinting of ancient oceanic lithosphere: Geological Society of America Bulletin. 123, 387–411.
- Ehler, E.G. and Blatt, H., 1987. Petrology - Igneous, Sedimentary and Metamorphic: CBS Publishers and Distributors, New Delhi, 732.
- Elthon, D., Casey, J.F., and Komor, S., 1982. Mineral chemistry of ultramafic cumulates from the North Arm Mountain massif of the Bay of Islands ophiolite: evidence of high pressure crystal fractionation of oceanic basalts: Journal of Geophysical Research. 87, 8717–8734.
- Emilio Saccani*, 2014. A new method of discriminating different types of post-Archean ophiolitic basalts and their tectonic significance using Th-Nb and Ce-Dy-Yb: Geoscience Frontiers xxx1e21).
- Evans, P., 1932. Explanatory notes to accompany a table showing the tertiary succession in Assam: Trans. Mining and Geol. Int. India, 27, 155-260.
- Gansser, A., 1964. Geology of the Himalayas.
- Gansser, A., 1980a. The significance of the Himalayan suture zone. Tectonophysics, 62(1-2), 37-52.
- Gansser, A., 1980b. The Peri-Indian suture zone. In: Aubouin, J., Debarnes, J., Latreille, M. Eds. Geology of the Alpine chains born of Tethys. Bureau de Recherches Geologiques et Minières, Memoire 115, 140–148. Gass, I.G., 1982. Ophiolites. Sci. Am. 247, 122–131.
- Gass, I.G., 1980, The Troodos massif-its role in unraveling of the ophiolite problem and its Significance in the understanding of constructive plate margin processes. In: Panayistou, A., eds. Ophiolites: Geol. Surv. Cyprus, 23-35.
- Gass, I.G., Neary, C.R., Plant, J., Robertson, A.H.F., Simonian, K.O., Smewing, J.D.,
- Spooner, E.T.C. and Wilson, R.A.M., 1975. Comments on “The Troodos ophiolitic complex was probably formed in an island arc”, by A. Miyashiro and subsequent correspondence by A. Hynes and A. Miyashiro. Earth and Planetary Science Letters. 25(2), 236-238.
- Ghosh, B., Ray, J., and Morishita, T., 2014. Grain-scale plastic deformation of chromite from podiform chromitite of the Naga-Manipur ophiolite belt, India: Implication to mantle dynamics: Ore Geology Reviews 56:199–208.
- Gnos, E., 1998. Peak metamorphic conditions of garnet amphibolites beneath the Semail Ophiolite. implications for an inverted pressure gradient: International Geology Review, 40(4), 281-304.

- Gnos, E., Immenhauser, A. and Peters, T.J., 1997. Late Cretaceous/early Tertiary convergence between the Indian and Arabian plates recorded in ophiolites and related sediments. *Tectonophysics*, 271(1-2), 1-19.
- Harte, B., 1983. Mantle peridotites and processes – the kimberlite sample, In: Hawkesworth, C.J. & Norry, M.J., eds. *Continental basalts and mantle xenoliths*: Nantwich, Shiva, 46-91.
- Hebert, R., Bezard, R., Guilmette, C., Dostal, J., Wang, C.S. and Liu, Z.F., 2012. The Indus–Yarlung Zangbo ophiolites from Nanga Parbat to Namche Barwa syntaxes, southern Tibet: First synthesis of petrology, geochemistry, and geochronology with incidences on geodynamic reconstructions of Neo-Tethys. *Gondwana Research*. 22, 377–397.
- Hemanta Singh, R.K., Rodríguez-Tovar, F.J. and Soibam, I., 2008. Trace Fossils of the Upper Eocene-Lower Oligocene Transition of the Manipur, Indo-Myanmar Ranges (Northeast India), Turkish. *Journal of Earth Sciences* 17, 821–834.
- Hess, 1962. History of ocean basin, petrologic studies: a volume to honor, 599-620.
- Hess, H.H., 1938. A primary peridotite magma: *Am. J. Sci.*, 35, 321-344.
- Hess, H.H., 1955a. Serpentine, Orogeny, and Epeirogeny. *Geol. Soc. Am. Spec. Paper*, 62, 391-407.
- Hess, H.H., 1955b. The oceanic crust: *J. Marine Res.*, 14, 423-439.
- Hyndman, D.W., 1985. *Petrology of igneous and metamorphic rocks*, 2nd edition, McGraw-Hill Company.
- Jackson, E.D. and Thayer, T.P., 1972. Some criteria for distinguishing between stratiform, concentric and alpine peridotite-gabbro complexes: 24th Intern. Geol. Congr. Sect., 2, 289-296.
- Kabui, G., 1990. Tribal profile of Manipur, Centre for Tribal Studies, Manipur University, Imphal.
- Kakar, M.I., Collins, A.S., Mahmood, K., Foden, J.D. and Khan, M., 2012. U-Pb zircon crystallization age of the Muslim Bagh ophiolite: Enigmatic remains of an extensive pre-Himalayan arc. *Geology*, 40 (12), 1099–1102.
- Kamenetsky, V.S., Crawford, A.J. and Meffre, S., 2001. Factors controlling chemistry of magmatic spinel: an empirical study of associated olivine, Cr-spinel and melt inclusions from primitive rocks. *J. Petrol.* 42, 655–671.
- Karson, J.A., 1998. Internal structure of oceanic lithosphere, A perspective from tectonic windows, In: Buck, W.R., Delaney, P.T., Karson, J.A. and Lagabriele, Y., eds., *Faulting and magmatism at mid-oceanic ridges*. *Am. Geophy. Union Mono.*, 106, 177-218.

- Karson, J.A., 2001. Oceanic crust when Earth was young. *Science*, 292, 1076-1079.
- Kerr A.C., Tamey J., Nivia A., Marriner, G.F. and Saunders A.D., 1998. The internal structure of oceanic plateaus: Inferences from obducted Cretaceousterranes in Western Colombia and the Caribbean. *Tectonophysics*, 292, 173-188.
- Khan, S.R., 1995. A Preliminary Geological Report on Part of Waziristan Ophiolite, North Waziristan, NW. Pakistan. International Symposium on Himalayan Suture Zone of Pakistan. 4.
- Khan, S.R., 1999. Stratigraphy of the passive margin of the Indian plate, North Waziristan, NW Pakistan. Geological Survey of Pakistan, Geoscience Laboratory, *Geologica*, 4, 48–68.
- Khan, S-R., Jan, M. Q., Khan, T. and Khan, M. A. 2007. Petrology of the dykes from the Waziristan Ophiolite, NW Pakistan. *Journal of Asian Earth Sciences*, 29(2), 369-377.
- Khuman, M. Ch. and Soibam, I., 2010. Ophiolite of Manipur - its field setting and petrotectonic significance. *Memoir Geological Society of India* 75, 255-290.
- Khuman, M. Ch., 2009. Petrological and Geochemical Studies of the Ophiolite Belt in Parts of Chandel and Ukhrul Districts Manipur and Their Tectonic Significance. Unpublished PhD Thesis of Manipur University, Imphal, 238.
- Lagabriele, Y., Guivel, C., Maury, R.C. and Bourgois, J., 2000. Magmatic-tectonic effects of high thermal regime at the site of active ridge subduction: the Chile Triple junction model: *Technophysics* 326, 255-268.
- Lagabriele, Y. and Cannat, M., 1990. Alpine Jurassic ophiolites resemble the modern central Atlantic basement. *Geology*, 18, 319-322.
- Lagabriele, Bideau, D. Cannat, M., Jeffrey, A., Karson and Mevel, C., 1998. Ultramafic-mafic plutonic rock suites exposed along the mid-Atlantic ridge (10°N - 30°N). Symmetrical-Asymmetrical Distribution and Implication for seafloor spreading Processes In: Buck, W.R., Delaney, P.T., Karson, J.A. & Lagabriele, Y., eds. *Faulting and magmatism at mid-oceanic ridges: Am. Geophy. Union Mono.*, 106, 153-176.
- Leeman, W.P., Smith, D.R. and Hildreth, W., 1990). Compositional diversity of Late Cenozoic basalts in a transect across the southern Washington Cascades – Implications for subduction zone magmatism: *Jour. of Geophy. Res.*, 95, 19561-19582.
- Loney, R.A., Himelberg, G.R. and Coleman, R.G., 1971. Structure and petrology of the alpine-type peridotite at Burro Mountain, California, U.S.A.: *J. Petrol.*, 12, 245-309.

- Macdonald, K.C., 1998. Linkage between faulting, volcanism, hydrothermal activity and segmentation on fast spreading centers, In: Buck, W.R., Delaney, P.T., Karson, J.A. and Lagabriele, Y., eds., *Faulting and magmatism at mid-oceanic ridges*. Am. Geophy. Union Mono., 106, 27-58.
- Macdonald, K.C., 1998. Linkage between faulting, volcanism, hydrothermal activity and segmentation on fast spreading centers, In: Buck, W.R., Delaney, P.T., Karson, J.A. and Lagabriele, Y., eds., *Faulting and magmatism at mid-oceanic ridges*. Am. Geophy. Union Mono., 106, 27-58.
- Mallet, F.R., 1876. On the coal fields of Naga hills bordering the Lakhimpur and sibsagar districts, Assam: Geol. Sur. India, Memoirs, 12(2), 166-363.
- Manatschal, G. and Muntener, O., 2009. A type sequence across an ancient magma-poor ocean-continent-transition: the example of the western Alpine Tethys ophiolites. *Tectonophysics*, 437, 4-19.
- Mathur, L.P. & Evans, P., 1964. Oil in India: 22nd Int. Geol. Congr. Proc. Comptes Rendus Brochure, 1-86.
- McDermid, I., Aitchison, J., Davis, A., Harrison, T. and Grove, M., 2002. The Zedong terrane: Late Jurassic intra-oceanic magmatic arc within the Yarlung-Tsangpo Suture Zone, southeastern Tibet. *Chemical Geology* 187, 267–277.
- Medlicott, H.B., 1865. The coal of Assam etc. with geological notes of Assam and the hills to the south of it: Geol. Sur. India Memoirs, 4, 387-442.
- Merangsoba, 2011. Petrology and Geochemistry of Serpentinites in Ophiolite Suite from parts of Phek District, Nagaland with Emphasis on Their Genesis. Unpublished PhD Thesis of Nagaland University, Kohima.
- Minster, J. B. and Jordan, T. H. 1978. Present day plate motions. *Journal of Geophysical Research*, 83, 5331–5354.
- Mitchell, A.H.G. and McKerrow, W.S., 1975. Analogous evolution of the Burma orogen and the Scottish Caledonides. *Geological Society of America Bulletin*, 86(3), 305-315.
- Mitchell, A.H.G., 1993. Cretaceous–Cenozoic tectonic events in the western Myanmar (Burma) Assam region. *J. Geol. Soc. Lond.* 150, 1089–1102.
- Miyashiro, A., 1973. The Troodos ophiolitic complex was probably formed in an island arc. *Earth and Planetary Science Letters*, 19(2), 218-224.
- Mohn, G., Manatschal, G., Beltrando, M., Masini, E. and Kusznir, N. 2012. Necking of continental crust in magma-poor rifted margins: evidence from the fossil Alpine Tethys Margins. *Tectonics*, 31, 1-28.
- Mondal, S.K., Ripley, E.M., Li, C. and Frei, R., 2006. The genesis of Archean chromitites from the Nuasahi and Sukinda massifs in the Singhbhum craton, India. *Precamb. Res.* 148, 45–66.

- Moore, E.M. and Vine, F.J., (1971). Troodos Massif, Cyprus and other ophiolites as oceanic crust -evaluation and implications. Roy. Soc. London Philos. Trans., A268, 443-466.
- Moore, E.M., 1982. Origin and emplacement of ophiolites. Rev. Geophys. Space Phys., 20, 737-760.
- Moore, E.M., 2002. Pre-1Ga (pre-Rodinian) ophiolites, their tectonic and environmental Implications. GSA Bull., 114(1), 80-95.
- Moore, E.M., 1975. Discussion of "Origin of Troodos and other ophiolites: a reply to Hynes", by Akiho Miyashiro. Earth and Planetary Science Letters, 25(2), 223-226.
- Nelson S A , 2007. Basaltic and gabbroic rocks, retrieve from : Ophiolite/Basaltic and gabbroic rocks.htm.
- Nicolas, A., 1989. Structure of ophiolites and dynamics of oceanic lithosphere, Kluwer Academic Publishers, Dordrecht.
- Nixon, P. H., 1987. Mantle Xenoliths. Wiley, Chichester.
- O'Hanley, D.S., 1992. Solution to the volume problem in serpentinisation: Geology, 20, 705-708.
- O'Hanley, D.S., 1996. Serpentine-Records of tectonic and petrological history, New York, Oxford University Press.
- Pascoe, E.H., 1912. A traverse across the Naga Hills of the Assam from Dimapur to neighbouring of Saramati peak, Rec. v. 40 (i), 1- 269.
- Pearce, J.A. and Cann, J.R., 1973. Tectonic setting of basic volcanic rocks determined using trace element analyses. Earth and planetary science letters, 19(2), 290-300.
- Pearce, J.A., 1983. Role of the sub-continental lithosphere in magma genesis at active continental margins. In: Hawkesworth, C.J., and Norry, M.J. eds. Continental basalts and mantle xenoliths, Nantwich, Cheshire: Shiva publication, 230-249.
- Pearce, J.A., Harris, N.B. and Tindle, A.G., 1984. Trace element discrimination diagrams for the tectonic interpretation of granitic rocks. Journal of petrology, 25(4), 956-983.
- Pedersen, R.B., Searle, M.P. and Corfield, R.I., 2001. U-Pb zircon ages from the Spontang Ophiolite, Ladakh Himalaya. Journal of the Geological Society of London 158, 513-52.

- Piccardo, G. B., 2015. Passive rifting and continental splitting in the Jurassic Ligurian Tethys: the mantle perspective, In Gibson, G. M., Roure, F. and Manatschal, G. eds., *Sedimentary Basins and Crustal Processes at Continental Margins: From Modern hyper-extended Margins to Deformed Ancient Analogues*. Geological Society, London, Special Publications, 413, 239-267.
- Pober, E. and Fauph., 1980. The chemistry of detrital chromian spinels and its implications for the geodynamic evolution of Eastern Alps. *Geologische Rundschau*, 77, 641-670.
- Ranga Rao, A., 1983. Geology and hydrocarbon potential of a part of Assam , Arakan basin and its adjacent region, symp. *Petroliferous basin of Ind.*, 127-158.
- Raymond, L.A., 2002. *The study of igneous, sedimentary and metamorphic rocks*. Mc. Graw Hills.
- Robinson, P.T. and Malpas, J., 1990. The Troodos ophiolite of Cyprus: new perspectives on its origin and emplacement. *Ophiolites: Oceanic Crustal Analogues*, 13-36.
- Pearce, J.A., Harris, N.B. and Tindle, A.G., 1984. Trace element discrimination diagrams for the tectonic interpretation of granitic rocks. *Journal of petrology*, 25(4), 956-983.
- Rollinson, H., 2008. The geochemistry of mantle chromitites from the northern part of the Oman ophiolite: inferred parental melt compositions. *Contrib. Mineral. Petrol.* 156, 273–288.
- Romendro, L., Khuman, Ch., and Ibotombi, S., 2017. Petrographic and Geochemical studies of ultramafic rocks of the Ophiolite Belt in Manipur, North-East India. *Journal of applied geochemistry*, vol.19, No. 4 (2017). 436-449.
- Romendro and Khuman, 2021. Petrography and Mineral Chemistry of Podiform Chromite of Ophiolite Belt in Manipur, Northeast India and their Implication. In: *Recent Advances in Earth Science Research in North East India*. South-eastern Book Agencies, 22-51.
- Salisbury, M.H. and Christensen, N.I., 1978. The seismic velocity structure of a traverse through the Bay of Islands ophiolite complex, Newfoundland, an exposure of oceanic crust and upper mantle: *J. Geophys. Res.*, 83, 805-817.
- Sheymaan, Y.M. and Lutts, B.G., 1975. Composition group of ultrabasic rocks and their significance in tectonic analysis : *Geotectonics* (Eng. Ed.), 6.

- Singh, A.K., Devi, L.D., Singh, N.I., Subramanyam, K.S.V., Bikramaditya Singh, R.K. and Satyanarayanan, M., 2013. Platinum-group elements and gold distributions in peridotites and associated podiform chromitites of the Manipur Ophiolitic Complex, Indo-Myanmar Orogenic Belt, Northeast India. *Chem. Erde – Geochem.* 73, 147–161.
- Soibam and Hemanta, 2007. Transtentional Basin in Oblique Subduction Margin: Imphal Valley, an example, Himalaya (Geological Society). vol. 5, 273-297.
- Soibam Ibotombi and Pradipchandra Singh, M., 2006. Analysis of drainage system of Manipur and implications on the tectonics of the Indo-Myanmar Ranges, In: Saklani, P.S., eds., Himalaya (Geological Aspects), 4, 281-302.
- Soibam Ibotombi, 1993. Geology, Structure and tectonics of Manipur, India, Unpublished M.Sc./DIC Thesis, University of London, 131.
- Soibam Ibotombi, 1998. Structural and Tectonic Analysis of Manipur with special reference to evolution of the Imphal valley, Unpublished Ph.D. Thesis of Manipur University, Imphal, 283.
- Soibam, I. and Khuman M, Ch., 2011. Basic rocks of Manipur Ophiolite in the Indo-Myanmar hill ranges, NE India and the petroTECTONIC significance. *J. Nepal Geological Society*, 43, 13-28.
- Soibam, I. and Khuman, M. Ch., 2008. Geological and tectonic setting of Manipur: implications on the tectonics of Indo-Myanmar Ranges. In: Seminar on Indo-Myanmar Ranges in the tectonic framework of the Himalayas and Southeast Asia, Souvenir, November 27-29, Manipur University, Imphal, 51-62.
- Soibam, I., 1998. On the geology of Manipur. In Souvenir: IX Manipur Science Congress (March, 25-27), 12-19.
- Soibam, I., Khuman, M. Ch. and S. S. Subhamenon, 2015. Ophiolitic rocks of the Indo-Myanmar Ranges, NE India: relicts of of an inverted hyper-extended continental margin basin? In Gibson, G. M., Roure, F. And Manatschal, G. eds. *Sedimentary Basins and Crustal Processes at Continental Margins: From Modern Hyper-extended Margins to Deformed Ancient Analogues*. Geological Society, London, Special Publications, 413, 239-267.
- Soibam Ibotombi, 2000. Structural and tectonic framework of Manipur, In: X Manipur Science congress, 15-17 March, 2000, 26-37.
- Steinmann, G., 1927. Die ophiolithischen zonen in dem mediterranen kettegebirge. 14th Intern. Geol. Congr., Madrid, 2, 638-667.
- Stevens, R.E., 1944. Composition of some chromites of the western Hemisphere. *Amer. Mineral.* 29, 1–34.

- Sun, S.S. and Mcdonough, W.F., 1989. Chemical and isotopic systematics of oceanic basalts – implications for mantle compositions and processes, In: Saunders, A.D. & Norry, M.J., (eds.), *Magmatism in the ocean basins: Jour. of Geol. Soc. London, Spl. Publ.*, 42, 313-345.
- Talkington, R.W. and Malpas, J.G., 1984. The formation of spinel phases of white Hill peridotite. St. Anthony complex, Newfoundland, *Neues Jahrbuch Mineralogie, Abhandlunger*, 149, 65-90.
- Tapponnier, P., Mattauer, M., Proust, F. and Cassaigneau, C., 1981a. Mesozoic ophiolites, sutures, and arge-scale tectonic movements in Afghanistan. *Earth and Planetary Science Letters*, 52(2), 355-371.
- Tapponnier, P., Mercier, J.L., Proust, F., Andrieux, J., Armijo, R., Bassoullet, J.P., Brunel, M., Burg, J.P., Colchen, M., Dupre, B. and Girardeau, J., 1981b. The Tibetan side of the India–Eurasia collision. *Nature*, 294(5840), 405.
- Thakur, V.C., 1981. Regional framework and geodynamic evolution of the Indus-Tsangpo suture zone in the Ladakh Himalayas. *Earth and Environmental Science Transactions of the Royal Society of Edinburgh*, 72(2), 89-97.
- Thayer, 1973. U.S Geol. Survey Prof. Paper, 820, 111-121.
- Vaughan, A.P.M., and Scarrow, J.H., 2003. Ophiolite obduction pulses as a proxy indicator of superplume events? *Earth and Planetary Science Letters*. 213, 407-416.
- Vredenburg, E, 1901 : A geological sketch of the Baloschistan desert and part of Eastern Persia. *India Geol. Survey Mem.* 21, 179-302.
- White, L.T. and Lister, G.S., 2012. The collision of India with Asia. *Journal of Geodynamics*, 56, 7-17.
- White, R.S., McKenzie, D. and O’Nions, R.K., 1992. Oceanic crustal thickness from seismic measurements and rare earth element inversions. *Journal of Geophy. Res.*, 97, 19683-19716.
- Windley, B. F., Alexeiev, D., Xiao, W., Kroner, A. and Badarch, G., 2007. Tectonic models for accretion of the Central Asian Orogenic Belt, *J. Geol. Soc.* 164(1), 31-47.
- Wyllie, P.J. eds., 1967. *Ultramafics and related rocks*, Willey, New York, 464.
- Xia, B., Li, J.F., Liu, L.W., Xu, L.F., He, G.S., Wang, H., Zhang, Y.Q. and Yang, Z.Q., 2008. SHRIMP U–Pb dating for dolerite in Sangsang ophiolite, Xizang, China: geochronological constraint for development of eastern Tethys basin. *Geochimica* 37, 399–403.

- Zhou, M.F., Robinson, P.T., Malpas, J. and Li, Z., 1996. Podiform chromitites in the Luobusa ophiolite (southern Tibet): implications for melt/rock interaction and chromite segregation in the upper mantle. *J. Petrol.* 37, 3–21.

Annexure – I

List of the Conference and Seminar

1. 35th International Geological Congress,
27 August to 2 September **2016**, Cape Town, South Africa.
2. National Seminar on Geology, Geochemistry, Tectonics, Energy and Mineral Resources of Northeast India, 9-11 November, 2016, Orgd. by Department of Geology Nagaland University, Kohima Campus , Meriema.
3. Centennial Celebration (1919-2019) And Conference On “Recent Trends In Science Research” 12-14 October 2019. Orgd. by Department of Geology, Centre of Advanced Study Institute Of Science, BHU, Varanasi.
4. NACETER 2019 “National Conference On Emerging Trends In Environmental Research” 31 October- 2 November 2019 Orgd. by Department of Environmental Science, Pachhunga University College, Aizawl.